UNIVERSITY OF CALIFORNIA,
IRVINE

Using a naturally occurring viral protein and a small molecule compound to inhibit B cell immunoglobulin class-switch DNA recombination

DISSERTATION

submitted in partial satisfaction of the requirements
for the degree of

DOCTOR OF PHILOSOPHY

in Biological Sciences

by

Tonika Lam

Dissertation Committee:
Professor Michael J. Buchmeier, Chair
Professor Paolo Casali, Thesis Mentor
Professor Melissa B. Lodoen
Professor Albert Zlotnik

2014

DEDICATION

To my mother, Silene Lam, and my father, Tony Lam

for our *family*

to my brother, Alex Lam, and my cousin, Elizabeth Lyv

for our *childhood*

and to my love, Nicholas Molino

for our *future*.

TABLE OF CONTENTS

LIST OF ABBREVIATIONS

7-AAD	7-Amino-actinomycin D
AFC	Antibody forming cells
AICD	Activation-induced cell death
AID	Activation induced cytidine deaminase
AP-1	Activator protein 1
APC	Antigen presenting cell
APE	Apurinic/apyrimidinic endonuclease
APOBEC2	Apolipoprotein B mRNA editing enzyme, catalytic polypeptide-like 2
BCR	B cell receptor
BiFC	Bimolecular fluorescence complementation assay
CFSE	Carboxyfluorescein succinimidyl ester
C_H	Constant region of heavy chains
ChIP	Chromatin immunoprecipitation
C_L	Constant region of light chains
CpG	DNA containing unmethylated, 5'-Cytosine-phosphate-Guanosine-3' sequence(s)
CSR	Class-switch DNA recombination
DC	Dendritic cell
ELISA	Enzyme-linked immunosorbent assay
Fab	Fragment antigen binding
Fc	Fragment crystallizable
GC	Germinal center
GCK	Germinal center kinase

GFP	Green fluorescent protein
GLT	Germline transcription
HIGM	Hyper IgM Syndrome
ICOS	Inducible costimulator
ICOSL	Inducible costimulator ligand
IFNγ	Interferon gamma
Ig	Immunoglobulin
IgH	Ig heavy chain
IκB	Inhibitor of κB
IKK	Inhibitor of NF-κB kinase
IL	Interleukin
IP	Immunoprecipitation
IRAK	IL-1 receptor associated kinases
JAK	Janus kinase
ITAM	Immunotyrosine-based activation motif
LPS	Lipopolysaccharide
LRR	Leucine-rich repeat
LTA	Lipoteichoic acids
MAL	MyD88-adaptor-like
MAMP	Microbe-associated molecular pattern
MAPK	Mitogen-activated protein kinase
MFI	Mean fluorescence intensity
MHC II	Major histocompatibility complex II
MyD88	Myeloid differentiation primary response 88
NF-κB	Nuclear factor κB

NK	Natural killer cells
ODN	Oligodeoxynucleotide
PAMP	Pathogen-associated molecular pattern
PBMC	Peripheral blood mononuclear cells
PCR	Polymerase chain reaction
PKA	Protein kinase A
PI3K	Phosphoinositide 3 kinase
PLCγ	Phospholipase Cγ
PNA	Peanut agglutinin
PRR	Pattern recognition receptor
PST	Post-recombination transcript
RAG	Recombination activating gene
RPA	Replication protein A
SDS-PAGE	Sodium dodecyl sulphate-polyacrylamide gel electrophoresis
SLE	Systemic lupus erythematosus
SHM	Somatic hypermutation
STAT	Signal transducers and activators of transcription
T-bet	T box expressed in T cells
TCR	T cell receptor
T_{FH}	T follicular helper
TGFβ	Transforming growth factor beta
TIR	Toll/IL-1 receptor
TIRAP	Toll/IL-1 receptor domain containing adaptor protein
TLR	Toll-like receptor

TLS	Translesion synthesis
TNF	Tumor necrosis factor
TRAF	Tumor necrosis factor receptor-associated factor
TRIF	Toll/interleukin 1 receptor protein domain-containing adaptor inducing interferonβ
V(D)J	Variable(Diversity)Joining
V_L	Variable region of light chains
V_H	Variable region of heavy chains

LIST OF FIGURES

LIST OF TABLES

ACKNOWLEDGMENTS

I would like to express the deepest appreciation to my mentor, Dr. Paolo Casali, who has the substance of a true advisor. Dr. Paolo Casali is a scholar who possesses profound knowledge and insight. He continually supported me through my growth in regard to research and scholarship. Without his mentorship and i feedback, my dissertation would not have been possible.

I would like to thank my committee members: Dr. Melissa Lodoen, Dr. Albert Zlotnik and Dr. Michael Buchmeier (Committee Chair) for stimulating discussion and their work and expertise in immunology and infectious diseases has guided me throughout my dissertation work.

I would also like to thank Dr. Craig Walsh, Dr. David Fruman and Dr. Grant MacGregor. Their lectures in signal transduction and cellular biology initiated my aspirations to purse a PhD in immunology.

Lastly, I would like to thank my colleagues, Dr. Zhenming Xu, Dr. Hong Zan, Dr. E.J. Pone, Dr. Clayton A. White, Dr. Guideng Li, Dennis Kulp and Crystal LaFleur who have all supported me through my dissertation work.

Our work was supported by the National Institutes of Health grants 45011, AI 105813, AI 79705 (to P.C.) and NIAID Immunology Research Training Program grant T32 AI 60573 (for T.L.).

DECLARATION REGARDING THE AUTHORSHIP OF WORK THAT APPEARS IN THIS DISSERTATION

All experiments were designed and conducted by Tonika Lam, under the guidance of Dr. Paolo Casali, with the exception of contributions from the following individuals in the following figures:

CHAPTER 1	
Figure 1.2	Tonika Lam
Figure 1.4	Dr. Zhenming Xu, Dr. Hong Zan
Figure 1.5	Dr. Zhenming Xu
CHAPTER 2	
Figure 2.1	Tonika Lam
Figure 2.2	Dr. Zhenming Xu
Figure 2.3	Dr. Zhenming Xu
Figure 2.4	Tonika Lam and Lisa Thomas
Figure 2.5	Tonika Lam and Lisa Thomas
Figure 2.6	Tonika Lam
Figure 2.7 – 2.10	Tonika Lam and Lisa Thomas
Figure 2.11	Tonika Lam
Figure 2.12	Tonika Lam
Figure 2.13	Lisa Thomas and Tonika Lam
Figure 2.14	Tonika Lam and Dr. Egest J. Pone
CHAPTER 3	
Figure 3.1 – 3.7	Dr. Zhenming Xu, Dr. Egest J. Pone and Tonika Lam
Figure 3.8	Tonika Lam
Figure 3.9	Tonika Lam, Dennis Kulp, Dr. Egest J. Pone
Figure 3.10	Dr. Zhenming Xu
CHAPTER 4	
Figure 4.1	Dr. Guideng Li
Figure 4.2 – 4.3	Tonika Lam and Dennis Kulp
Figure 4.4 – 4.6	Tonika Lam
CHAPTER 5	
Figure 5.1	Dr. Zhenming Xu
Figure 5.2	Tonika Lam

CURRICULUM VITAE

Tonika Lam

2007 – 2008	Research Assistant, Organic Chemistry Laboratory Saddleback College
2008 – 2010	Research Assistant, Bioinorganic Chemistry Laboratory University of California, Irvine
2010	BSc in Molecular Biology and Biochemistry University of California, Irvine
2012	Teaching Assistant, School of Biological Sciences University of California, Irvine
2014	Editorial Assistant, *Autoimmunity*, Informa Healthcare
2014	Visiting PhD Student University of Texas Health Science Center at San Antonio

FIELD OF STUDY

B cell immunoglobulin class-switching in antibody and autoantibody responses.

PUBLICATIONS AND PRESENTATIONS

Publications

Lam, T., L. M. Thomas, E. J. Pone, T. Mai, C. A. White, G. Li, Z. Xu and P. Casali. 2013. Scaffold functions of 14-3-3 adaptors in B cell immunoglobulin class switch DNA recombination. ***PLOS ONE***, 8(11): e80414. doi:10.1371/journal.pone.0080414.

Lam, T., D. V. Kulp, Z. Lou, R. Wang, P. Casali and Z. Xu. 2014. Inhibition of antibody class switching and blocking of pathogenic autoantibody responses and disease development in lupus-prone mice by a small molecule compound that targets Rab7. ***J. Immunol.***, *in preparation*.

Li, G., C.A. White, **T. Lam**, E.J. Pone, D. C. Tran, K.L. Hayama, H. Zan, Z. Xu and P. Casali. 2013. Combinatorial H3K9acS10ph histone modifications in *IgH* locus S regions target 14-3-3 adaptors and AID to specify antibody class-switch DNA recombination. ***Cell Rep.,*** 5(3): 702-714.

Mai T., E.J. Pone, G. Li, **T. Lam**, J. Moehlman, Z. Xu, and P. Casali. 2013. Induction of activation-induced cytidine deaminase – targeting adaptor 14-3-3γ is mediated by NF-kB–dependent recruitment of CFP1 to the 5'-CpG-3'-rich 14-3-3γ promoter and is sustained by E2A. ***J. Immunol.*** 191(4): 1895-1906.

Morgando, P., D. Sudarshana, **T. Lam**, P. Casali and M. B. Lodoen. 2014. Type II Toxoplasma gondii induction of CD40 on infected macrophages enhances IL-12 responses. ***Infect and Immun***. doi:10.1128/IAI.0165

White, C.A., E.J. Pone, **T. Lam**, C. Tat, K.L. Hayama, Guideng Li, H. Zan and P. Casali. 2014. HDAC inhibitors upregulate selected B cell microRNAs that silence AID and Blimp-1 expression for epigenetic modulation of antibody and autoantibody Responses. ***J. Immunol****, in press.*

Pone E.J., **Lam, T.**, Z. Xu and P. Casali. 2014. B Cell Rab7 Mediates Induction of AID Expression and Class-Switching in T-dependent and T-independent Antibody Responses. ***J. Immunol.*** *in revision.*

Pone, E.J., Z. Lou, **T. Lam**, M. L. Greenberg, R. Wang, Z. Xu and P. Casali. 2014. LPS induction of B cell class switching and its modulation by TLR1/2, TLR7, TLR9 and CD40: relevance to T-independent antibody responses. ***Autoimmunity***. *in review*.

Select Presentations

Scaffold functions of 14-3-3 adaptors in B cell immunoglobulin class-switch DNA recombination. AAI Annual Meeting, May 5, 2014.

Rab7 and B cell autophagy in maturation of the antibody response. Molecular Biology and Biochemistry Lake Arrowhead Retreat, March 24, 2013. *Honorable mention*.

Viral protein R disrupts 14-3-3 adaptors scaffold functions and AID recruitment to inhibit class-switch DNA recombination. 2nd UC Irvine School of Medicine Clinical Basic & Translational Science Festival, May 24, 2012.

Probing scaffolding functions of 14-3-3, AID, PKA and Ung in class-switch DNA recombination through mutagenesis and naturally occurring Vpr/Vpr peptides. 9th UC Irvine Immunology Fair, November 18-19, 2011.

ACADEMIC DISTINCTIONS AND AWARDS

2014	AAI 2014 Travel Trainee Abstract Award
2013 – 2014	NIH Immunology Research Training Program grant T32 AI 60573
2008 – 2010	Science, Mathematics, And Research for Transformation Scholarship
2006 – 2008	Dean's List, Saddleback College
2004 – 2005	Young Artist Scholarship, Laguna College of Art and Design

ABSTRACT OF THE DISSERTATION

Using a naturally occurring viral protein and a small molecule compound to inhibit B cell immunoglobulin class-switch DNA recombination

By

Tonika Lam

Doctor of Philosophy in Biological Sciences

University of California, Irvine, 2014

Professor Michael Buchmeier, Chair

Immunoglobulin (Ig) gene class-switch DNA recombination (CSR) and somatic hypermutation (SHM), which requires activation-induced cytidine deaminase (AID), underpins autoantibody class-switching from the non-harmful, protective IgM class to the potentially pathogenic IgG and IgA classes. CSR replaces the Ig heavy chain (*IgH*) constant (C_H) region, e.g., Cμ of IgM, with Cγ, Cε or Cα, thereby producing IgG, IgE or IgA antibodies. Aberrant CSR results in a variety of diseases, including atopic IgE reactions (e.g., in asthma), hyper-IgM syndrome, and systemic or organ-specific autoimmunity.

I have explored the in-depth molecular mechanisms underlying antibody class-switching to IgG, IgA or IgE, with emphasis on the targeting and induction of CSR factors. Our work seeks to establish a paradigm that intervention at any of these two levels of regulation can modulate class-switching. Such a paradigm will be critical in shaping research in vaccines, whose efficacies depends on generation of high-affinity antibodies and on therapeutics to inhibit unwanted class-switching in a variety of clinical conditions. We first explored CSR inhibition mechanisms by quantifying direct interaction between 14-3-3, AID, PKA or Ung and viral protein R (Vpr). As we have shown in activated B cells, 14-3-3 adaptors specifically recruit AID

on *IgH* switch (S) region DNA. Our research has been focused on using a naturally occurring viral protein R (Vpr) to disrupt 14-3-3–mediated recruitment of the AID-centered CSR machinery to S region DNA, which inhibited CSR. We then focused on using a small molecule compound for therapeutic treatment in preventing high titers of autoantibodies in systemic lupus erythematosus (SLE). MRL/$Fas^{lpr/lpr}$ mice treated with CID 1067700, the only known inhibitor of Rab7, displayed reduced decreased glomerular hypercellularity and proteinuria, virtually abolished skin lesions, and extended life span. Accordingly, serum titers of anti-dsDNA IgG1, IgG2a, IgG2b and IgG3 autoantibodies were reduced in treated mice, in association with reduced generation of IgG^+ B cells. These mice, however, showed increased proportion of IgM^+ B cells, but normal proportions of $CD4^+$ and $CD8^+$ T cells as well as $CD138^+$ plasma cells. These together with reduced AID expression in treated mice indicate that CID 1067700 selectively inhibits B cell class-switching. Indeed, CID 1067700 treatment blunted the antibody response NP-LPS, a T cell-independent antigen, and inhibited CSR to IgG1 and IgA in purified B cells *in vitro*, but did not affect B cell proliferation, survival or differentiation into plasma cells. Overall, our data have further confirmed the specific role of Rab7 in mediating AID expression and CSR, and strongly suggest Rab7 as a therapeutic target for systemic lupus.

CHAPTER 1

INTRODUCTION TO INNATE AND ADAPTIVE IMMUNITY

1.1 PRINCIPLES OF INNATE AND ADAPTIVE IMMUNITY

The individual is protected from infectious pathogens or agents by effector cells and molecules that are highly organized and trained to communicate together to form an armory, that is the immune system. In response to an immune challenge, higher organisms have evolved distinct immune systems. In vertebrate animals, there are two types of immune responses to infection: the innate and adaptive responses.

The innate and adaptive immune systems protect the individual from infectious pathogens or host disease, such as cancer; parasites or agents from the damage that they cause that may compromise the health and/or longevity of the host organism. To effectively combat invading pathogens or agents, the immune system must complete four critical tasks: (1) immunological recognition, (2) immune effector functions, (3) immune regulation and (4) immunological memory. In immunological recognition, the immediate presence of an invader or infection must be identified, both by white blood cells of the innate system and adaptive system (Table 1.1).

Table 1.1. Comparison of the innate and adaptive systems.

Feature	Innate Immunity	Adaptive Immunity
Antigen-specific	No	Yes
Clonal distribution	No	Yes
Receptor diversity	Germline	Rearranged
Time of response	Fast	Slow
Efficiency of response	Moderately efficient	Highly efficient
Memory	No	Yes

The innate immune system uses receptors that are inherited in the germline (nonclonal distribution). In contrast, the adaptive immune system uses receptors that are assembled (rearranged) during lymphocyte development endowing a single cell with unique specificity towards a specific antigen (clonal distribution).

The innate immune response: The First Lines of Defense

The innate immune response is evolutionarily ancient and is found in plants, fungi, insects and higher organisms and universally based on the – discrimination of self and non-self – detection of conserved products of microbial metabolisms or danger signals from diseased or dying host cells[1]. For example, lipopolysaccharide (LPS), lipoproteins, peptidoglycan and lipoteichoic acids (LTAs) are molecules produced metabolically by bacteria, but not eukaryotic cells, which can be recognized as microbial signatures of microbial invaders by the innate immune system[2, 3]. One critical aspect of the innate recognition is that microbial signatures are not always absolutely identical between different species. Although there are several species–specific and strain–specific variations of the chemical structure, including their synthetic counterparts, these are highly conserved and invariant among microbes of the same class. Due to the conserved molecular patterns of the microbial signatures, these are called pathogen-associated molecular patterns (PAMPs).

Accordingly, pattern-recognition receptors (PRR) of innate immune system recognize PAMPs. In addition to immunological recognition, the downstream events of PRRs recognition with PAMPs include: opsonization, activation of complement and coagulation cascades, phagocytosis, activation of pro-inflammatory signaling pathways and apoptosis. PRR evolved before the adaptive immune response – seen in vertebrates – where receptors undergo rearrangement to further enhance the possibility to recognize foreign antigen[3]. The innate immune system has various PRRs that are expressed on the cell surface of varying white blood cells, intracellular compartments within a cell, or secreted in the blood stream[1]. The Toll-like receptors (TLRs) are PRRs that have a unique and critical function in vertebrate, as well as invertebrate innate

immunity (**Figure 1.1**). TLRs belong to a family of type I transmembrane receptors characterized by an extracellular leucine-rich repeat domain (LRR) and together with IL-1 receptors, TLRs have an intracellular Toll/IL-1 receptor (TIR) domain. The TIR domain superfamily can be divided into three subgroups: the first subgroup include receptors most similar to IL-1R, the second subgroup are classical TLRs and the third subgroup include cytosolic signaling adaptors MyD88 (Myeloid differentiation primary response 88**)** and TIRAP (Toll/IL-1 receptor domain containing adaptor protein), both of which function in TLR signal transduction[4].

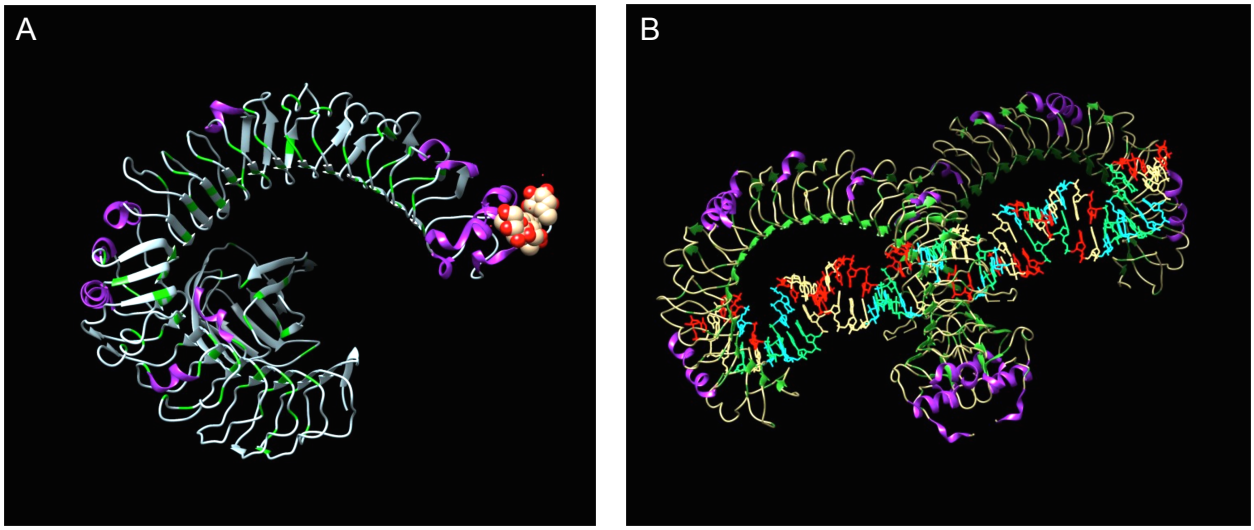

Figure 1.1. Crystal structure of TLR4 and TLR3 and their ligands. The extracellular domain of a TLR, like TLR4 (**A**) and TLR3 (**B**) shown here, is composed of tandem leucine rich repeats (green) which form a sickle-shaped beta-coil and confer specificity in sensing a particular class of TLR ligands. (**A**) Mouse TLR4 shown as a monomer complexed with LPS analog, Eritoran (PDB ID 2z64). (**B**) Mouse TLR3 shown as a homodimer complexed with dsRNA (PDB ID 3ciy). Structures were rendered using the UCSF Chimera program.

There are now at least ten known TLRs and their ligands in mammals (**Table 1.2**), with TLR1 through TLR9 abundantly expressed in mouse B cells[5, 6, 7].

Table 1.2. Cellular expression of TLRs and their ligands.

TLR	Cellular Expression	TLR Ligand (microorganism)	Signal Adaptor
Cell surface TLRs			
TLR1/2	Mo, MΦ, DC, B	Lipomannans (mycobacteria) Lipoproteins (diacly lipoproteins; triacly lipopeptides) Lipoteichoic acids (Gram-positive bacteria) Zymosan (fungus)	TIRAP, MyD88, MAL
TLR5	Mo, MΦ, DC, IE	Flagellin (bacteria) Diacyl lipopeptides (mycoplasma)	MyD88
TLR2/6	Mo, MΦ, DC, B	Diacyl lipopeptides	TIRAP, MyD88, MAL
Cell surface and endosomal TLRs			
TLR4	Mo, MΦ, DC, MC, B	Lipopolysaccharides (LPS, Gram-negative bacteria) Lipoteichoic acids (Gram-positive bacteria)	TIRAP, MyD88, MAL
Endosomal TLRs			
TLR3	B, T, NK, DC	dsRNA (viruses) tRNA, siRNA	TRIF
TLR7/8	Mo, MΦ, DC, B	ssRNA (viruses)	MyD88
TLR9	Mo, MΦ, DC, T, T	Unmethylated CpG containing DNA (bacteria and herpesviruses)	MyD88

Different TLRs have cellular distributions between Mo: monocytes, MΦ: macrophages, DC: dendritic cells, MC: Mast cells, B: B cells, T: T cells, IE: Intestinal epithelium and activate an immune response by direct interaction with their respective ligands. TLR1:TLR2 and TLR2:TLR6 for heterodimers.

Most TLRs function as homodimers, however TLR1 functions as a heterodimer with either TLR2 or TLR6, and TLR7 functions as a heterodimer with TLR8. TLRs 1, 2, 4, 5 and 6 are expressed on the cell surface, whereas TLRs 3, 7, 8 and 9 are expressed in endosomal vesicles inside the cell. TLR1/2 heterodimer senses triacyl lipopeptides from bacteria; TLR2/6 heterodimer senses diacyl lipopeptides from mycoplasma; TLR3 senses dsRNA from viruses; TLR4 senses LPS from bacteria and O-linked mannoses on fungus; TLR7/8 heterodimer senses ssRNA from viruses and bacteria; and, finally TLR9 senses unmethylated CG- rich, or ssDNA containing repeats of the CG motif from replicating viruses and bacteria[8, 9, 10].

Upon sensing pathogens via their PRRs, macrophages and mast cells are activated to phagocytose the pathogen, display peptide fragments on MHC II and I receptors, and secrete pro-inflammatory cytokines and lipid mediators. Similarly, stimulation of PRRs on immature dendritic cells (DCs) leads to their activation, which in turn activates adaptive immunity.

The rearrangement and clonal distribution of receptors is different from the previously described PRRs, which do not rearrange and usually have the same sequence in all cells of an organism. If antigen receptors of a lymphocyte happen to bind an antigen on a bacterium, virus, or parasite, their clustering, or crosslinking, brings into proximity intracellular signaling molecules that contribute to the activation of the lymphocyte. The clonal theory of immunity holds that only those B and T lymphocytes with receptors that have a high enough affinity for antigen will respond by becoming activated and differentiated.

Dynamics of the Adaptive Immune Response

The adaptive immune system is activated when a pathogen overcomes the first line defenses of the innate immune system.

The adaptive immune systems of vertebrates utilize elegantly efficient mechanisms of somatic diversification to generate unlimited repertoires of diverse antigen receptors that are unique and clonally expressed on the surface of B and T lymphocytes. Although, the adaptive immune response is activated in part by innate immune components, once an effective immune response is mounted against a specific antigen, B and T lymphocytes are able to differentiate into memory cells that will recognize the same antigen upon a second exposure. Immunological memory is

the last yet critical and elegant task of the adaptive immune response that allows such high effectiveness against disease, and has contributed to the past developments and future therapeutic designs of vaccines.

The adaptive immune response has at its core B and T lymphocytes, which are generated and mature in the bone marrow and thymus, respectively. During their development, lymphocytes rearrange those portions of their genomes, which code for B cell receptors (BCRs) and T cell receptors (TCRs). Lymphocytes then display on the extracellular surface of their plasma membranes multiple (hundreds to thousands) of identical copies of their BCR or TCR, each cell usually having unique antigen receptor specificity among the pool of millions of lymphocytes. $Ig\mu^+$ $Ig\delta^+$ mature B cells migrate to secondary lymphoid organs, such as the spleen and lymph nodes, where they complete their maturation and are ready to be activated and respond to infection as needed[11, 12]. In this way, there will be a quick amplification of antigen-specific lymphocytes without a change in the number of non-specific lymphocytes. The activation of antigen-specific lymphocytes results in their differentiation to either an effector cell, which in the case of B lymphocytes an antibody-producing plasma cell, or to a memory lymphocyte. The effector and the memory cell have the same antigen specificity towards the initial pathogenic antigen as the lymphocyte that gave rise to them. In the case of B cells, the antigen receptor is further diversified during B cell activation[13]

Upon initial pathogen recognition, innate immune cells such as macrophages or DCs are activated when their PRRs are engaged by PAMPs. Once activated, DCs migrate to secondary lymphoid organs, such as the spleen and lymph nodes, where they process and present peptides

(non-self and self) to T follicular helper (T_{FH}) cells, which regulate the stepwise development of antigen-specific B cell immunity[14]. B cells that contain an antigen receptor (BCR) with affinity for antigen will bind to and internalize pathogenic proteins for processing and display antigen derived peptide fragments as peptide:MHC class II complexes. This allows B cells to be targeted by antigen-specific CD4 T helper cells. In addition, T cells and B cells further contact each other through the membrane receptor pairs CD28:CD80 and ICOS:ICOSL.

Activation of CD4 T helper cells by cognate B cells or DCs leads to upregulation of surface CD40 ligand (also known as CD154) on T cells. Accordingly, CD40, a member of the TNF family of transmembrane receptor is expressed on the surface of B cells[15, 16]. CD154:CD40 engagement activates the CD40 signaling pathway, through which tumor necrosis factor receptor-associated factor (TRAF) adaptors molecules activates transcription factors such as nuclear factor κB (NF-κB) and activator protein 1 (AP-1), leading to vigorous B cell proliferation and differentiation[17]. In addition to membrane protein receptor interactions, several types of interleukin (IL) molecules secreted by both cells greatly influence the nature of the differentiation program for T and B cells. These interactions are known as T-dependent and eventually give rise to effector B cells known as plasma cells, which secrete high affinity antibodies against specific antigens, and also give rise to memory B cells, that can be rapidly activated by the presence of antigen upon re-infection.

The adaptive antibody response unfolds mainly in germinal centers (GC) of spleen and lymph nodes. The maturation of the antibody response, are critical for effective vaccines and the generation of neutralizing antibodies to defend against bacterial and viral infections and tumoral

cells as well as atoptic anaphylaxis, depends on two B lymphocyte differentiation processes: immunoglobulin (Ig) class-switch DNA recombination (CSR) and somatic hypermutation (SHM).

In GCs, the generation of affinity antibodies increases dramatically due to the B cell intrinsic process of SHM[18, 19, 20]. During the GC reaction (**Figure 1.2**), the constant heavy chain of the antibodies changes to acquire new biological effector functions that are more suitable to the clearance of a particular type of infecting pathogen.

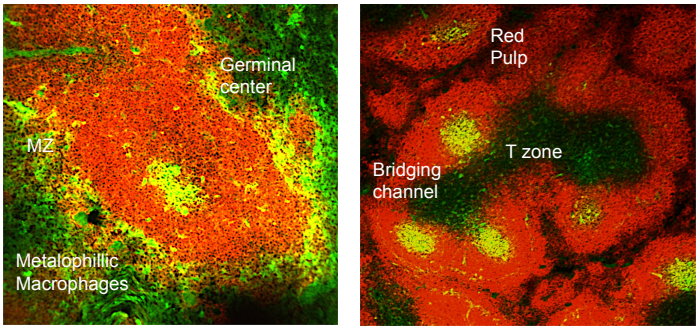

Figure 1.2. Germinal centers. (Left) PNA (green) a marker for GCs, a special microenvironment where $CD19^+$ B cells (red) proliferate, differentiate and mutate their antibody genes. Marginal zone (MZ) B cells, metalophillic macrophages lining between follicles (left) and the T zone (right).

The change in the constant heavy chain (C_H) of antibodies occurs through the process of immunoglobulin (Ig) class-switch DNA recombination (CSR)[21, 22, 23]. Naïve B cells display IgM and IgD surface Igs, and part of the differentiation process entails CSR, i.e., the substitution of the IgM original isotype (or class) with IgG, IgA and IgE antibody isotypes, as will be detailed in section 1.3. SHM and CSR occur primarily in activated GC B cells having threshold affinity (or higher) for antigen. There are two distinct zones in the germinal center: the dark zone, where B cells are in a stage of differentiation known as centroblasts and proliferate vigorously, and the light zone, where centroblasts stop proliferating, and are known as centrocytes. Centrocytes compete for antigen displayed by DCs and T_{FH} and only those centrocytes who's BCRs have the highest affinity for antigen will survive, while the rest undergo apoptosis and are no longer

selected. The selected high affinity centrocytes then can either differentiate to short-lived plasma cells that exists for a few days after infection and produce mostly IgM antibody against the antigen, or re-enter the same GC or adjacent GC to undergo further rounds of proliferation, hypermutation, class-switching, and finally emerge as either long-lived plasma cells or memory cells[24, 25, 26].

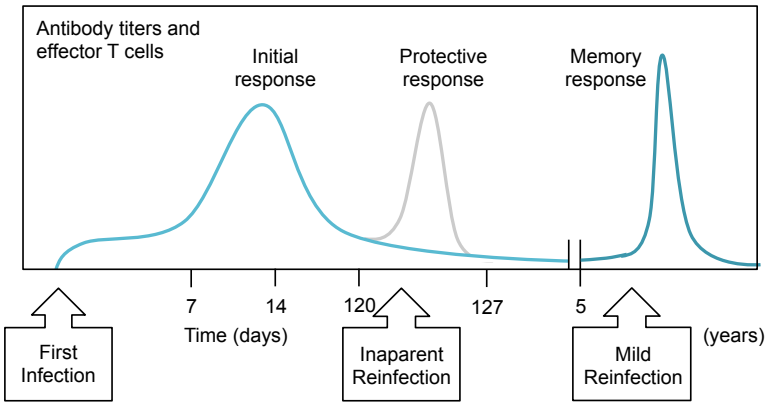

Figure 1.3. Immunological memory. Upon encounter of a particular antigen, antigen-specific B cells produce high-affinity antibodies against foreign antigen. Early reinfection is rapidly and efficiently cleared. Reinfection years afterwards lead to immediate and efficient clearance.

After a primary immune response to a specific pathogen, the adaptive immune response will establish a more rapid and effective immunological memory. Memory responses, also called secondary immune responses, tertiary immune responses, and so forth, differ qualitatively from primary responses. This is particularly clear in antibody response, which is characteristic of antibodies produced by memory B cells in subsequent responses (**Figure 1.3**). Memory T cell responses can be distinguished from the responses of naïve or effector T cells. Memory cells are in a constant resting state and are sustained by long-lived antigen-specific lymphocytes until a second encounter with the same antigen. Upon a subsequent exposure, memory cells will reactivate and proliferate to mount a rapid and efficient response.

1.2 HISTORICAL DISCOVERIES IN INNATE AND ADAPTIVE IMMUNITY

Over the last century there has been tremendous progress in the field of immunology due to the tireless efforts of several outstanding immunologists, many of which were rewarded with the Nobel Prize for their pioneering research. It is of critical importance then, to acknowledge some of the key scientists and their discoveries relating to the roles of components of immune responses, such as cellular and humoral, and innate and adaptive, that are relevant to this dissertation.

Edward Jenner (1749-1823)

Edward Jenner was an English physician and scientist and is often referred to as "the father of immunology" whose research lead to the discovery of vaccination and whose initial work has been the foundation for all other immunologists over the years. Jenner observed that milkmaids who were infected with the non-lethal cowpox virus were immune to subsequent exposure to the often-fatal smallpox. He then hypothesized that the pus in the blisters of milkmaid's hands contributed to their immunity to smallpox. On May 14, 1796 he tested his hypothesis on James Phipps along with other subjects; Jenner had successfully developed a vaccination with cowpox to provide immunity to smallpox.

Louis Pasteur (1822-1895)

Louis Pasteur was a multidimensional scientist, but is perhaps most remembered for his work in organic chemistry, microbiology, and vaccines. Pasteur developed vaccines against chicken cholera and anthrax by using the respective attenuated forms of bacteria. As Pasteur used the

attenuated forms of the pathogens, it would be more promising to experiment with ways of preparing attenuated microorganisms that can be safely used in vaccines. Of most significant is his research also showed the growth of microorganisms was responsible for spoiling beverages. Pasteur developed a process in which liquids, like milk or more importantly, beer, are heated to kill most bacteria – this process is famously termed pasteurization.

Robert Koch (1843-1910)

Robert Koch is best known as the founder of modern bacteriology and for identifying the specific causative agents of tuberculosis, cholera and anthrax. In addition to his contribution to bacteriology, he developed and improved laboratory technologies and techniques in the microbiology field and principles to help link specific microorganisms to a specific disease. Robert Koch received he Nobel Prize in Physiology or Medicine on 1905.

Ilya Mechnikov (English as Elie Metchnikoff, 1845-1915)

Elie Metchnikoff was awarded the Nobel Prize in Medicine in 1908 for his great contributions to cellular immunology, especially his landmark discovery of phagocytosis in immunity. Metchnikoff pioneered research on the immune system when he first described macrophages and phagocytosis in 1882. Skeptics, such as Louis Pasteur, doubted Metchnikoff's theory that specific white blood cells could engulf/phagocytose pathogens, such as bacteria. Metchnikoff focused his research on how the body combated infections by microbial pathogens. He initially studied the interaction of microbes with the immune system of various lower animals, and was the first to discover phagocytosis by phagocytes of larvae of starfish against rose thorns introduced by the researchers, and later, discovered the action of phagocytes of water flees

(Daphnia) against infection by spores from a natural pathogenic fungus. One lesson here is that frequently basic research that appears not to have immediate applications to human health, later turns out to have profound implications and applications for future research and therapeutic treatments. Therefore, lessons from reduced systems (as in the case of simple, transparent marine animals that can be studied by microscopy) can lay the foundation for more advanced research applicable to human health. Metchnikoff was convinced that an effective immune response as a general rule always requires successful phagocytosis, and rejected experimental data published by other researchers who showed that in many cases immunity can be due solely to humoral factors (mainly antibodies) in the absence of significant phagocytosis[27]. It has been suggested that the adaptive immune system may have independently evolved twice, once in a lineage that gave rise to jawless vertebrates and again in the lineage that gave rise to jawed vertebrates[28].

Paul Ehrlich (1854-1915)

One of the most prominent researchers in the separate field of humoral immunity at the time was Paul Ehrlich. Ehrlich started out as a histologist, and was initially interested in selective staining of tissues as well as microbes. He showed that sera from animals, which are immune against a pathogen, can confer protection against the same pathogen when transferred to another animal. He envisioned the production of antibodies as being triggered by the binding of specific pathogens or antigens on receptors of different shapes on the surface of immune cells (now known as B cells), with each unique antigen somehow triggering the production of only the antibodies that have high affinity for the given antigen. Around the middle of the 20th century, advancements in several fields of biology, including immunology, which itself made possible the

advancement of other fields of biology by the applications of antibodies as tools for the identification and isolation of biomolecules, and for activating or inhibiting their interactions with other biomolecules. Nils Jerne had proposed the antigen-dependent stimulation of amplification of pre-existing antibodies, and later, Macfarlane Burnet proposed the clonal selection hypothesis[29, 30] where each lymphocyte displays identical antibodies of a single specificity on its surface, each lymphocyte expressing different and unique antibodies, and only those that are triggered by antigen expand, as was described in more detail earlier in this section. Looking back, the tremendous progress and precocious vision of Paul Ehrlich cannot be emphasized enough. His partly incorrect hypothesis of different antibody receptors of multiple specificities residing on the same cell[27] was corrected by Burnet's modification and extension of Jerne's hypotheses, by postulating that each B cell express only one type of antibody on its surface, with a virtually unlimited pre-existing repertoire residing in the total population of millions of B cells, each with unique antigen receptors of a single sequence and specificity. However, in its larger aspects, Ehrlich's hypothesis and his work not only stood the test of time, but also formed the basis for subsequent research in antibodies.

Karl Landsteiner (1868-1943) and Merrill Chase (1905-2004)

Karl Landsteiner is best known for his work on distinguishing the main blood groups and helped establish successful blood transfusion. Merrill Chase is credited for discovering that white blood cells and not just antibodies alone are critical components of the immune response. Together, Karl Landsteiner and Merrill Chase showed that antibodies could be generated to virtually any synthetic chemical compound, provided it was conjugated to a protein, and the animal was also immunized with killed-bacteria[31]. These observations were crucially important in three distinct

ways. First, it showed that the antibody specificities were pre-existing and not simply induced by natural pathogens, since chemical compounds not known to occur naturally could generate antibodies. Second, the need for a protein carrier was later found to be due to the difficulty of antibodies binding molecules below a minimal size (known as haptens), as well as provide T cell help via the TCR on T cells interacting with MHCII on B cells bridged by antigenic peptide-hapten conjugate, as was described earlier. Third, and perhaps more perplexing was the need for killed-bacteria to potentiate the response to haptenated protein. The need for killed-bacteria as potentiators, or adjuvants, of antibody responses to haptenated proteins then prompted the development of empirically derived adjuvants such as Freund's complete adjuvant, Freund's incomplete adjuvant, and Ribbi's adjuvant. In our own research, we commonly use NP-CGG (nitrophenol-chicken gamma globulin) to immunize mice and induce a strong NP-specific response. In addition to containing oils for forming adjuvant depots upon injection, these adjuvants also contain mycoplasma lysates (which contain various TLR ligands) in order to elicit robust immune responses to soluble protein antigens. This fact was referred to by the famous Charles Janeway as the immunologists' "dirty little secret"[32].

Charles Janeway (1943-2003) and Ruslan Medzhitov

Finally, these stunning developments were followed in 1997 by the seminal discovery by Charles Janeway and Ruslan Medzhitov of a human Toll-like receptor 4 (TLR4), homologous to the *Drosophila* Toll, which signaled to NF-κB, and resulted in the upregulation of B7 (marker for activated APC) family proteins and production of cytokines, which were known to initiate the activation of adaptive immune responses. It was found that Toll contained a cytoplasmic domain which was homologous to IL1R (which also signals to NF-κB) and to a protein important in

plants for resistance against tobacco mosaic virus (N protein)[33]; hence the domain fold was named TIR after Toll/IL1R/Resistance[34]. This was then followed in 1998 by the identification, via positional cloning of the *lps* locus in C3/HEJ strain of LPS-unresponsive mice, of this mammalian Toll receptor as TLR4[35]. Over the next few years, the details of the signaling pathways of TLRs were uncovered[36, 37, 38, 39, 40], all the way to recent connections between innate and adaptive immune modules between different immune cells, or in the same cell as is particularly prominent in B lymphocytes[41, 42, 43, 44].

1.3 TARGETING AND INDUCTION FOR ANTIBODY CLASS-SWITCHING

Our laboratory has extensively studied the mechanisms that modulate the antibody response.

We have made two important discoveries focused on the targeting of CSR: (i) 5'-AGCT-3' repeats are characteristic S region motifs highly conserved across unrelated species[23, 45]; and (ii) **14-3-3 adaptors**, a family of seven (β, ε, γ, η, σ, τ and ζ) highly homologous proteins, specifically target 5'-AGCT-3' repeats and mediate CSR by directly interacting with activation-induced cytidine deaminase (AID) and PKA catalytic subunit (PKA-Cα), and recruiting/stabilizing them to/on S regions[46]. We have also made three recent and compelling discoveries on the induction of CSR: (i) B cell Rab7 is critical for T-dependent and T-independent antibody responses; (ii) and CSR of $Igh^{+/C}\gamma^{1\text{-}cre}$ $Rab7^{fl/fl}$ B cells (in these mice, the Cre recombinase is expressed only in B cells activated to undergo IgH germline Iγ1-Sγ1-Cγ1 transcription, as induced by IL-4[47] – IL-4 specifies CSR to IgG1 and IgE, but not to other IgG isotypes or IgA) *in vitro*; (iii) Rab7 is upregulated in lupus B cells and treatment using a Rab7-inhibitor on autoimmune mice prevents the development of lupus immunopathology.

The significance of the studies described here derives primarily from an in-depth understanding of the mechanisms underpinning the generation of effective anti-microbial antibodies and pathogenic autoantibodies. Our studies are also important to unveil mechanisms of immunoglobulin gene expression. Finally, by devising tools and reagents to inhibit CSR, our research will have a significant impact on the development of therapeutics that block unwanted CSR, e.g., CSR to IgG autoantibodies or atopic IgE.

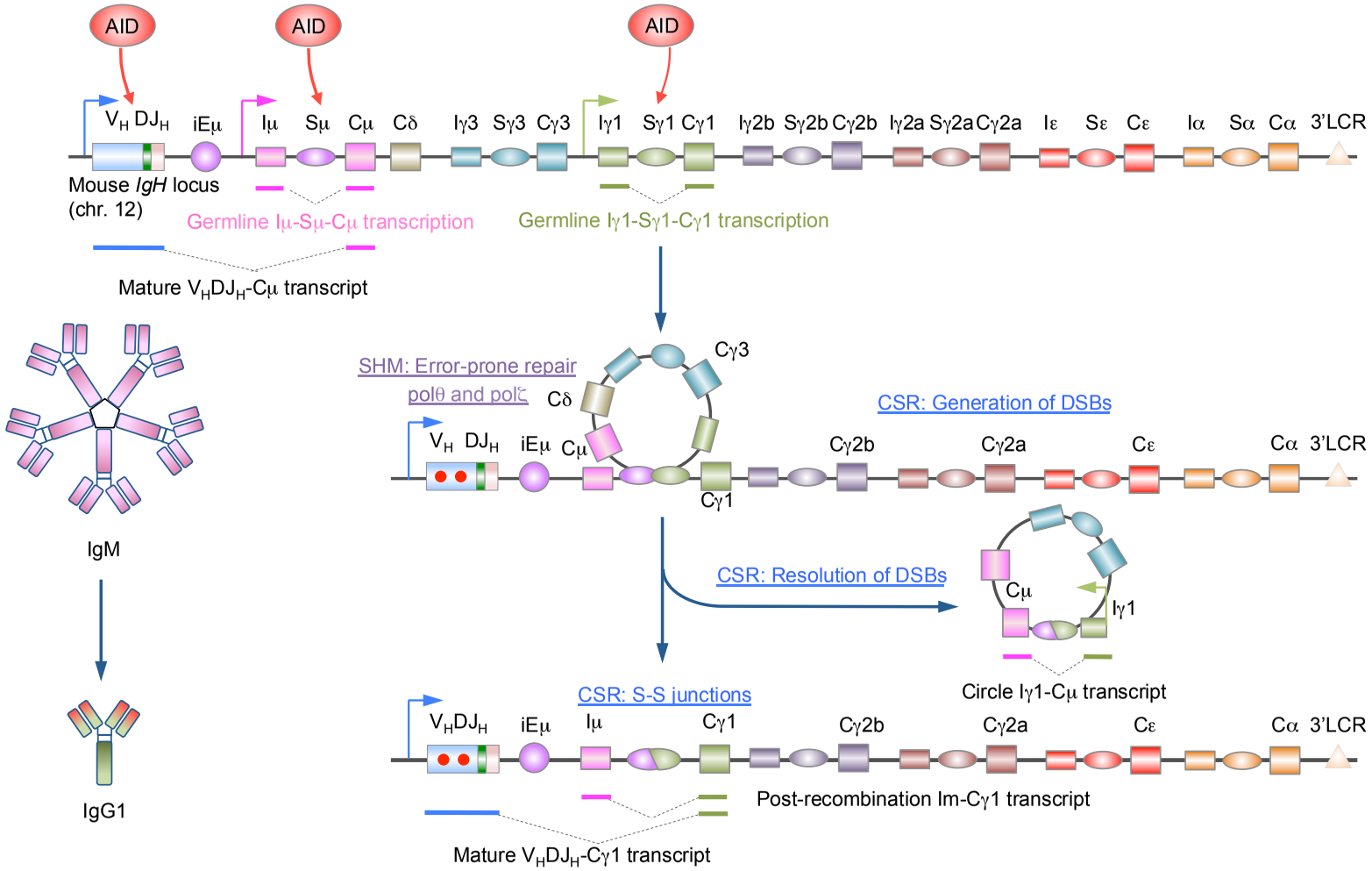

Figure 1.4. Schematic depiction of AID-mediated CSR and SHM in antibody diversification. Class-switch DNA recombination (CSR) exchanges the gene encoding the immunoglobulin heavy chain constant region (C_H) with one of a set of downstream CH genes (the figure depicts CSR between Sμ and Sγ1 in the human immunoglobulin heavy chain (IgH) locus). This deletion–recombination reaction requires activation-induced cytidine deaminase (AID) and involves the generation of DNA double-strand breaks (DSBs) in switch (S) regions (which lie upstream of the C_H gene) followed by DSB repair. This leads to the juxtaposition of rearranged V_HDJ_H DNA (which encodes the heavy chain variable region) with a downstream CH exon cluster and deletion of the intervening sequence between S regions as an extrachromosomal circle. Modified from Xu et al., 2012.

CSR and generation of neutralizing antibodies

CSR is central to the generation of antibodies capable of clearing microbial pathogens or killing tumoral cells as well as the antibodies that underlie the efficacy of vaccines (**Figure 1.4**). Such antibodies are mutated for a better fit (high-affinity) for antigen and class-switched, mostly to IgG and IgA. IgG readily pass into extravascular spaces, where they eradicate bacteria and viruses, and IgA are abundant on digestive and respiratory mucosae, where they effectively oppose microbial pathogens. The first antibodies to be produced against a foreign-antigen initially are IgM, which contain the pathogen in the first hours to days of infection.

CSR impairment leads to hyper-IgM syndrome, as characterized by low/undetectable IgG, IgA and IgE levels and susceptibility to infections. As shown by us[48, 49, 50] and others[22, 51], like anti-microbial antibodies, pathogenic autoantibodies in systemic autoimmune diseases, such as systemic lupus erythematosus, or organ-specific autoimmunity, such as thyroiditis or type I diabetes mellitus, are also class-switched, mostly to IgG. Antibodies mediating allergic reactions, such as asthma or anaphylaxis, are switched to IgE.

Targeting of CSR: Scaffold functions of 14-3-3 adaptors

14-3-3 proteins derive their unique name from the number of fractions that were purified during liquid chromatography of brain lysates conducted in the 1960s [52]. These proteins are widely conserved and found as different isoforms from plants to animals. Their roles are revealed by their structures: they are concave shaped proteins of bundles of alpha helices. They form homo and heterodimers, and are uniquely structured to either sequester other proteins or bring two identical or different partners together. The several phosphorylation substrates in 14-3-3 make

them amenable to regulation in response to extracellular or intracellular signals[53]. The unique structures that 14-3-3 proteins form has allowed them to play a variety of diverse functions in the cell, mainly as scaffolds and adapters in cellular signaling, as well as cruciform DNA binding proteins involved in the initiation of DNA replication.

14-3-3 adaptor proteins (seven homologous isoforms, 14-3-3β, 14-3-3ε, 14-3-3γ, 14-3-3η, 14-3-3σ, 14-3-3τ and 14-3-3ζ)[54] specifically bind to 5'-AGCT-3' repeats, but are selectively recruited to the upstream and downstream switch (frequently abbreviated S in diagrams) regions that are set to undergo S–S DNA recombination by the H3K9acS10ph combinatorial histone modification[23, 55]. AID deaminates efficiently at dC nucleotides in the WRCY motif [56, 57] (where, W = A or T, R = purine, and Y = pyrimidine) found in S regions before each constant heavy chain. Because of the potentially catastrophic consequences if its mutator activity were uncontrolled, AID is expressed only transiently in B cells undergoing CSR and SHM, and must be downregulated thereafter.

In addition to 14-3-3 adaptors, which are bona fide scaffolding proteins, CSR enzymatic elements, such as AID, PKA, and Ung, may possess non-enzymatic scaffolding functions for their recruitment/stabilization to/on the recombining S regions. Our proposed studies to outline these scaffolding functions are very novel and will likely provide important information on the assembly of DNA/multi-protein macromolecular complexes on S regions. Here, we hypothesized that 14-3-3 nucleate the assembly of CSR factors by binding 5'-AGCT-3' repeats; and function as structural scaffolds to stabilize multiple enzymatic elements through many DNA-protein and homotypic/heterotypic protein-protein interactions (14-3-3[58, 59], AID[60] and PKA are

all dimers/multimers); and, as strongly suggested by our findings that 14-3-3 enhance AID DNA deamination activity[50], enzymatic activities of AID, PKA and/or Ung are enhanced by scaffolding proteins in DNA/protein complexes. The results of our findings will be discussed in Chapter 2.

CSR inhibition: Naturally occurring Vpr and synthetic small molecules to inhibit targeting of CSR

The level of innovation of our work is further heightened by the experiments addressing how interactions/scaffolding functions of 14-3-3[61], AID, PKA[62] and/or Ung[63] can be subverted by Vpr. Vpr, which is present in circulation[64] in HIV-1$^+$ individuals, can be "picked-up" by immune cells, including B cells[65]. Here we hypothesized that naturally occurring or synthetic molecules can interfere with scaffolding functions of 14-3-3, AID, PKA and/or Ung and can therefore, inhibit CSR. Analysis of how Vpr interfere with the CSR machinery would help to understand the mechanisms of CSR and potentially lead to development of therapeutics that inhibit unwanted CSR, e.g., to IgG in autoimmunity and IgE in atopy. The results of our findings will be discussed in Chapter 2. Here we also hypothesized that small molecules could inhibit the induction of AID expression in autoimmune lupus mice and therefore, generation of autoantibodies and lupus immunopathology. The results of our findings will be discussed in Chapter 4.

Induction of CSR/SHM: B cell Rab7-dependent induction of AID

The induction of AID must be greatly expressed for efficient CSR. CSR requires both primary and secondary stimuli (**Figure 1.5 and Table 1.3**). Primary CSR-inducing stimuli, whether T cell dependent or T cell independent, induce AID expression (encoded by *AICDA* in humans and

Aicda in mice) depends on NF-κB, and other CSR proteins. Secondary CSR-inducing stimuli cannot induce the expression of AID but are required for directing class-switching to IgG, IgA or IgE. These secondary stimuli include interleukin-4 (IL-4), transforming growth factor-β (TGFβ) or interferon-γ (IFNγ; in mice but not humans).

Transcription of the AID gene depends on NK-κB, which is activated in B cells mainly by engagement of: CD40L on the surface of T cells with CD40, agonists with TLRs, and B cell-activating factor with TACI, but not BCR alone, induces the recruitment of the (non-canonical) NF-κB p52 subunit to the AID gene promoter and the (canonical) p65 subunit to an upstream enhancer element for AID expression.

Table 1.3. Cytokines direct CSR to specific isotypes.

Stimulus	IgM	IgG1/IgE	IgG2a	IgG2b	IgG3	IgA
IL-4		+	–	–	–	+
IL-5						+
IL-10					+	–
IL-13		+				
IFNγ	–	–	+	–	+	
TGFβ	–			+		+
BCR	+	+	+	+	+	+

"+" denotes promotion, and "-" denotes inhibition of CSR. Empty spaces denote that there is no conclusive information available.

IL-4 induces STAT6 the Iγ1 and Iε upstream promoters to initiate germline Iγ1-Sγ1-Cγ1 and Iε-Sε-Cε transcription and therefore, CSR to IgG1 and IgE respectively. TGF-β induces RUNX expression which directs CSR to IgA, and IFN-γ induces STAT1/2 expression which directs CSR to IgG2a.

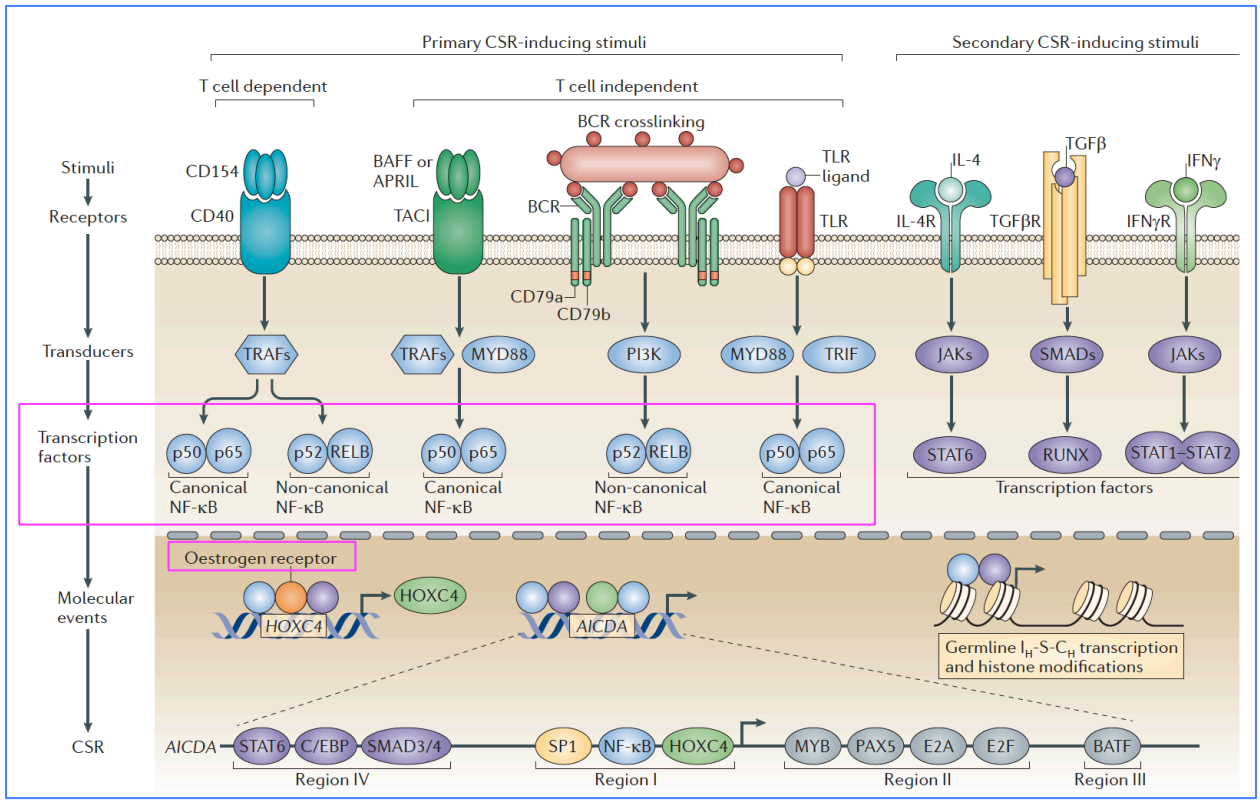

Figure 1.5. CSR induction entails multiple levels of regulation. During class-switch DNA recombination (CSR), primary CSR-inducing, such as T cell-dependent (namely, CD40 signals) or T cell-independent (namely, dual Toll-like receptor (TLR)–B cell receptor (BCR), TACI–BCR or TLR–TACI engagement) activates nuclear factor κB (NF-κB). This transcription factor induces HOCX4 expression (which is enhanced by estrogen), and both NF-κB and HoxC4 induce the expression of AID. The ability of primary CSR-inducing stimuli to induce AID expression and CSR correlates with their activation of either the canonical or non-canonical (or both, e.g., CD40) NF-κB pathways. Secondary CSR-inducing stimuli, namely, interleukin-4 (IL-4), transforming growth factor-β (TGF-β) and interferon-γ (IFN-γ) activate transcription factors that bind to immunoglobulin heavy chain intervening region (I_H) promoters to initiate germline I_H-S_H-C_H transcription, thereby specifying the S regions that are to undergo S–S DNA recombination. Adopted from Xu et al., 2012[23].

In addition to NF-κB, HoxC4, a homeodomain transcription factor that is highly expressed by B cells and is induced by the same stimuli that induce AID and CSR. HoxC4 is upregulated by oestrogen. Together, HoxC4 and NF-κB bind to the region I promoter of AID, thereby

potentiating AID expression. IL-4 induces STAT6 expression; STAT6 will bind to the region IV locus of the AID gene to help induce AID expression.

Germline I_H-S-C_H transcription is initiated by specific I_H promoters in a manner generally dependent on cytokine-activated transcription factors. IL-4 activates STAT6, which binds to the Iγ1 and Iε promoters to initiate germline transcription that proceeds through Sγ1 and Sε, thereby enabling class-switching to IgG1 and IgE, respectively. TGFβ activates SMAD3, SMAD4 and/or RUNX proteins to promote transcription proceeding through Sγ2b and Sα for class-switching to IgG2b and IgA, respectively. Finally, IFNγ activates T-bet, STAT1 and/or STAT2 for the initiation of germline transcription that proceeds through Sγ2a for class-switching to IgG2a. Competition between different IH promoters for the transcription machinery enhances isotype selection. For example, Ikaros mediates suppression of germline Iγ2a-Sγ2a-Cγ2a and Iγ2b-Sγ2b-Cγ2b transcription, thereby downregulating class-switching to IgG2a and IgG2b, and promotes class-switching to IgG3 and IgG1.

Thus, whereas primary CSR-inducing stimuli activate transcription factors that regulate the transcription of the AID gene and various other genes, secondary stimuli activate transcription factors that bind to different I_H promoters to initiate germline I_H-S-C_H transcription, thereby specifying the acceptor S regions that are to undergo CSR. Full induction of germline I_H-S-C_H transcription requires the interplay of both sets of transcription factors.

1.4 COMMON IMMUNOLOGICAL METHODS TO STUDY ANTIBODY CLASS-SWITCHING

Antibody class-switching has been intensively studied for the last several decades, and empirical observations about the induction of CSR both *in vivo* and *in vitro* are extensive. Th1 and Th2 CD4 T cells make contact with B cells through the interaction of CD154:CD40 surface receptor pair, which provides a general activation stimulus. The specificity in inducing CSR to a particular isotype is generally considered to be due to the soluble cytokines that Th1 and Th2 cells secrete, which bind to and stimulate their appropriate receptors on B cells to induce transcription factors that bind to I promoters and stimulate GLT, eventually resulting in CSR to Th1 or Th2 antibody classes. CSR has been measured by several methods that detect either DNA recombination, generation of post-recombination Iμ-C_H and circle I_H-Cμ transcripts, expression of membrane Ig, and finally, the secreted antibody levels[66].

Post-recombination Iμ-C_H and circle I_H-Cμ transcript analysis

The protocol for analyzing CSR-related RNA transcripts employs qRT-PCR to make a cDNA library from B cells activated with various stimuli. Primers for specific regions can be used to detect germline I_H-C_H transcripts from the original IgM (Iμ-Cμ), the germline transcripts of other isotypes (e.g. Iγ1-Cγ1), and finally or PSTs, e.g. Iμ-Cγ1[67, 68] (**Figure 1.6**). While GLT may function to open up DNA and thus make it more accessible to AID and other CSR factors, PST levels have been found to be a better predictor of CSR than GLT levels in that the higher the PST levels, the more antibodies will be translated from their mature, spliced forms. There is no established quantitative relationship between GLT and CSR, whereas there is a generally linear relationship between the levels of PSTs and CSR.

Flow cytometry analysis

Flow cytometry is an advanced biophysical technology that utilizes cell surface biomarkers that can be bound by fluorophore-conjugated antibodies. Cells bearing fluorophore-conjugated antibodies are suspended in a fluid stream and passed through a laser to be acquired (data recorded) based on the light scattering and fluorescent characteristics of each cell. Measurement of the levels of class-switched BCRs expressed on the B cell surface is used to reliably identify the class-switched B cells (**Figure 1.6**). This is accomplished by employing flow cytometry to detect the different isotypes by means of isotype-specific antibodies that target the Fc regions. In our flow cytometry experiments, each antibody is carefully titrated so that the optimal concentration is used. An excessive antibody will result in a high background (i.e. in an increase in false positives) as well as false MFI values, which can complicate the analysis of the data as spectral compensation will overestimate the bleeding of that fluorescence in the other channels. Thus, our flow cytometry protocol provides an accurate and reproducible measure of the distribution of surface antibody isotypes and other proteins on B cells.

Enzyme-linked immunosorbent assay (ELISA)

Indirect and sandwich ELISA are used to measure antigen-specific and total antibody titers, respectively, of the various classes secreted from cultures stimulated *in vitro*, or in the serum of immunized mice (**Figure 1.6**). However, as our ELISA assays measure both total antibody titers and antigen-specific antibody titers, the influence of plasmacytoid differentiation which includes the extensive golgi and ER secretory network, cell proliferation, and cell death, are intrinsically linked in determining overall antibody titers, and these factors must be taken into account when using ELISA data to evaluate CSR.

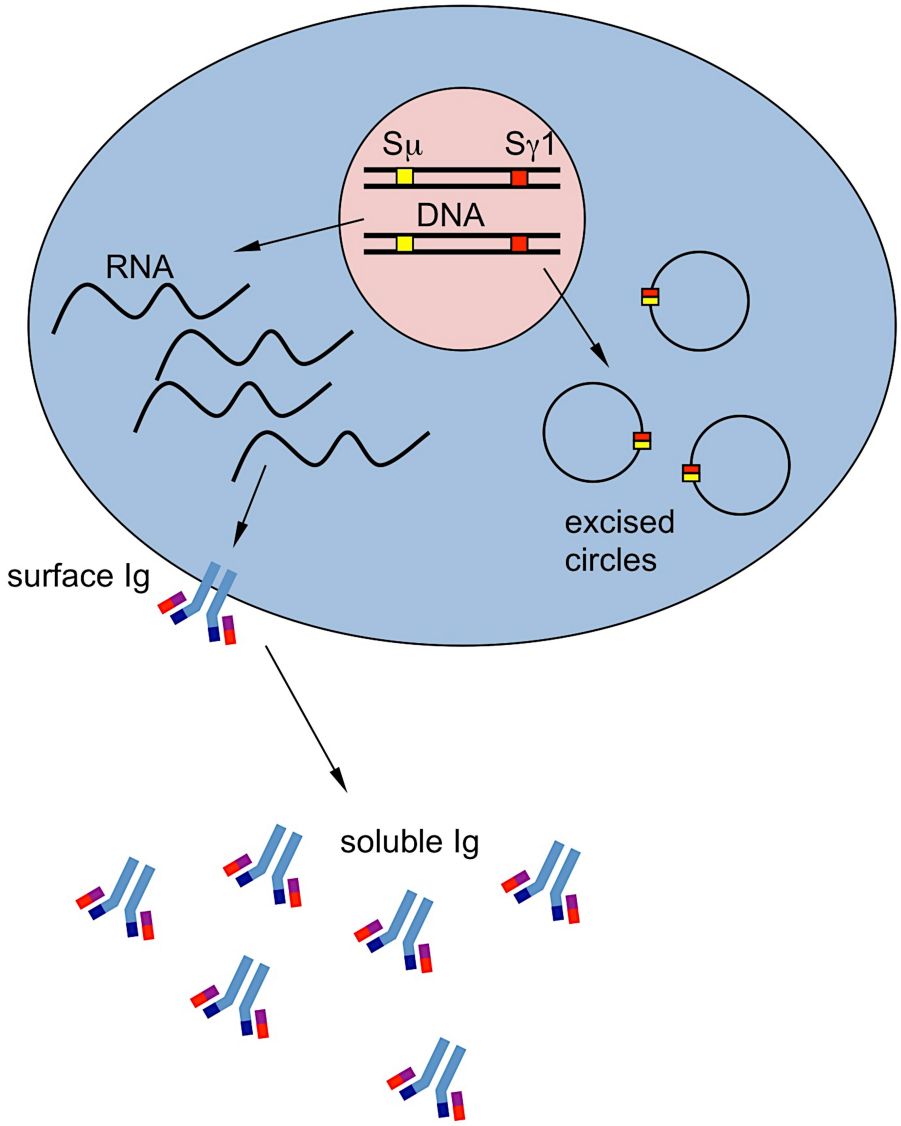

Figure 1.6. Experimental methods for analyzing CSR. Upon completion of CSR in the chromosome, circle transcripts (used to analyze ongoing CSR by qRT-PCR) are excised and the post-recombined IgH region serves as a template for transcription of mRNAs (used to analyze completed CSR by qRT-PCR), which are then spliced and used to translate them to the membrane-bound form of Ig (used to analyze class-switched B cells by flow cytometry). As an activated B cell further differentiates to a plasma cell, alternative splicing of Ig transcripts results in the production of soluble antibodies (used to analyze secreted/soluble antibodies by ELISA). CSR can be detected and quantitatively measured at any of these stages, but was most extensively measured at the surface Ig level in our work.

1.5 PLASMA CELLS, MEMORY B CELLS AND GENERAL PROPERTIES OF ANTIBODIES

When B cells recognize pathogenic antigens via their BCRs, and after they receive the other previously described signals from DCs and T_H cells, they become activated and ultimately secrete antibodies targeting the pathogen. The secreted antibody molecules are identical to the BCR except that they lack the membrane spanning tail of the heavy chains of the BCR critical for anchoring to the plasma membrane on B cells (**Figure 1.7**). Antibodies are chimeric proteins composed of a variable region, important for the specific antigen binding site, and a constant region, which confers the specialized effector functions that determine the mode of clearing of the pathogen[69] (**Table 1.4**).

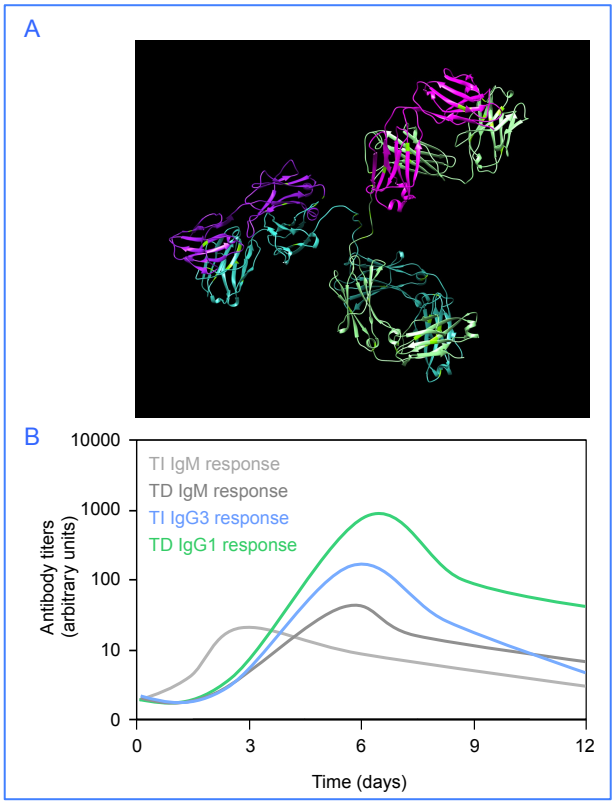

Figure 1.7. Features of an antibody. (**A**) The antibody is composed of two identical heavy chains and two identical light chains. Each heavy chains is about 50 kDa and contains one variable region (V_H) which binds antigen, and several constant regions (C_H) unique of each class or isotype, conferring immune effector specificity (1IGT). Each light chain is 25 kDa and contains one variable region (V_L) that also contributes to antigen binding, and one constant region (C_L). (**B**) Kinetics of T-independent and T-dependent primary antibody responses. The fastest response is the production of IgM from B cells that were stimulated by BCR crosslinking triggered by pathogens. Some IgG3 is also made early on, likely due to TLR-initiated CSR. The appearance of the other isotypes typically takes longer and requires T cell help in the form of receptor-coreceptor interactions and stimulation via cytokines.

An antibody is composed of two identical heavy chains and two identical light chains. Each heavy chain is 50 kDa and contains one variable region (V_H), and one constant region (C_H) (**Figure 1.7**). The constant region has 3-4 domains, called C_H1, C_H2, C_H3, C_H4. Of these, C_H1 is the constant region of the fragment antigen binding (Fab) of the antibody, which contains the variable V_H and V_L domains, and the last 2-3 C_H form the constant fragment (Fc) of the antibody. The Fab varies with each antibody due to the generated diversity prior to, and during, B cell activation. Unlike the Fab, the Fc is constant for antibodies of the same class, which in the mouse are IgM/IgD, IgG1, IgG2a, IgG2b, IgG3, IgE, IgA. Each Fc interacts with its specific Fc receptor (FcR) on cells such NK, macrophages, DCs, eosinophils and basophils, and therefore directs the appropriate effector mechanisms to clear the pathogen that the antigen-specific Fab parts have bound. For example, IgE Fc interacts with its high-affinity FcRs on eosinophils and basophils, leading to their degranulation to kill the parasite that IgE has bound. IgM and IgG2a/b antibodies have Fc that bind C1q and activate complement. IgG2a and IgG2b antibodies are appropriate for clearing viral infections, and are induced respectively by IFNγ and TGFβ. IgM and IgG3 are effective at activating complement and are secreted upon B cell activation by TLR ligands such as LPS[57, 69, 70].

The large size of the pentameric IgM limits its distribution mainly to blood and prevents it from moving efficiently across epithelia and binding pathogen systemically. However, the monomeric IgG3 is distributed systemically, and therefore class-switching from IgM to IgG3 upon recognition of LPS and the ensuing activation and differentiation response are advantageous during a bacterial infection. IgM compensates in part for being a large pentameric structure by having a total of ten identical Fab arms, and therefore a higher avidity than a monomer (two

arms) due to the gain in local entropy when antigen binding has been initiated in one of the ten arms[71].

Table 1.4. Distinct features of different antibody isotypes in the mouse.

Feature	IgM	IgG1	IgG2a	IgG2b	IgG3	IgA	IgE
Neutralization	+	++	++	++	++	++	–
Opsonization	+	+	+++	++	NA	+	–
NK cell sensitization	–	–	++	++	–	–	–
Mast cell sensitization	–	–	+	+	–	–	+++
Complement activation	+++	–	++	+++	+	+	–
Transport across epithelium	+	–	–	–	–	+++	–
Transport across placenta	–	+/–	+++	++	+	–	–
Extravascular diffusion	+/–	+++	+++	+++	+++	++	+

There are five main antibody isotypes or classes with subclasses in the mouse, and they play distinct functions and are selectively distributed throughout the body. IgM antibodies (which mainly exists a pentamer) predominate in the blood serum and heart and functions to activate the complement system in the early stages of the B cell response (before there is sufficient IgG). IgD and IgG antibodies predominate in the extracellular fluid or blood serum, IgD mainly functions as an antigen receptor on B cells (mature Igδ Igμ double positive B cells) that have not been exposed to antigens; IgG antibodies mainly function to neutralize and opsonize pathogens. IgA antibodies predominate in the mucosa (linings of mostly endodermal origin, covered in epithelium, which are involved in absorption and secretion) and functions to neutralize pathogens. IgE antibodies predominate beneath epithelia surfaces (such as the respiratory and gastrointestinal tract and skin) and functions to sensitize mast cells to induce a type 1 hypersensitivity response (allergic reaction).

In fact, all antibody isotypes other than IgM diffuse efficiently to extravascular sites and therefore their generation is critical during an infection. Whether due to intrinsic or extrinsic causes, if a B cell fails to undergo class-switching of the constant chain from IgM to one of the other isotypes, the organism cannot mount an efficient antibody response during an infection, such as occurs in the HIGM syndrome in humans[72, 73, 74, 75]. These individuals are highly susceptible to infection and require injections of IgG fractions from pooled sera from many healthy donors.

1.6 ABERRANT IMMUNE RESPONSE: GENERATION OF AUTOANTIBODIES

AID, is a potent DNA mutator and must be tightly regulated in order to prevent off-target effects, which may lead to mutations in non-Ig genes, genomic instability and autoimmune diseases. Accordingly, AID is expressed in B cells and in a differentiation stage-specific fashion. AID is tightly regulated, at several levels, including transcription, post-transcription, and targeting and enzymatic activity[76].

Primary inducing stimuli induce not only AID expression, but also expression or activation of upstream factors that mediate *Aicda* induction, including Rab7 and NF-κB[47]. In addition, there must be highly ordered recruitment of AID to the *IgH* S region, where CSR replaces the C_H thereby giving rise to class-switched IgG, IgA and IgE antibodies, these class-switched antibodies can potentially be pathogenic such as those of anti-dsDNA IgG and IgA, and IgA nephropathy. Self-reactive B cells are usually anergized or deleted during development[77, 78, 79]. The failure of a B cell to have self-tolerance leads to self-reactive B cell clones that is further compounded by T cell dependent autoantibody responses. This leads to the generation of pathogenic anti-dsDNA IgG and IgA that triggers fulminant autoimmune disease, as seen in systemic lupus erythematosus[80].

My dissertation work has been focused on (**i**) disrupting the targeting of AID, by 14-3-3, to *IgH* S regions by using a naturally occurring small protein/peptides (viral protein R) to blunt antibody responses; and (**ii**) inhibiting the induction of AID, using a small molecule, Rab7 inhibitor (CID 1067700) to blunt autoantibody responses that lead to the generation of pathogenic anti-dsDNA IgGs in lupus-prone mice.

1.7 REFERENCES

1. Medzhitov R. Toll-like receptors and innate immunity. *Nature reviews Immunology* 2001, **1**(2)**:** 135-145.

2. Janeway CA, Jr. Approaching the asymptote? Evolution and revolution in immunology. *Cold Spring Harbor symposia on quantitative biology* 1989, **54 Pt 1:** 1-13.

3. Janeway CA, Jr. The immune system evolved to discriminate infectious nonself from noninfectious self. *Immunology today* 1992, **13**(1)**:** 11-16.

4. Pasare C, Medzhitov R. Toll-like receptors: linking innate and adaptive immunity. *Advances in experimental medicine and biology* 2005, **560:** 11-18.

5. Peng SL. Signaling in B cells via Toll-like receptors. *Current opinion in immunology* 2005, **17**(3)**:** 230-236.

6. Lanzavecchia A, Sallusto F. Toll-like receptors and innate immunity in B-cell activation and antibody responses. *Current opinion in immunology* 2007, **19**(3)**:** 268-274.

7. Pone EJ, Zhang J, Mai T, White CA, Li G, Sakakura JK*, et al.* BCR-signalling synergizes with TLR-signalling for induction of AID and immunoglobulin class-switching through the non-canonical NF-kappaB pathway. *Nature communications* 2012, **3:** 767.

8. Lee MS, Kim YJ. Signaling pathways downstream of pattern-recognition receptors and their cross talk. *Annual review of biochemistry* 2007, **76:** 447-480.

9. Miyake K. Innate immune sensing of pathogens and danger signals by cell surface Toll-like receptors. *Seminars in immunology* 2007, **19**(1)**:** 3-10.

10. West AP, Koblansky AA, Ghosh S. Recognition and signaling by toll-like receptors. *Annual review of cell and developmental biology* 2006, **22:** 409-437.

11. Janeway CA, Jr., Medzhitov R. Innate immune recognition. *Annual review of immunology* 2002, **20:** 197-216.

12. Medzhitov R, Janeway CA, Jr. Innate immune recognition and control of adaptive immune responses. *Seminars in immunology* 1998, **10**(5)**:** 351-353.

13. Murphy K, Travers P, Walport M, Janeway C. *Janeway's immunobiology*, 8th edn. Garland Science: New York, 2012.

14. Fazilleau N, Mark L, McHeyzer-Williams LJ, McHeyzer-Williams MG. Follicular helper T cells: lineage and location. *Immunity* 2009, **30**(3)**:** 324-335.

15. Kawabe T, Naka T, Yoshida K, Tanaka T, Fujiwara H, Suematsu S*, et al.* The immune responses in CD40-deficient mice: impaired immunoglobulin class switching and germinal center formation. *Immunity* 1994, **1**(3)**:** 167-178.

16. Renshaw BR, Fanslow WC, 3rd, Armitage RJ, Campbell KA, Liggitt D, Wright B*, et al.* Humoral immune responses in CD40 ligand-deficient mice. *The Journal of experimental medicine* 1994, **180**(5)**:** 1889-1900.

17. Elgueta R, Benson MJ, de Vries VC, Wasiuk A, Guo Y, Noelle RJ. Molecular mechanism and function of CD40/CD40L engagement in the immune system. *Immunological reviews* 2009, **229**(1)**:** 152-172.

18. Muramatsu M, Kinoshita K, Fagarasan S, Yamada S, Shinkai Y, Honjo T. Class switch recombination and hypermutation require activation-induced cytidine deaminase (AID), a potential RNA editing enzyme. *Cell* 2000, **102**(5)**:** 553-563.

19. Casali P, Pal Z, Xu Z, Zan H. DNA repair in antibody somatic hypermutation. *Trends in immunology* 2006, **27**(7)**:** 313-321.

20. Peled JU, Kuang FL, Iglesias-Ussel MD, Roa S, Kalis SL, Goodman MF*, et al.* The biochemistry of somatic hypermutation. *Annual review of immunology* 2008, **26:** 481-511.

21. Stavnezer J. Molecular processes that regulate class switching. *Current topics in microbiology and immunology* 2000, **245**(2)**:** 127-168.

22. Honjo T, Kinoshita K, Muramatsu M. Molecular mechanism of class switch recombination: linkage with somatic hypermutation. *Annual review of immunology* 2002, **20:** 165-196.

23. Xu Z, Zan H, Pone EJ, Mai T, Casali P. Immunoglobulin class-switch DNA recombination: induction, targeting and beyond. *Nature reviews Immunology* 2012, **12**(7)**:** 517-531.

24. Honjo T. A memoir of AID, which engraves antibody memory on DNA. *Nature Immunol* 2008, **9:** 335-337.

25. McHeyzer-Williams LJ, Pelletier N, Mark L, Fazilleau N, McHeyzer-Williams MG. Follicular helper T cells as cognate regulators of B cell immunity. *Current opinion in immunology* 2009, **21**(3)**:** 266-273.

26. McHeyzer-Williams M, Okitsu S, Wang N, McHeyzer-Williams L. Molecular programming of B cell memory. *Nature Rev Immunol* 2012, **12:** 24-34.

27. Roit I. *Essetial Immunology*. Blackwell Sci. Pub.: Oxford, 1994.

28. Boehm T. Design principles of adaptive immune systems. *Nature reviews Immunology* 2011, **11**(5)**:** 307-317.

29. Burnet FM. A modification of Jerne's theory of antibody production using the concept of clonal selection. *Aust J Sci* 1957, **20:** 67-69.

30. Hodgkin PD, Heath WR, Baxter AG. The clonal selection theory: 50 years since the revolution. *Nat Immunol* 2007, **8**(10)**:** 1019-1026.

31. Landsteiner K, Chase MW. Studies on the sensitization of animals with simple chemical compounds. *J Exp Med* 1941, **73:** 431-438.

32. Janeway CA, Jr. Approaching the asymptote? Evolution and revolution in immunology. *Cold Spring Harb Symp Quant Biol* 1989, **54 Pt 1:** 1-13.

33. Whitham S, Dinesh-Kumar SP, Choi D, Hehl R, Corr C, Baker B. The product of the tobacco mosaic virus resistance gene N: similarity to toll and the interleukin-1 receptor. *Cell* 1994, **78**(6)**:** 1101-1115.

34. Medzhitov R. Approaching the asymptote: 20 years later. *Immunity* 2009, **30**(6)**:** 766-775.

35. Poltorak A, He X, Smirnova I, Liu MY, Van Huffel C, Du X*, et al.* Defective LPS signaling in C3H/HeJ and C57BL/10ScCr mice: mutations in Tlr4 gene. *Science* 1998, **282**(5396)**:** 2085-2088.

36. Doyle SL, O'Neill LA. Toll-like receptors: from the discovery of NFkB to new insights into transcriptional regulations in innate immunity. *Biochem Pharmacol* 2006, **72**(9)**:** 1102-1113.

37. West AP, Koblansky AA, Ghosh S. Recognition and signaling by toll-like receptors. *Annu Rev Cell Dev Biol* 2006, **22:** 409-437.

38. Lemaitre B, Hoffmann J. The host defense of Drosophila melanogaster. *Annu Rev Immunol* 2007, **25:** 697-743.

39. Lee MS, Kim YJ. Signaling pathways downstream of pattern-recognition receptors and their cross talk. *Annu Rev Biochem* 2007, **76:** 447-480.

40. Beutler B, Moresco EM. The forward genetic dissection of afferent innate immunity. *Curr Top Microbiol Immunol* 2008, **321:** 3-26.

41. Yi AK, Yoon JG, Krieg AM. Convergence of CpG DNA- and BCR-mediated signals at the c-Jun N-terminal kinase and NF-κB activation pathways: regulation by mitogen-activated protein kinases. *Int Immunol* 2003, **15**(5)**:** 577-591.

42. Chaturvedi A, Dorward D, Pierce SK. The B cell receptor governs the subcellular location of Toll-like receptor 9 leading to hyperresponses to DNA-containing antigens. *Immunity* 2008, **28**(6)**:** 799-809.

43. Chaturvedi A, Pierce SK. How Location Governs Toll-Like Receptor Signaling. *Traffic* 2009, **10**(6)**:** 621-628.

44. Eckl-Dorna J, Batista FD. BCR-mediated uptake of antigen linked to TLR9-ligand stimulates B-cell proliferation and antigen-specific plasma cell formation. *Blood* 2009.

45. Pone EJ, Zan H, Zhang J, Al-Qahtani A, Xu Z, Casali P. Toll-like receptors and B-cell receptors synergize to induce immunoglobulin class-switch DNA recombination: relevance to microbial antibody responses. *Crit Rev Immunol* 2010, **30**(1)**:** 1-29.

46. Lam T, Thomas LM, White CA, Li G, Pone EJ, Xu Z*, et al.* Scaffold functions of 14-3-3 adaptors in B cell immunoglobulin class switch DNA recombination. *PloS one* 2013, **8**(11)**:** e80414.

47. Pone EJ, Lam T, Edinger AL, Xu Z, Casali P. B cell Rab7 mediates induction of AID expression and class-switching in T-dependent an T-independent antibody responses. *Journal of immunology* 2014.

48. Zan H. Endonuclease G plays a role in immunoglobulin class switch DNA recombination by introducing double-strand breaks in switch regions. *Mol Immunol* 2011, **48:** 610-622.

49. Zan H, Casali P. AID- and Ung-dependent generation of staggered double-strand DNA breaks in immunoglobulin class switch DNA recombination: a post-cleavage role for AID. *Mol Immunol* 2008, **46:** 45-61.

50. Xu Z, Fulop Z, Wu G, Pone EJ, Zhang J, Mai T*, et al.* 14-3-3 adaptor proteins recruit AID to 5'-AGCT-3'-rich switch regions for class switch recombination. *Nature structural & molecular biology* 2010, **17**(9)**:** 1124-1135.

51. Shlomchik M, Weigert M. Is the hypothesis alive that IgM anti-IgG1 rheumatoid factor specificity is determined by framework regions? *European journal of immunology* 1990, **20**(11)**:** 2529-2531.

52. Moore BW, Perez, V.J. Specific acidic proteins of the nervous system. In: Carlson FD (ed). *Physiological and Biochemical Aspects of Nervous Integration*. Prentice Hall, 1967.

53. Fu H, Subramanian RR, Masters SC. 14-3-3 proteins: structure, function, and regulation. *Annu Rev Pharmacol Toxicol* 2000, **40:** 617-647.

54. Fu H, Subramanian RR, Masters SC. 14-3-3 proteins: structure, function, and regulation. *Annu Rev Pharmacol Toxicol* 2000, **40:** 617-647.

55. Li G, White CA, Lam T, Pone EJ, Tran DC, Hayama KL*, et al.* Combinatorial H3K9acS10ph histone modification in IgH locus S regions targets 14-3-3 adaptors and AID to specify antibody class-switch DNA recombination. *Cell reports* 2013, **5**(3)**:** 702-714.

56. Xu Z, Pone EJ, Al-Qahtani A, Park SR, Zan H, Casali P. Regulation of aicda expression and AID activity: relevance to somatic hypermutation and class switch DNA recombination. *Crit Rev Immunol* 2007, **27**(4)**:** 367-397.

57. Stavnezer J, Guikema JE, Schrader CE. Mechanism and regulation of class switch recombination. *Annu Rev Immunol* 2008, **26:** 261-292.

58. Athwal GS, Lombardo CR, Huber JL, Masters SC, Fu H, Huber SC. Modulation of 14-3-3 protein interactions with target polypeptides by physical and metabolic effectors. *Plant & cell physiology* 2000, **41**(4)**:** 523-533.

59. Fu H, Subramanian RR, Masters SC. 14-3-3 proteins: structure, function, and regulation. *Annual review of pharmacology and toxicology* 2000, **40:** 617-647.

60. Chaudhuri J, Alt FW. Class-switch recombination: interplay of transcription, DNA deamination and DNA repair. *Nature Rev Immunol* 2004, **4:** 541-552.

61. Kino T, De Martino MU, Charmandari E, Ichijo T, Outas T, Chrousos GP. HIV-1 accessory protein Vpr inhibits the effect of insulin on the Foxo subfamily of forkhead transcription factors by interfering with their binding to 14-3-3 proteins: potential clinical implications regarding the insulin resistance of HIV-1-infected patients. *Diabetes* 2005, **54**(1)**:** 23-31.

62. Barnitz RA, Wan F, Tripuraneni V, Bolton DL, Lenardo MJ. Protein Kinase A phosphorylation activates Vpr-induced cell cycle arrest during Human Immunodeficiency Virus Type-1 infection. *J Virol* 2010, **In press**.

63. Begum NA. Further evidence for involvement of a noncanonical function of uracil DNA glycosylase in class switch recombination. *Proc Natl Acad Sci USA* 2009, **106:** 2752-2757.

64. Tungaturthi PK, Sawaya BE, Singh SP, Tomkowicz B, Ayyavoo V, Khalili K*, et al.* Role of HIV-1 Vpr in AIDS pathogenesis: relevance and implications of intravirion, intracellular and free Vpr. *Biomed Pharmacother* 2003, **57**(1)**:** 20-24.

65. Sherman MP, Schubert U, Williams SA, de Noronha CM, Kreisberg JF, Henklein P*, et al.* HIV-1 Vpr displays natural protein-transducing properties: implications for viral pathogenesis. *Virology* 2002, **302**(1)**:** 95-105.

66. Gu H, Rajewsky, K. *B Cell Protocols*. Humana Press, 2004.

67. Zan H, Casali P. AID- and Ung-dependent generation of staggered double-strand DNA breaks in immunoglobulin class switch DNA recombination: A post-cleavage role for AID. *Mol Immunol* 2008, **46**(1)**:** 45-61.

68. Zan H, Shima N, Xu Z, Al-Qahtani A, Evinger Iii AJ, Zhong Y*, et al.* The translesion DNA polymerase theta plays a dominant role in immunoglobulin gene somatic hypermutation. *EMBO J* 2005, **24**(21)**:** 3757-3769.

69. Murphy KM, Travers, P., Walport, M. *Janeway's Immunobiology*. Garland Science: New York, 2007.

70. DeFranco AL, Locksley, R.M., Robertson, R.M. *Immunity: the immune response in infectous and inflammatory disease*. New Science Press: Sunderland, MA, 2007.

71. Casali P. *Immunoglobulin M*, Second Edition edn. Academic Press Ltd.: London, 1998.

72. Ta VT, Nagaoka H, Catalan N, Durandy A, Fischer A, Imai K*, et al.* AID mutant analyses indicate requirement for class-switch-specific cofactors. *Nat Immunol* 2003, **4**(9)**:** 843-848.

73. Durandy A, Peron S, Fischer A. Hyper-IgM syndromes. *Curr Opin Rheumatol* 2006, **18**(4)**:** 369-376.

74. Durandy A, Taubenheim N, Peron S, Fischer A. Pathophysiology of B-cell intrinsic immunoglobulin class switch recombination deficiencies. *Adv Immunol* 2007, **94:** 275-306.

75. Durandy A. Immunoglobulin class switch recombination: study through human natural mutants. *Philos Trans R Soc Lond B Biol Sci* 2009, **364**(1517)**:** 577-582.

76. Stavnezer J. Complex regulation and function of activation-induced cytidine deaminase. *Trends in immunology* 2011, **32**(5)**:** 194-201.

77. Goodnow CC, Crosbie J, Jorgensen H, Brink RA, Basten A. Induction of self-tolerance in mature peripheral B lymphocytes. *Nature* 1989, **342**(6248)**:** 385-391.

78. Goodnow CC, Basten A. Self-tolerance in B lymphocytes. *Seminars in immunology* 1989, **1**(2)**:** 125-135.

79. Goodnow CC. Cellular mechanisms of self-tolerance. *Current opinion in immunology* 1989, **2**(2)**:** 226-236.

80. Oracki SA, Tsantikos E, Quilici C, Light A, Schmidt T, Lew AM*, et al.* CTLA4Ig alters the course of autoimmune disease development in Lyn-/- mice. *Journal of immunology* 2010, **184**(2)**:** 757-763.

CHAPTER 2

THE ROLE OF 14-3-3 ADAPTORS IN B CELL IMMUNOGLOBULIN CLASS-SWITCHING

2.1 14-3-3 ADAPTORS IN B LYMPHOCYTES

14-3-3 adaptors are highly conserved multidomain proteins that function as structural scaffolds that, by switching the conformation of their ligands, coordinate the spatiotemporal organization of macromolecular complexes. This brings enzymatic elements into close proximity with substrate(s), to transmit specific biological outputs. 14-3-3 adaptors have the striking ability to bind to diverse signaling proteins, such as kinases, phosphatases, and transmembrane proteins and contingent with specific effectors, 14-3-3 play major roles in cell cycle, survival, and cell migration, among others[1] (**Figure 2.1**).

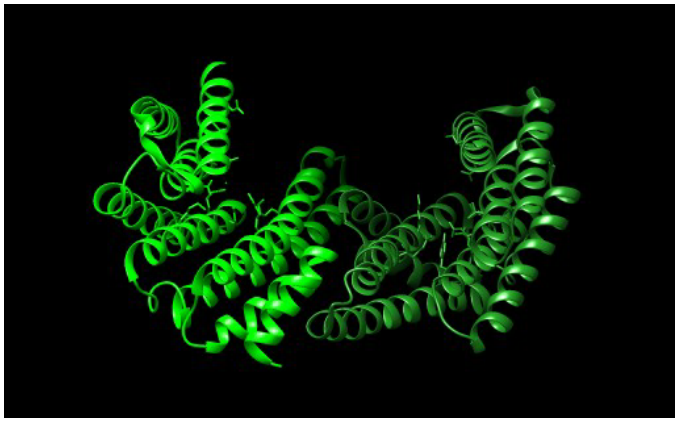

Figure 2.1 Crystal structural model of the recognition of phosphorylated and phosphoacetylated histone H3 by 14-3-3ζ. 14-3-3 proteins (seven homologous isoforms defined with Greek letters, β, ε, γ, η, σ, τ and ζ) form dimers. The dimeric structure of 14-3-3 can bind to two ligands simultaneously allowing 14-3-3 proteins to bind diverse signaling proteins and act as scaffolds to direct protein-protein interaction.

We have made two important discoveries focused on the targeting of CSR: (i) 14-3-3 family of seven isoforms bind to 5'-AGCT-3' repeats that are characteristic within the immunoglobulin heavy chain (IgH) switch (S) region and is highly conserved across unrelated species (**Figure 2.2**) and (ii) 14-3-3 adaptors mediates immunoglobulin class-switch DNA recombination (CSR) by directly interacting with activation-induced cytidine deaminase (AID) and protein kinase A (PKA)[2].

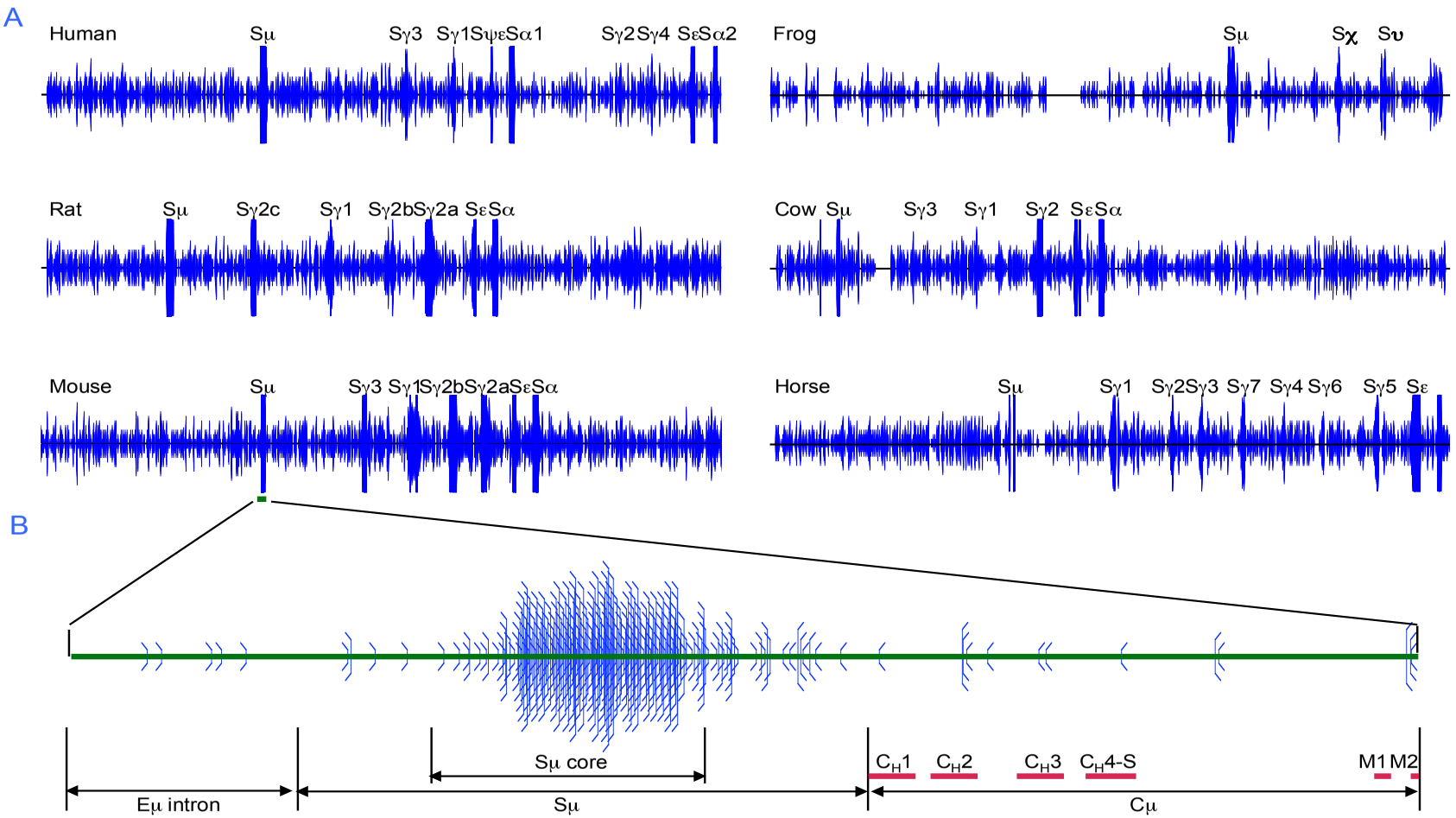

Figure 2.2 5'-AGCT-3' repeats recur at a high frequency in S regions.

(**A**) High density 5'-AGCT-3'-rich repeats in S regions of the IgH locus in species that used CSR to diversity their antibody repertoire. 5'-AGCT-3' repeats are evolutionarily conserved and are preferential targets of S–S junctions.

(**B**) Magnified map of the mouse *Igh* DNA from the end of the J_H4 gene segment to Cμ region, including the Eμ intron, Sμ and the C_H1, C_H2, C_H3, C_H4-S, M1 and M2 exons of Cμ, shows the high density of 5′-AGCT-3′ motifs in the Sμ core. The graphs were generated using MacVector® software (MacVector, Inc.). Modified from Xu et al., 2010.

2.2 TARGETING OF CSR: SCAFFOLD FUNCTIONS OF 14-3-3 ADAPTORS

For CSR to unfold, AID and the whole CSR machinery must be targeted to the S regions that are set to undergo recombination to introduce DSBs, the resolution of which leads to S–S DNA recombination – dysregulation of AID expression and targeting has been associated with chromosomal translocations, lymphomagenesis and autoimmunity. In species that use CSR to diversify their antibodies, all S region "cores", within which DSBs and S–S junctions preferentially segregate, contain high-density repeats of the 5'-AGCT-3' motif[2]. 14-3-3 adaptor proteins (seven homologous isoforms, 14-3-3β, 14-3-3ε, 14-3-3γ, 14-3-3η, 14-3-3σ, 14-3-3τ and 14-3-3ζ)[1] specifically bind to 5'-AGCT-3' repeats and are selectively recruited to the upstream and downstream S regions that are set to undergo S–S DNA recombination by the H3K9acS10ph combinatorial histone modification[3]. Once docked onto S regions, 14-3-3- adaptors, which are *bona fide* scaffolding proteins, mediate the assembly of macromolecular complexes on S region DNA. In addition to 14-3-3 adaptors, CSR enzymatic elements, such as AID, PKA, and Ung, may possess non-enzymatic scaffolding functions for their recruitment/stabilization to/on the recombining S regions. We outline these novel scaffolding functions and will likely provide important information on the assembly DNA/multi-protein macromolecular complexes on S regions. Here, we show that 14-3-3 nucleate the assembly of CSR factors through many DNA–protein and homotypic/heterotypic protein-protein interactions (14-3-3[1, 4], AID[5] and PKA are all dimers/multimers); and, as strongly suggested by our findings that 14-3-3 enhance AID DNA deamination activity[2], enzymatic activities of AID, PKA and/or Ung are enhanced by scaffolding proteins in DNA/protein complexes (**Figure 2.3**).

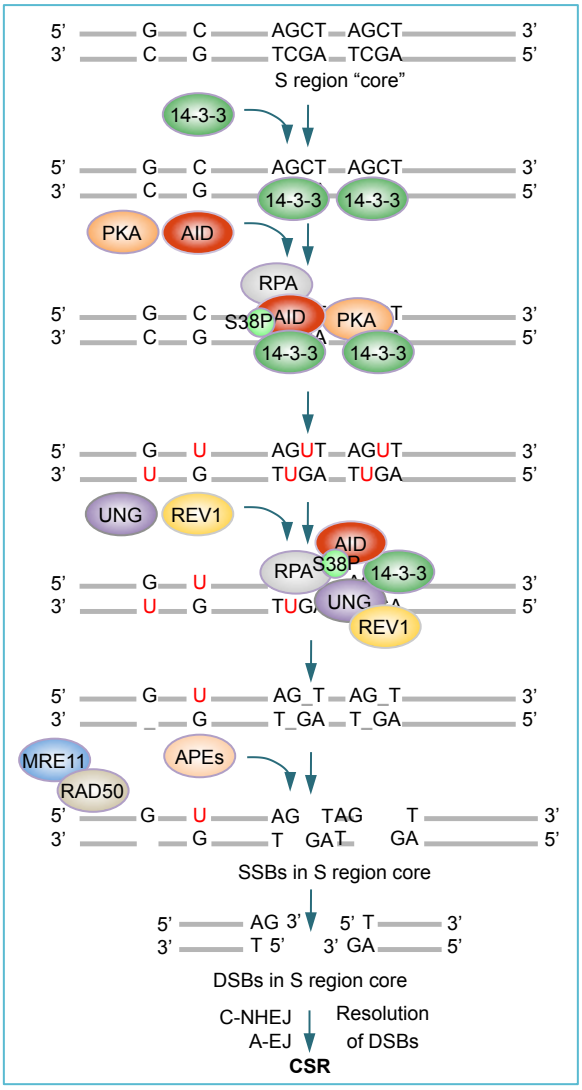

Figure 2.3 Schematic depiction of 14-3-3 binding to 5'-AGCT-3' repeats in S regions and recruiting enzymes to unfold CSR. Class-switch DNA recombination (CSR) is initiated by activation-induced cytidine deaminase (AID), which is targeted to switch (S) regions by 14-3-3 adaptor proteins that specifically bind to 5′-AGCT-3′ repeats in the S region core and recruit AID and protein kinase A (PKA) to S region DNA. AID is phosphorylated at serine 38 in its amino-terminal region by PKA, generating a binding site for replication protein A (RPA). RPA enhances AID-mediated deamination of deoxycytidine in transcribed S region DNA. The resulting deoxyuracils are removed by uracil DNA glycosylase (Ung), which is thought to be recruited to and stabilized on S regions by the scaffold functions of 14-3-3 adaptors, RPA and the translesion DNA polymerase REV1. Excision of Ung-generated abasic sites by apurinic/apyrimidinic endonucleases (APEs) and/or the MRE11–RAD50 results in single-strand breaks (SSBs), which either directly form double-strand breaks (DSBs) owing to the close proximity of SSBs on opposite strands or is converted to DSBs. DSB resolution by classical non-homologous end joining (C-NHEJ) or alternative end joining (A-EJ) leads to class-switching. Modified from Xu et al., 2012[2].

The direct interaction between 14-3-3 and AID was addressed using BiFC assays. In our BiFC assays, EYFP was split into two complementary moieties: the N-terminal 154 amino acids (EYFP1–154) and the C-terminal 84 amino acids (EYFP155–238)[6]. EYFP1–154 was fused with Flag–tagged AID (Flag–AID–EYFP1–154), AID C-terminal truncation mutant (Flag–AIDΔ(180–198)–EYFP1–154), AID C-terminal point mutants (Flag–AIDR190A–EYFP1–154, Flag–AIDF193A–EYFP1–154, Flag–AIDL196A–EYFP1–154) or AID S38A mutant (Flag–AIDS38A–EYFP1–154). EYFP155–238 was fused with influenza hemagglutinin (HA)–tagged

14-3-3β, ε, γ, η, σ, τ or ζ, (HA–14-3-3β–EYFP155–238, HA–14-3-3ε–EYFP155–238, HA–14-3-3γ–EYFP155–238, HA–14-3-3η–EYFP155–238, HA–14-3-3σ–EYFP155–238, HA–14-3-3τ–EYFP155–238 or HA–14-3-3ζ–EYFP155–238, respectively). Upon coexpression of Flag–AID–EYFP1–154 and HA–14-3-3–EYFP155–238 in HeLa cells, the two EYFP moieties complement each other and give off fluorescence complex ($EYFP^+$) only when juxtaposed, as a result of direct interaction between AID and 14-3-3. By contrast, if AID and 14-3-3 interact though a third molecule, this 'spacer' molecule will prevent the direct interaction between AID and 14-3-3, and therefore, hamper EYFP1–154 and EYFP155–238 reciprocal complementation (**Figure 2.4A**). We have previously shown[2], and confirmed here, that all seven 14-3-3 isoforms interacted with AID and that 14-3-3ζ failed to interact with AIDΔ(190–198) or AIDΔ(180–198), which was expressed at a higher level than AID (**Figure 2.4B, C**), two AID C-terminal truncation mutants that are defective in mediating CSR despite their normal DNA dC deamination activity[7]. In addition, 14-3-3ζ displayed reduced (by 66%) interaction with AID C-terminal point-mutant AIDF193A, which fails to mediate CSR[8]. 14-3-3ζ also displayed reduced interaction with another CSR-defective AID C-terminal point-mutant AIDL196A. By contrast, 14-3-3ζ directly interacted with AIDR190A (**Figure 2.4C**), which can fully rescue CSR in *Aicda*$^{-/-}$ B cells[8]. Like 14-3-3ζ, the other six 14-3-3 isoforms interacted with AIDR190A, but failed to interact with AIDΔ(180–198), AIDF193A or AIDL196A. Finally, all seven 14-3-3 adaptors directly interacted with AIDS38A mutant, which can be recruited to S region DNA[9], but cannot be phosphorylated by PKA and mediates limited CSR[10] (**Figure 2.4D**). Thus, 14-3-3 adaptors interact with AID and a CSR-proficient AID C-terminal point-mutant, but not with CSR-defective AID C-terminal truncation mutant or point-mutants.

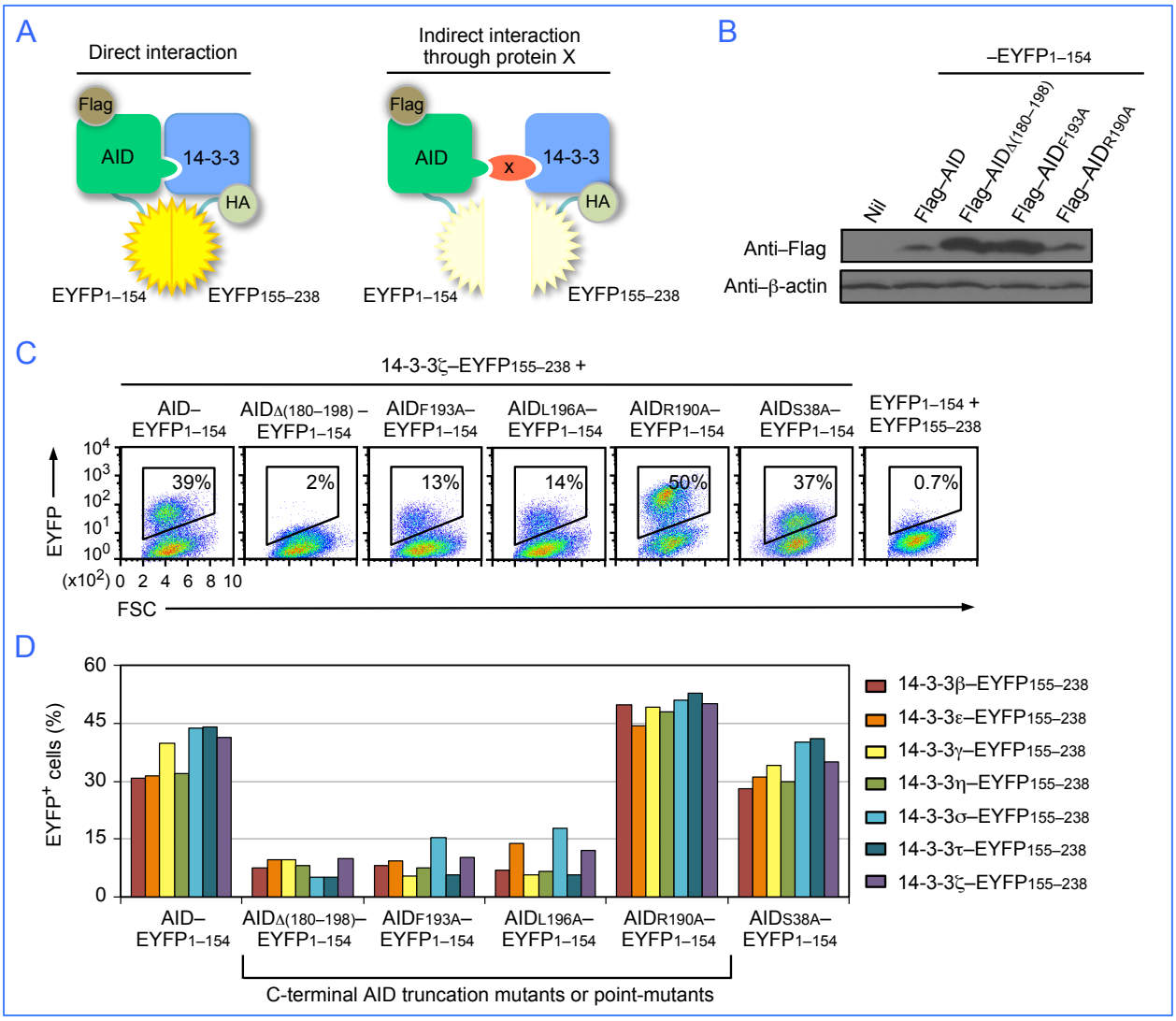

Figure 2.4 14-3-3 adaptors interact with AID through the AID C-terminus.

(A) Schematics of the principle of the BiFC assays to analyze interaction of 14-3-3 (HA–14-3-3–EYFP155–238) and AID (Flag–AID–EYFP1–154). (B) Immunoblotting using specific mAbs to identify Flag and β-actin in HeLa cell e xpressing nil (pcDNA3 vector), Flag–AID, Flag–AIDΔ(180–198), Flag–AIDF193A, Flag–AIDR190A (fused to EYFP1–154). (C) BiFC assays of the interaction between 14-3-3ζ (fused to EYFP155–238) and AID, and AIDR190A and AIDS38A, but not AIDΔ(180–198), AIDF193A or AIDL196A (fused to EYFP1–154) in HeLa cells (at 24 hours), as analyzed by flow cytometry. (D) Quantification of the interaction between each of the seven 14-3-3 isoforms (β, ε, γ, η, σ, τ, ζ; fused to EYFP155–238) and AID, AIDΔ(180–198), AIDF193A, AIDL196A, AIDR190A or AIDS38A (fused to EYFP1–154), in HeLa cells (at 48 hours) depicted as percentage of $EYFP^+$, as analyzed by flow cytometry.

The direct interaction between 14-3-3 and PKA-Cα and PKA-RIα or RPA1 was addressed using BiFC assays. The kinase activity of the two catalytic subunits PKA-Cα and PKA-Cβ within the PKA holoenzyme is inhibited by the two regulatory inhibitory subunits PKA-RIα and PKA-RIIα; upon allosteric binding of cAMP, these two regulatory subunits are released – PKA-RIα is the major PKA regulatory subunit and has been shown to interact with AID and be recruited to S region DNA, as part of the PKA holoenzyme[11]. In our BiFC assays, HA–tagged 14-3-3β, ε, γ, η, σ, τ or ζ–EYFP155–238 and Flag–PKA-Cα–EYFP1–154, Flag–PKA-RIα–EYFP1–154 or Flag–RPA1–EYFP1–154 were coexpressed in human HeLa cells. All seven 14-3-3 adaptors directly interacted with PKA-Cα and PKA-RIα. 14-3-3 adaptors, however, did not interact with RPA1 (**Figure 2.5A, B, C**), a 70 kDa subunit that binds ssDNA[5].

The direct interaction between 14-3-3 and Ung was also addressed using BiFC assays. As we have previously shown, Ung is recruited/stabilized on S region DNA by Rev1, a translesion DNA synthesis (TLS) polymerase, which functions as a scaffold protein in CSR[12], through direct interactions to mediate CSR by processing dUs in S regions for the generation of high density of DSBs. In our BiFC assays, HA–tagged 14-3-3β, ε, γ, η, σ, τ or ζ–EYFP155–238 and Flag–Ung–EYFP1–154 and Ung N-terminal truncation mutant Flag–Ung Δ(1-84)–EYFP1–154 and Ung C-terminal truncation mutant Flag–UngΔ(152–313)–EYFP1–154 were coexpressed in human HeLa cells. 14-3-3 adaptors directly interacted with Ung and with Ung N-terminal truncation mutant UngΔ(1-84), which can rescue CSR in *Ung*$^{-/-}$ B cells[13, 14]. 14-3-3 adaptors, however, did not bind Ung C-terminal truncation mutant UngΔ(152–313), which was expressed at a higher level than Ung or UngΔ(1-84) (**Figure 2.5**). Thus, 14-3-3 adaptors interact with PKA and with Ung C-terminal amino acid residues, but not with RPA.

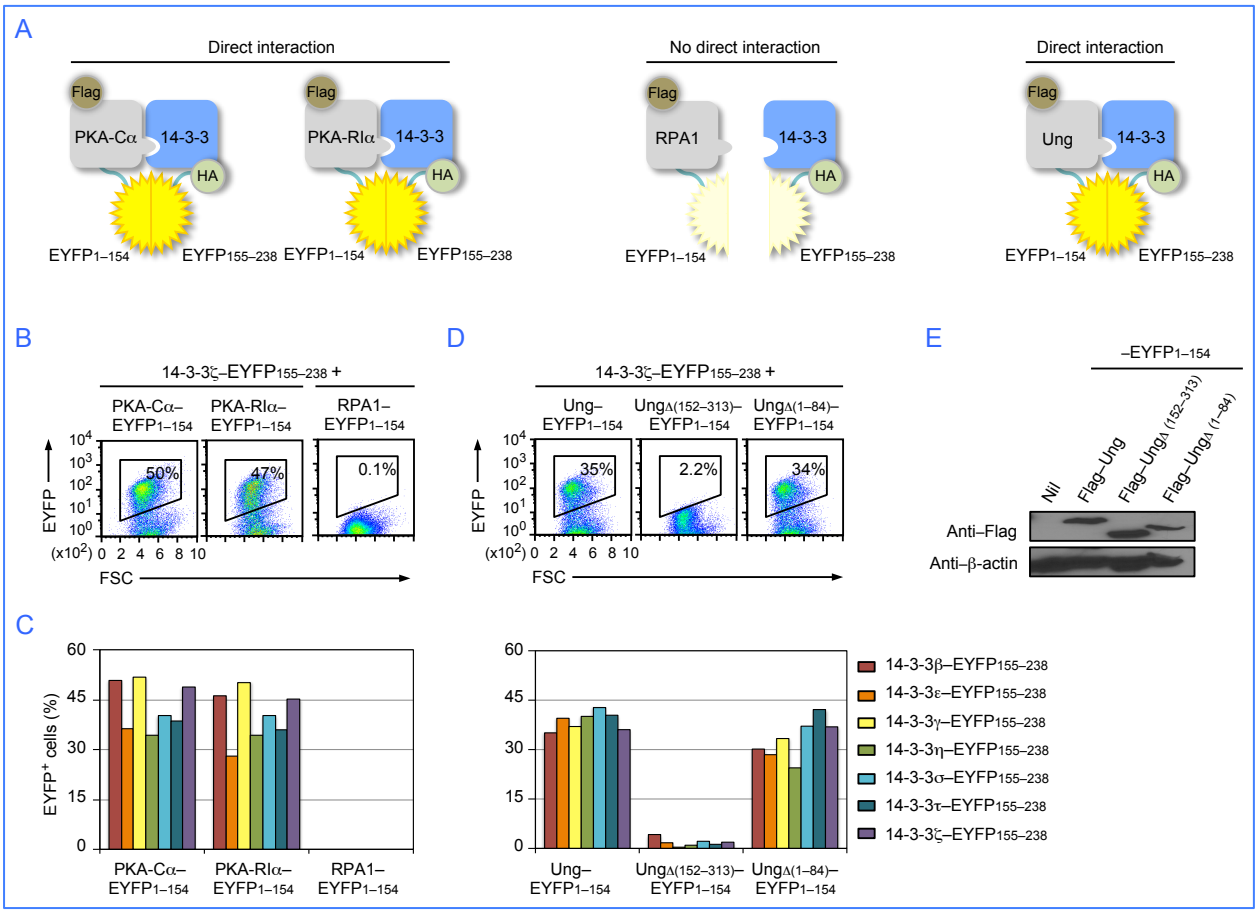

Figure 2.5 14-3-3 adaptors interact with PKA and Ung.

(**A**) Schematics of the principle of the BiFC assays to analyze interaction of 14-3-3 (HA–14-3-3–EYFP155–238) with PKA-Cα (Flag–PKA-Cα–EYFP1–154), PKA-RIα (Flag–PKA-RIα–EYFP1–154), RPA1 (Flag–RPA1–EYFP1–154) or Ung (Flag–Ung–EYFP1–154). (**B**) BiFC assays of the interaction between 14-3-3ζ (fused to EYFP155–238) and PKA-Cα and PKA-RIα, but not RPA1 (fused to EYFP1–154) in HeLa cells, as analyzed by flow cytometry. (**C**) Quantification of the interaction between each of the seven 14-3-3 isoforms (β, ε, γ, η, σ, τ, ζ; fused to EYFP155–238) and PKA-Cα, and PKA-RIα or RPA1 (fused to EYFP1–154, left panel), and Ung, and UngΔ(152–313) or UngΔ(1–84) (fused to EYFP1–154, right panel) in HeLa cells depicted as percentage of $EYFP^+$, as analyzed by flow cytometry. (**D**) BiFC assays of the interaction between 14-3-3ζ (fused to EYFP155–238) and Ung and N-terminal truncation mutant UngΔ(1–84), but not C-terminal truncation mutant UngΔ(152–313) (fused to EYFP1–154) in HeLa cells, as analyzed by flow cytometry. (**E**) Immunoblotting using specific mAbs to identify Flag and β-actin in HeLa cell expressing nil (pcDNA3 vector), Flag–Ung, Flag–UngΔ(152-313), Flag–UngΔ(1–84) (fused to EYFP1–154).

To confirm that 14-3-3γ can interact with AID, PKA-Cα and Ung in B cells undergoing CSR, we

performed glutathione S-transferase (GST) pull-down experiments using 14-3-3γ fused to GST (GST–14-3-3γ) and whole cell lysates prepared from mouse B cells stimulated with LPS plus mIL-4 for 48 hours. Using immunoblotting, we readily detected AID, PKA-Cα and Ung among protein molecules after pull-down by GST–14-3-3γ, but not GST (**Figure 2.6**). GST-14-3-3γ was also detected, as expected, and endogenous 14-3-3γ was detectable when a higher amount of GST–14-3-3γ–precipitated proteins were analyzed.

Thus, 14-3-3γ interacts with AID, PKA-Cα and Ung in switching B cells, consistent with its direct interactions with these CSR factors shown by our BiFC assays.

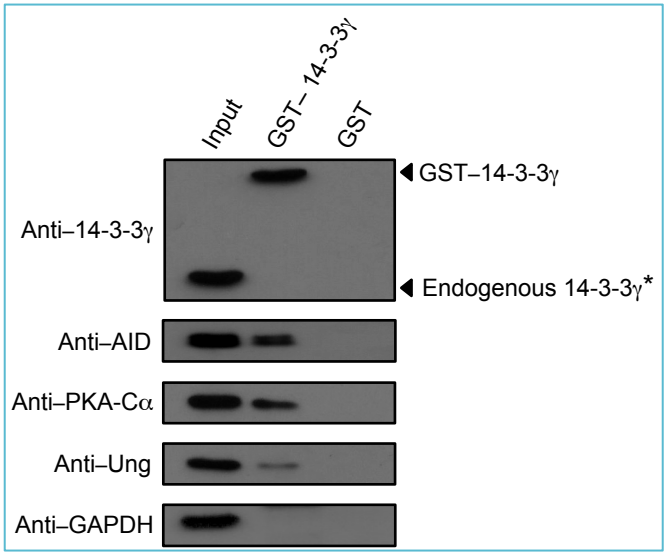

Figure 2.6 14-3-3γ interacts with AID, PKA-Cα and Ung expressed in B cells undergoing CSR.
Immunoblotting using specific mAbs/Abs was performed to identify 14-3-3γ, AID, PKA-Cα and Ung in proteins pulled-down with GST–14-3-3γ or GST alone from whole lysates of mouse B cells stimulated with LPS plus mIL-4 for 48 hours. *Endogenous 14-3-3γ was detected when a higher amount of GST–14-3-3γ–precipitated proteins were analyzed, but no signal was detected for AID, PKA or Ung from GST–precipitated proteins.

As we have shown, 14-3-3ζ–AID interaction mainly occurs in the nucleus despite their predominant cytoplasmic localization [2]. Using confocal microscopy we found that, consistent with their direct interaction, 14-3-3 adaptors and AID were expressed and codistributed mainly in the cytoplasm and, to a lower degree, in the nucleus of human 4B6 B cells, which switch

spontaneously from IgM to IgG, IgA and IgE [2, 15] (**Figure 2.7A**). Also, 14-3-3 codistributed with AID and RPA in human 2E2 B cells upon stimulation by an agonistic anti–hCD40 mAb plus hIL-4, which induce human 2E2 B cells to undergo CSR from IgM to IgG and IgE (**Figure 2.7B**). To directly visualize the colocalization of 14-3-3 and AID or RPA in the nucleus, where CSR occurs, we adapted a protocol to deplete human and mouse B cells of cytosolic constituents and then identified 14-3-3, AID or RPA by specific Abs. As detected by this approach, 14-3-3, AID and RPA formed nuclear foci in spontaneously switching human 4B6 B cells (**Figure 2.8A, B**) and in mouse B cells stimulated by LPS plus mIL-4 to undergo CSR from IgM to IgG1 at high levels, after 24 and 48 hours (**Figure 2.8C, D**). We consistently detected two to four 14-3-3–containing nuclear foci that colocalized with AID–containing nuclear foci or RPA–containing nuclear foci, in spite of no direct interaction between 14-3-3 and RPA (**Figure 2.5B**).

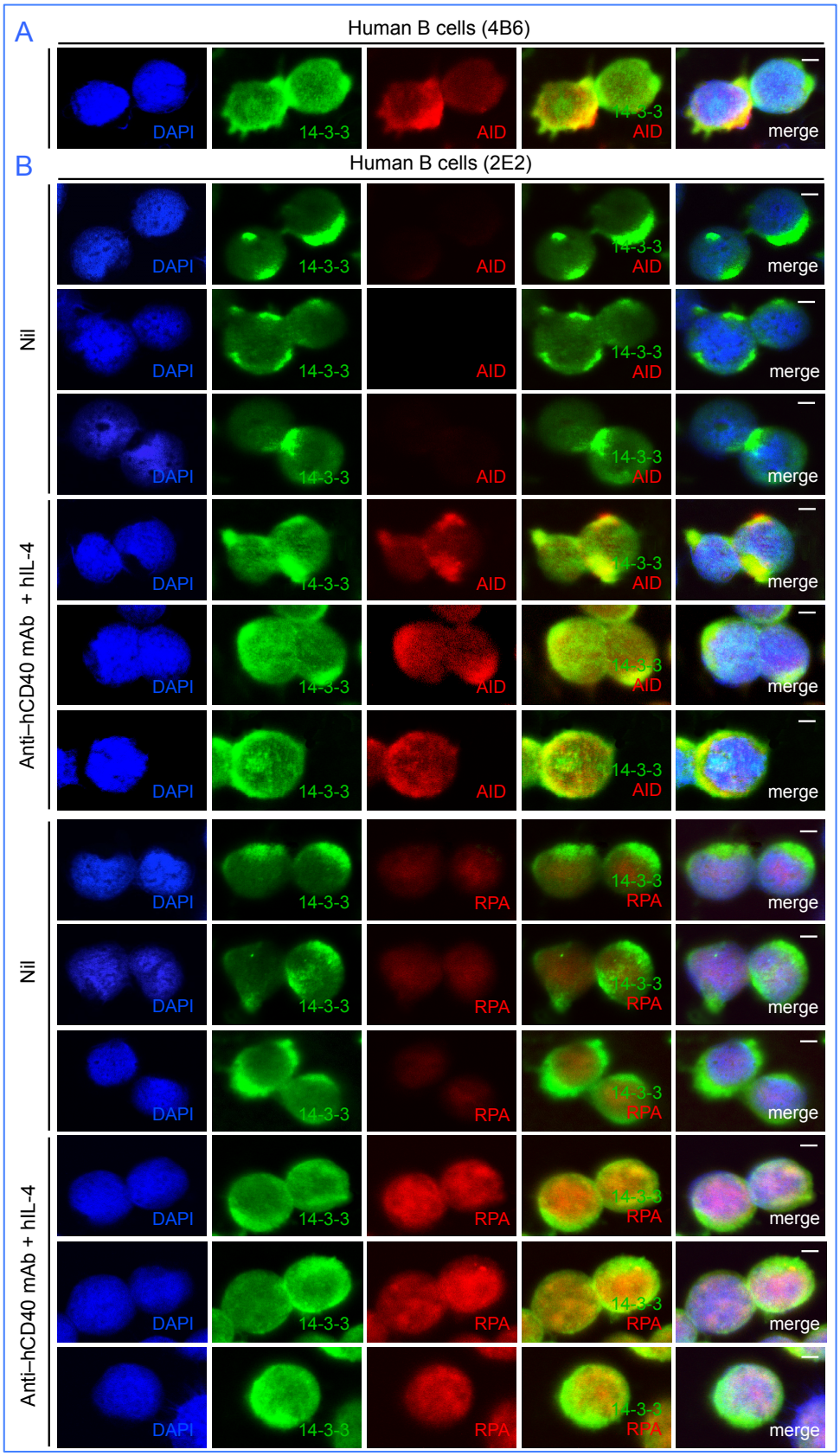

Figure 2.7 14-3-3 codistribute with AID and RPA in the nucleus of B cells undergoing CSR.

(A) Codistribution of 14-3-3 and AID in human 4B6 B cells (spontaneous CSR).

(B) Codistribution of 14-3-3 with AID or RPA in human 2E2 B cells stimulated with agonistic anti–hCD40 mAb plus hIL-4 (to induce CSR to IgG1) for 48 hours. Scale bars: 5 μm.

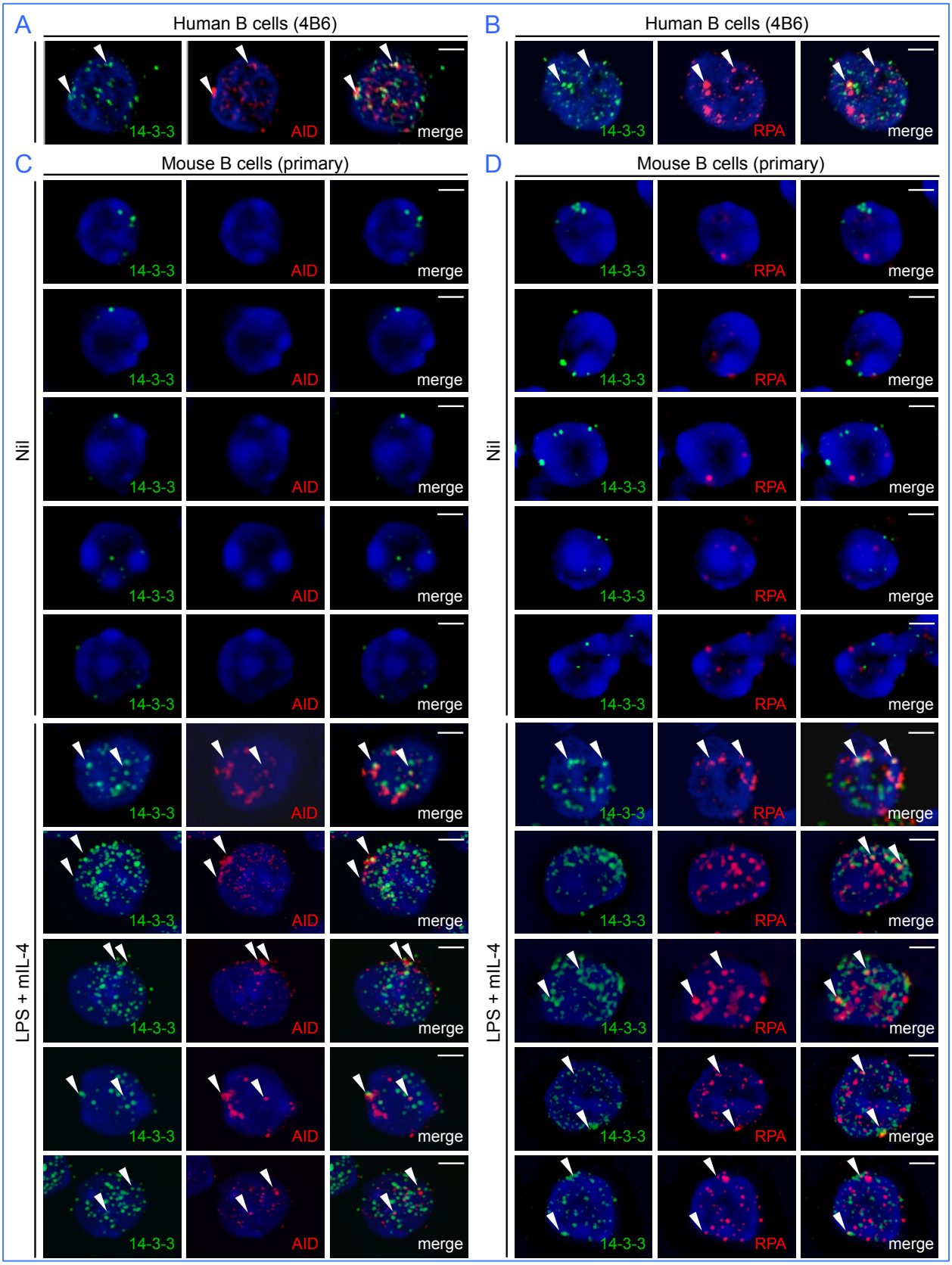
A
Human B cells (4B6)
14-3-3
AID
merge
B
Human B cells (4B6)
14-3-3
RPA
merge
C
Mouse B cells (primary)
Nil
LPS + mIL-4
14-3-3
AID
merge
D
Mouse B cells (primary)
Nil
LPS + mIL-4
14-3-3
RPA
merge

Figure 2.8 14-3-3 adaptors colocalize with AID and RPA in the nucleus of B cells undergoing CSR.
(**A**) Formation of 14-3-3 nuclear foci that colocalized with AID nuclear foci in human 4B6 B cells. (**B**) Formation of 14-3-3 nuclear foci that colocalized with RPA nuclear foci in human 4B6 B cells. (**C**) Formation of 14-3-3 nuclear foci that colocalized with AID nuclear foci in mouse primary B cells stimulated with LPS plus mIL-4 (to induce CSR to IgG1) for 48 hours. (**D**) Formation of 14-3-3 nuclear foci that colocalized with RPA nuclear foci in mouse primary B cells stimulated with LPS plus mIL-4 for 48 hours. Scale bars: 5 μm.

The percentages of human 2E2 B cells showing 14-3-3 molecules codistributing (%) with AID or RPA that were stimulated with agonistic anti–hCD40 mAb plus hIL-4 were higher than those of 2E2 B cells stimulated with nil (**Figure 2.9A**).

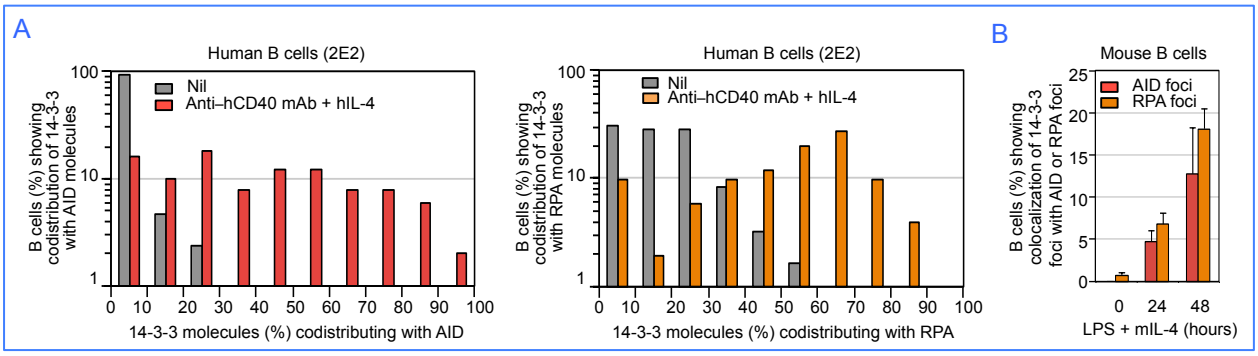

Figure 2.9 14-3-3 adaptors colocalize with AID and RPA at 24 hours and 48 hours.
(**A**) Percentages of human 2E2 B cells showing 14-3-3 molecules codistributing (%) with AID (red) or RPA (orange) were calculated and depicted on the *y*-axis. At least 100 cells stimulated with nil or agonistic anti–hCD40 mAb plus hIL-4 were analyzed in each experiment.
(**B**) Quantification of cells showing colocalization of 14-3-3 nuclear foci with AID nuclear foci or RPA nuclear foci in mouse primary B cells stimulated with LPS plus mIL-4 for 0 hour, 24 hours and 48 hours.

The proportion of B cells that displayed colocalization of 14-3-3 nuclear foci with AID nuclear foci or RPA foci increased over time of stimulation from 0% to 12.7% within 48 hours for AID, or from 0.8% to 18.1% within 48 hours for RPA, consistent with increased proportions of $IgG1^+$ B cells under the same stimulation conditions (**Figure 2.9B**). Thus, 14-3-3 adaptors colocalize with AID and RPA in the nucleus of human and mouse B cells undergoing CSR.

2.3 INHIBITION OF CSR: DISRUPTION OF 14-3-3 AND AID INTERACTION BY VPR

Prompted by our findings that 14-3-3 adaptors directly interacted and colocalized with AID and other CSR factors in the nucleus of switching B cells, we hypothesized that 14-3-3–mediated recruitment of the AID-centered CSR machinery to S regions would be blocked when interactions of 14-3-3 with CSR factors were disrupted by **naturally occurring or synthetic molecules**, leading to CSR inhibition.

To test this hypothesis, we first analyzed CSR inhibition by utilizing the HIV-1 accessory protein Vpr, which has been suggested to bind to 14-3-3 proteins[16], Ung[13] and possibly PKA[17]. Primary mouse B cells were transduced with pTAC retrovirus to express green fluorescent protein (GFP) alone (pTAC-GFP) or Vpr linked to GFP (pTAC-GFP-Vpr) and then stimulated with LPS and mIL-4 for CSR from IgM to IgG1. CSR was inhibited by Vpr, as shown by reduced proportions of $IgG1^+$ cells (23%) among B cells expressing GFP-Vpr when compared to their counterparts (42%) expressing GFP (**Figure 2.10**). In addition, levels of circle Iγ1-Cμ and post-recombination Iμ-Cγ1 transcripts, which are accurate parameters of ongoing and completed CSR, respectively, were reduced in the presence of Vpr. However, levels of AID expression and germline Iμ-Cμ and Iγ-Cγ1 transcription were normal in B cells expressing Vpr (**Figure 2.10B**). To address the molecular mechanisms underlying CSR inhibition by Vpr, we analyzed 14-3-3γ and AID recruitment to S regions in the presence of Vpr. Binding of 14-3-3γ and AID to Sμ and Sγ1 DNA was inhibited by Vpr, as shown by our ChIP assays using a specific Ab to 14-3-3γ or AID and chromatin from B cells expressing GFP-Vpr or GFP that were stimulated with LPS plus mIL-4 (**Figure 2.10C**).

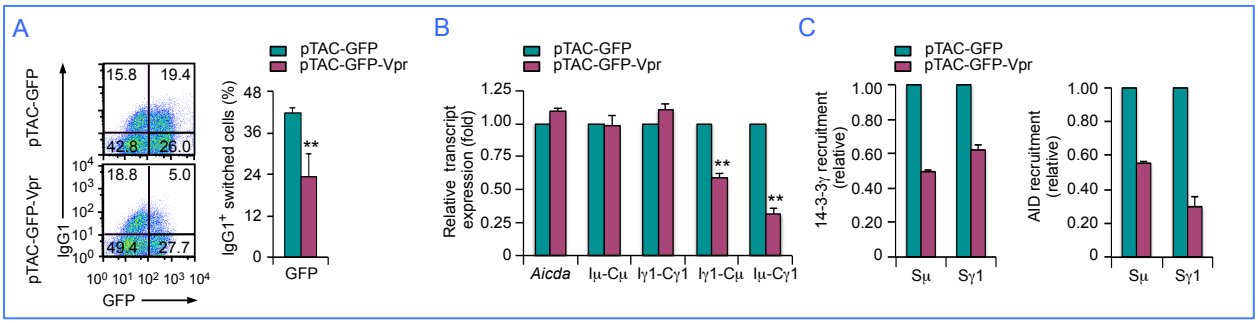

Figure 2.10 Inhibition of CSR and disruption of 14-3-3 recruitment to S regions by Vpr.

(**A**) Proportions of IgG1$^+$ cells in mouse primary B cells transduced with pTAC-GFP-Vpr or pTAC-GFP retrovirus (which mediated expression of GFP-Vpr or GFP, respectively) and stimulated with LPS plus mIL-4 for 72 hours (left; to induce CSR to IgG1), and quantification of class-switched surface IgG1$^+$ B cells expressing GFP (right; mean and s.e.m of data from three independent experiments), as analyzed by flow cytometry. (**B**) Levels of *Aicda*, germline Iμ-Cμ and Iγ1-Cγ1, circle Iγ1-Cμ and mature post-recombination Iμ-Cγ1 transcripts in mouse primary B cells expressing GFP-Vpr or GFP and stimulated with LPS plus mIL-4 for 48 hours. Data were normalized to the level of *Gapdh* transcripts and depicted as the ratio of expression of transcripts in B cells expressing GFP-Vpr to that in B cells expressing GFP (mean and s.e.m of data from three independent experiments). **, $P < 0.01$, t-test. (**C**) ChIP-qPCR analysis of the binding of 14-3-3γ and AID to the Sμ and Sγ1 region DNA in mouse primary B cells expressing GFP-Vpr or GFP and stimulated with LPS plus mIL-4 for 48 hours. Data were normalized to input chromatin DNA and depicted as enrichment of each DNA amplicon relative to baseline value obtained using irrelevant Ab.

To further dissect CSR inhibition by Vpr, we used an array of 22 Vpr peptides, each of 15–amino acid in length and each with a sequential 11–amino acid overlap, covering the entire 96–amino acid viral protein. We analyzed CSR inhibition by each peptide in mouse B cells induced by LPS plus mIL-4 – uptake of these peptides by B cells was efficient, possibly due to their small size. A differential CSR inhibitory activity was displayed from different Vpr peptides, which segregated into three inhibitory clusters (**Figure 2.11A**). The three clusters correlated with the three α-helices of Vpr[18], which are structurally independent (**Figure 2.11B**), and perhaps serve as distinct functional domains for the interaction of the retrovirus with host cell proteins.

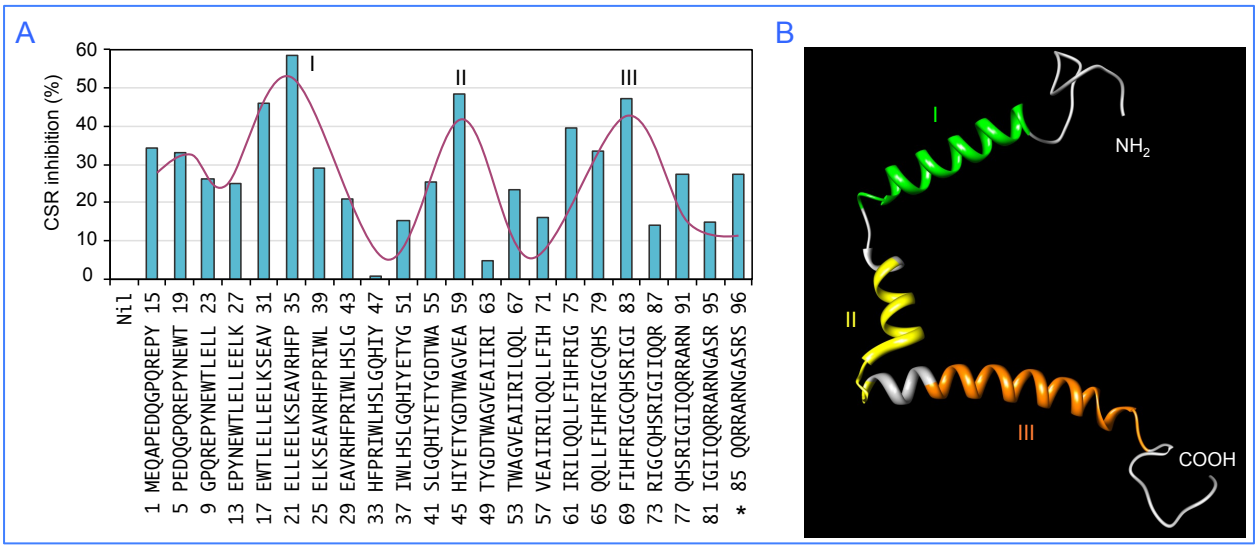

Figure 2.11 Vpr peptides inhibit CSR through segregated inhibitory clusters.

(A) Percent of inhibition of CSR to IgG1 in mouse primary B cells stimulated with LPS plus mIL-4 in the presence of 22 sequential Vpr peptides (*denotes the C-terminal peptide, which is 12–amino acid long). Three Vpr peptide clusters with the highest CSR inhibitory effects are depicted as I, II and III. Data are representative of those from three independent experiments. (B) The three Vpr peptide clusters with the highest CSR inhibitory effects correspond to the three α-helices of Vpr. The graph was rendered by the UCSF Chimera software using the NMR structure of Vpr (PDB ID 1esx).

Further, BiFC assays were utilized to address the direct interaction between 14-3-3 or AID and Vpr by coexpressing Flag–14-3-3ζ–EYFP1–154 or Flag–AID–EYFP1–154 and HA–Vpr–EYFP155–238, respectively, in HeLa cells. 14-3-3ζ and AID indeed interacted with Vpr and they did so in the nucleus. Further, in our BiFC assays involving Flag–AIDΔ(180–198)–EYFP1–154, Flag–PKA-Cα–EYFP1–154, Flag–PKA-RIα–EYFP1–154, Flag–Ung–EYFP1–154 or Flag–UngΔ(152–313)–EYFP1–154 with HA–Vpr–EYFP155–238, we showed that PKA-Cα and Ung, but not AIDΔ(180–198), PKA-RIα or UngΔ(152–313) interacted with Vpr (**Figure 2.12**). Thus, 14-3-3 adaptors function as scaffolds in mediating the recruitment of AID and possibly PKA and Ung to S regions, which can be inhibited by Vpr, likely due to the disruption of interactions between 14-3-3 and with those CSR factors, leading to the inhibition of CSR.

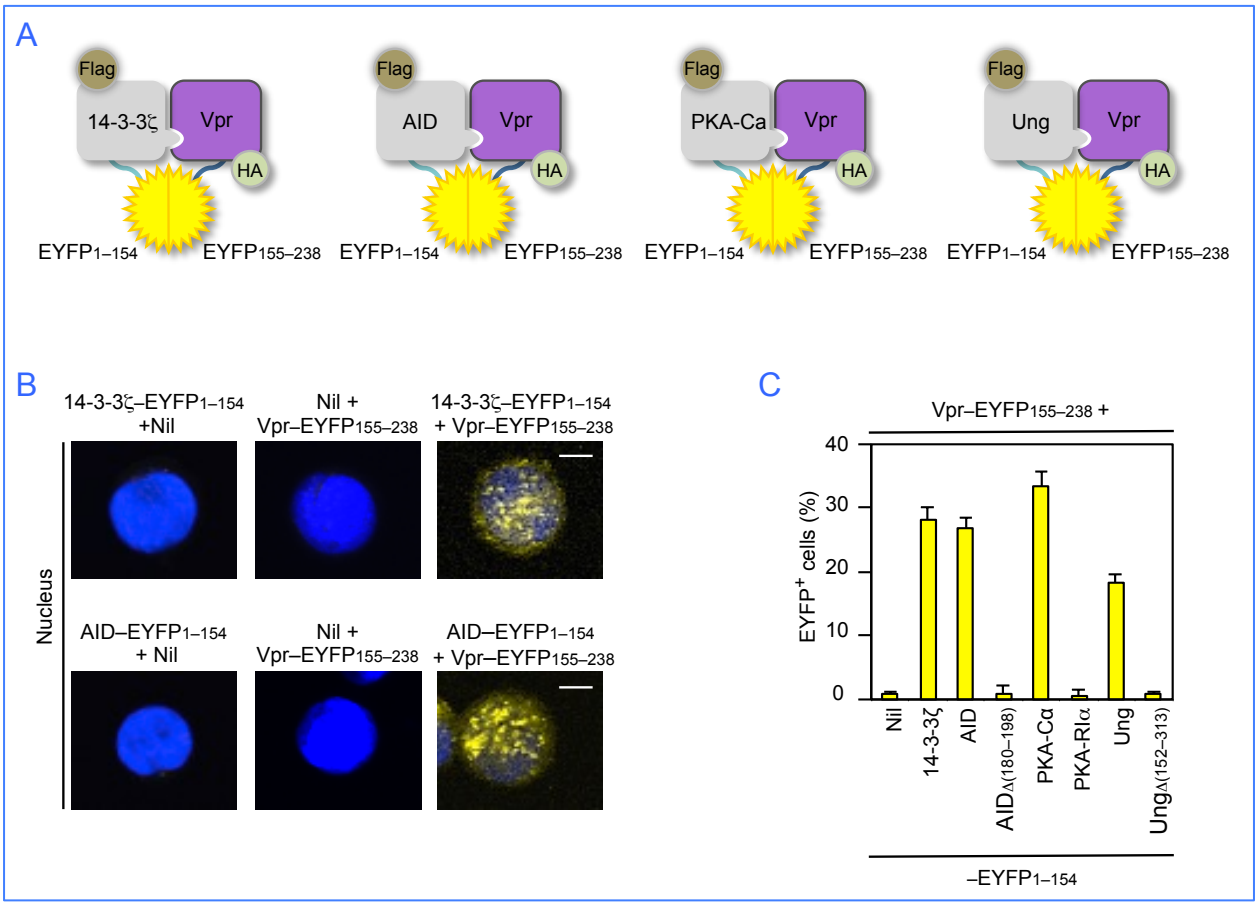

Figure 2.12 Essential CSR factors interact with Vpr.

(**A**) Schematics of the principle of the BiFC assays to analyze interaction of 14-3-3ζ (Flag–14-3-3ζ–EYFP1–154), AID (Flag–AID–EYFP1–154), PKA-Cα (Flag–PKA-Cα–EYFP1–154) or Ung (Flag–Ung–EYFP1–154) with Vpr (HA–Vpr–EYFP155–238). (**B**) BiFC assays of the interaction between 14-3-3ζ or AID (fused to EYFP1–154) and Vpr (fused to EYFP155–238) in HeLa cells. DAPI (blue) was used to visualize the nucleus. Scale bars: 5 μm. (**C**) Quantification of the interaction between nil (pcDNA3 vector), 14-3-3ζ, AID, AIDΔ(180–198), PKA-Cα, PKA-RIα, Ung or UngΔ(152–313) and Vpr in HeLa cells depicted as percentage of $EYFP^+$, as analyzed by flow cytometry. Data are representative of those from three independent experiments.

We next addressed the biological relevance of CSR inhibition by Vpr during HIV infection, in which a decrease in class-switched antibodies has been reported to occur. HIV does not infect B cells, but the HIV component such as Nef have been detected in B cells [19]. This prompted us to hypothesize that Vpr is present in secondary lymphoid structures during HIV infection. Here, we analyzed lymph node sections from HIV-1^+ patients and tonsil sections from HIV-1^- subjects by

immunohistochemistry using a specific Ab to Vpr. This revealed Vpr localized within germinal centers of HIV-1^{+} patients but not HIV-1^{-} subjects (**Figure 2.13A**). In addition, AID colocalized with Vpr within germinal center B cells of lymph nodes from HIV-1^{+} patients but not HIV-1^{-} subjects after double staining with an anti–Vpr Ab and anti–AID Ab or anti–CD20 Ab (**Figure 2.13B**). To demonstrate that B cells can acquire Vpr from an HIV-1^{+} source, we cocultured (HIV-1^{-}) human 4B6 B cells with (HIV-1^{-}) human CEM.NK^{R}-CCR5 T cells infected with nil or HIV-192US657 (a clinical isolate of the primary R5 HIV-1 strain[20, 21, 22]). 4B6 B cells displayed Vpr nuclear and cytoplasmic internalization, as indicated by the intracellular staining with FITC-conjugated anti–μ chain mAb staining and with Alexa 594-conjugated anti–Vpr Ab, only when cocultured with HIV-1-infected T cells, which were specified by staining with FITC-conjugated anti–CD4 mAb and positive for the intracellular staining of Vpr (**Figure 2.13C**).

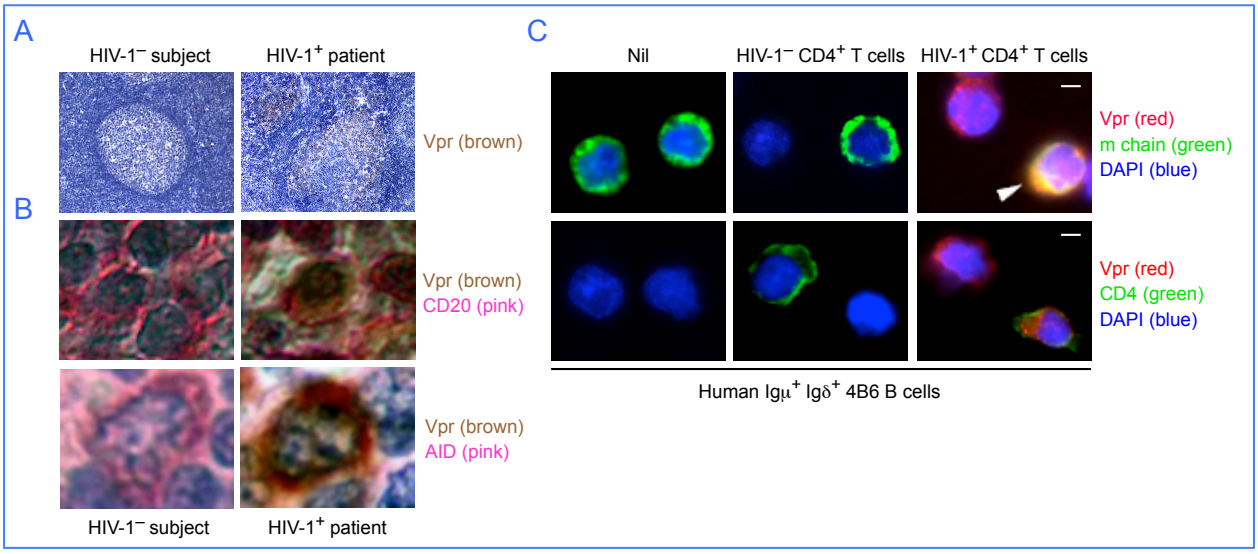

Figure 2.13 AID colocalized with Vpr in germinal center B cells from HIV-1^{+} patients.

(**A**) Immunohistochemistry analysis of Vpr in germinal centers in the tonsil from an HIV-1^{-} subject (left) or in lymph nodes from an HIV-1^{+} patient (right). Original magnification 100X. (**B**) Immunohistochemistry analysis of Vpr and CD20 (top) or Vpr and AID (bottom) in the tonsil from an HIV-1^{-} subject (left) or in lymph nodes from an HIV-1^{+} patient (right). Original magnification 100X. (**C**) Immunofluorescence staining and confocal microscopy analysis of Vpr in human 4B6 B cells cocultured with nil (left), CEM.NK^{R}-CCR5 T cells (middle) or CEM.NK^{R}-CCR5 T cells infected with HIV-192US657 (right). Human 4B6 B cells and CEM.NK^{R}-CCR5 T cells were stained

by FITC-conjugated anti–μ Ab (top) and anti-CD4 mAb (bottom), respectively. DAPI (blue) was used to visualize the nucleus. Scale bars: 5 μm. Data are representative of those from three independent experiments.

Thus, AID colocalizes with Vpr within germinal center B cells of HIV-1^+ patients and can be picked up by HIV-1^- B cells upon coculturing with HIV-1^+ T cells.

2.4 THERAPEUTICS USING A NATURALLY OCCURING VPR OR SMALL MOLECULE COMPOUNDS TO INHIBIT UNWANTED ANTIBODY CLASS-SWITCHING

CSR is central to the generation of antibodies capable of clearing microbial pathogens or killing tumoral cells as well as the antibodies that underlie the efficacy of vaccines. CSR impairment leads to hyper-IgM syndrome, as characterized by undetectable IgG, IgA and IgE levels and susceptibility to infections. Like anti-microbial antibodies, pathogenic autoantibodies in systemic autoimmune diseases, such as systemic lupus erythematosus, or organ-specific autoimmunity, such as thyroiditis or type I diabetes mellitus, are also class-switched, mostly to IgG. Antibodies mediating allergic reactions, such as asthma or anaphylaxis, are switched to IgE.

The significance of our studies described here derives primarily from an in-depth understanding of the mechanisms underpinning the generation of effective anti-microbial antibodies and pathogenic autoantibodies. Of added significance is the enhanced understanding of DNA targeting by AID, a potent mutagen that can generate genome-wide mutations and DSBs leading to chromosomal translocations and neoplastic transformation. By devising tools and reagents to inhibit CSR, our research will have a significant impact on the development of therapeutics that block unwanted CSR, e.g., CSR to IgG autoantibodies or atopic IgE (**Figure 2.14**).

In Chapter 3, we investigate the role of Rab7 small GTPase, which modulates AID expression and class-switching during T-dependent and T-independent antibody responses, and then utilize a small molecule compound to disrupt Rab7 function (CID 1067700) to inhibit class-switching. In Chapter 4, we describe our therapeutic treatment studies using CID 1067700 on lupus mice.

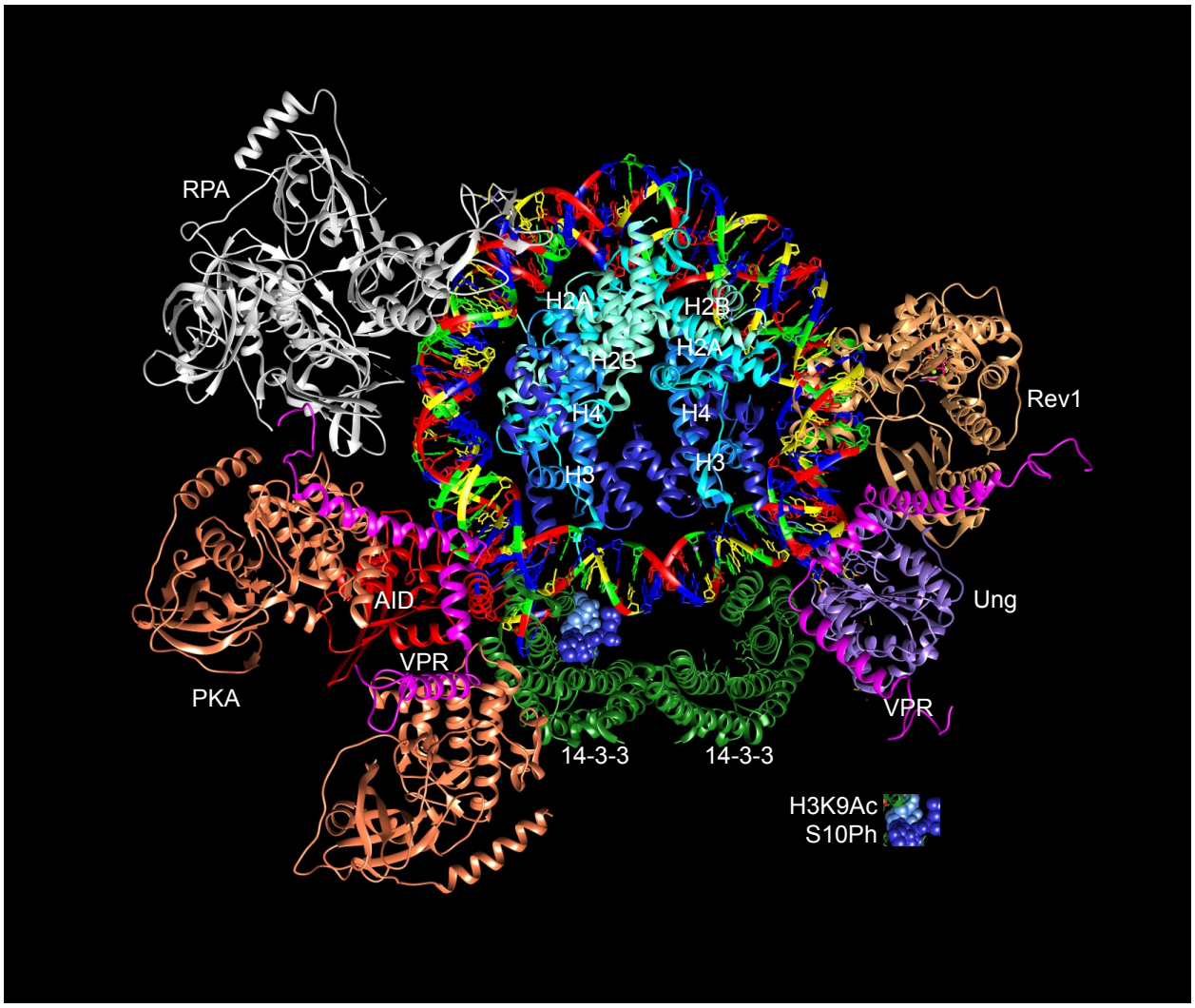

Figure 2.14 Schematic illustration of 14-3-3 scaffold functions in the assembly of S region DNA–protein complexes and disruption of such complexes by the naturally occurring Vpr molecule. A speculative model of a possible configuration of interacting proteins during CSR, and the disruption of some of these complexes by Vpr. The CSR macromolecular complex localizes to chromatin S regions through 14-3-3 adaptors (green) binding to the modified histone tail H3K9acS10ph (PDB ID 2c1j) as well as to 5'-AGCT-3' repeats (PDB ID 3afa), which specifically recur in S region DNA. Upon recruitment to S regions by 14-3-3, AID (red, homology modeled after human APOBEC2, PDB ID 2nyt) is phosphorylated at Ser38 by the PKA catalytic subunit (orange, PDB ID 3tnp), leading to the recruitment of RPA (silver, PDB ID 4gop) to S region DNA. Rev1 (brown, PDB ID 3gqc) is important for CSR by virtue of its ability to stabilize Ung (purple, PDB ID 3fci) on S region DNA. Vpr (magenta, PDB ID 1esx) impairs CSR, possibly by disrupting critical DNA–protein interactions, such as S region DNA–14-3-3 binding, and/or protein–protein interactions, such as those between 14-3-3 and AID, PKA or Ung. Graphics were rendered using the UCSF Chimera software (http://www.cgl.ucsf.edu/chimera).

2.5 SUMMARY TO CHAPTER 2

The recruitment and scaffold functions of 14-3-3 adaptors for the stabilization of enzymatic activity of AID and other CSR factors on S regions require multiple molecular interactions. Here, we showed that all seven isoforms of 14-3-3 adaptors directly interacted with AID, but failed to interact with AID C-terminal point mutants that have been shown to be defective in mediating CSR[8, 23]. In B cells undergoing CSR, 14-3-3 and AID formed nuclear foci of macromolecular complexes, as suggested by the colocalization of 14-3-3 nuclear foci and AID nuclear foci at 24 hours and 48 hours, but not at 0 hour. Non-colocalizing 14-3-3 nuclear foci may be involved in binding to H3K9acS10ph in the genome (outside the *IgH* locus) for transcription regulation[24]; non-colocalizing AID foci may be responsible for dC deamination outside the Ig locus[25, 26, 27], particularly in regions where RNA polymerase II stalls[28, 29].

All seven isoforms of 14-3-3 adaptors directly interacted with the catalytic and regulatory subunits of the PKA holoenzyme. These would lead to 14-3-3–mediated stabilization of CSR factors on S region DNA and enhancement of AID and PKA activity. 14-3-3 adaptors also directly interacted with Ung, which together with APEs mediates the dominant pathway of DSB generation in CSR[30, 31]. The direct interaction of 14-3-3 adaptors with Ung likely serves two important functions. First, 14-3-3 adaptors possibly facilitate AID and Ung reciprocal stabilization on S region DNA[32], as 14-3-3 possibly bridge AID and Ung to form an AID–14-3-3–Ung complex. This notion is further supported by findings that the reciprocal and cooperative stabilization of AID and Ung depends on the AID C-terminal region, which, as we showed[2], mediates 14-3-3–AID interaction. Second, 14-3-3 may enhance the processing of AID-inserted

dUs by Ung for the eventual generation of DSBs. This putative 14-3-3 function would complement and/or enhance that of Rev1, which serves as a scaffold for Ung by stabilizing Ung on S region DNA and enhancing its enzymatic activity[12]. Mismatch repair (MMR) proteins Msh2 and Msh6, recognize deoxyuracil:deoxyguanine mismatches and recruit 5'→3' exonuclease I (ExoI) to the generate DSBs[33], and they stabilize AID on S region DNA in a manner dependent on AID C-terminal region[32]. 14-3-3 adaptors have been shown to interact with ExoI[34], suggesting that 14-3-3 adaptors are also involved in MMR-dependent DSB generation. The critical importance of the interaction between 14-3-3 adaptors and essential CSR factors, likely contribute to the assembly of the CSR machinery, which includes AID, Ung, Msh2 and Msh6[32, 33].

14-3-3 nuclear foci colocalized with RPA nuclear foci despite no direct interaction between 14-3-3 and RPA1, the ssDNA-binding subunit, suggesting that RPA1 can only interact with 14-3-3 through another CSR-related factor, such as phosphorylated AID at S38 to form an RPA–AID–14-3-3 complex. RPA has been suggested to mark AID-mediated DNA damage sites[35] and can bind several CSR factors involved in DSB generation, such as Ung[36], MMR elements[37] and the Mre11/Rad50/Nbs1 complex[38]. RPA may also be key to the transition from formation of DSB-generating macromolecular complexes to DSB-resolving complexes on S regions, as RPA can also bind factors that are involved in CSR DSB resolution, such as γ-H2AX, 53BP1 and DNA-dependent protein kinase, catalytic subunit[30].

CSR to IgG1 in primary B cells was significantly reduced in the presence of HIV-1 viral component, Vpr; Vpr was also reported to inhibit CSR to IgA in CH12F3 B cells[13]. The CSR

inhibitory activities of Vpr segregated within three structural clusters (I, II and III) corresponding to the three Vpr helices. Therefore, our studies suggest the notion that CSR inhibition by Vpr is through a "multi-prong" strategy. Interestingly, cluster I peptides encompassed the Ung-binding Vpr region[39] and cluster III peptides straddled the 14-3-3- and PKA-interacting Vpr regions[17, 40]. Inhibition of CSR by Vpr did not affect AID expression or germline I_H-C_H transcription, suggesting that unlike HIV-1 Nef, which inhibits CSR by interfering with CD40-signaling and NF-κB activation[41], signaling events induced by primary CSR-stimuli and/or secondary CSR-stimuli is not affected by Vpr. By contrast, intimate CSR mechanisms was likely disrupted by Vpr, particularly the binding of 14-3-3 to S region 5'-AGCT-3' repeats, to H3K9acS10ph, or to important CSR factors, such as AID, PKA and Ung. This notion is supported by our data that recruitment of 14-3-3γ to Sμ and Sγ1 DNA was disrupted by Vpr, and that essential CSR factors such as 14-3-3ζ, AID, PKA-Cα and Ung directly interacted with Vpr. Reduced binding of 14-3-3γ to S regions, perhaps in conjunction with putative blocking of 14-3-3 and AID interaction by Vpr, lead to reduced AID recruitment to Sμ and Sγ1 DNA. Importantly, proliferation, survival or cell cycle of B cells was not affected in the presence of Vpr, by contrast Vpr–mediated cycle arrest in T cells has been reported [42].

As we have also shown here, AID colocalized with Vpr in HIV-1^+ patients lymph node germinal center B cells. In addition, HIV-1^- B cells internalized Vpr when cocultured with HIV-1-infected $CD4^+$ T cells. B cell internalization of HIV-1 Vpr is likely facilitated by CD21[43, 44], CD40 and/or binding of DC-SIGN[13] – Vpr can be released from virions or infected T cells in an extracellular form[45], which can be internalized by bystander B cells through protein transduction[46]. Irrespective of Vpr entry route, CSR and the generation of class-switched IgG,

possibly including HIV neutralizing IgG antibodies[19, 41], is efficiently inhibited by Vpr, leading to HIV-1 evading immune response and persistently infecting the host.

Overall, our findings provide evidence that 14-3-3 adaptor proteins nucleate the assembly of the AID-centered CSR machinery on 5'-AGCT-3' DNA repeats and H3K9acS10ph marks in S regions that are set to undergo S–S recombination (**Figure 2.14**). They also suggest that CSR DNA–protein and/or protein–protein complexes can be destabilized by naturally occurring molecules, leading to inhibition of CSR, thereby providing a basis for the identification of synthetic small molecule compounds, such as those that disrupt DNA–protein and/or protein–protein interactions involving 14-3-3[47, 48], or biologics that can effectively inhibit unwanted CSR, such as CSR underlying the generation of IgG and IgA autoantibodies in autoimmunity and atopic IgE antibodies in allergies and asthma.

2.6 MATERIALS AND METHODS

B lymphocytes

Spontaneously switching human sIgμ$^+$ sIgδ$^+$ 4B6 B cells and inducible switching human sIgμ$^+$ sIgδ$^+$ 2E2 B cells were derived from the CSR- and SHM-inducible human monoclonal sIgμ$^+$ sIgδ$^+$ CL-01 B cell line[2, 17, 49]. Single B cell suspensions were prepared from murine spleens using a 70-μm cell strainer. B cells were suspended in RPMI-1640 medium (Invitrogen) supplemented with FBS (10% v/v, Thermo Scientific), penicillin-streptomycin and amphotericin B fungizone (1% v/v) and 50 μM β-mercaptoethanol (FBS-RPMI) [50].

Class-switch DNA recombination

To analyze CSR by surface Ig, sIgμ$^+$ sIgδ$^+$ murine B cells were cultured at 10^5 cell/ml in FBS-RPMI in the presence of LPS deproteinized by chloroform extraction (3 μg/ml, from *E. coli*, serotype 055:B5, Sigma-Aldrich) plus recombinant mIL-4 (4 ng/ml, R&D Systems) for CSR from IgM to IgG1. B cells were harvested and stained using phycoerythrin (PE)-labeled anti–mouse B220 mAb (clone RA3-6B2, BD Biosciences), 7–aminoactinomycin D (7–AAD, Sigma-Aldrich) and allophycocyanin (APC)-labeled anti–mouse IgG1 mAb (clone X56, BD Biosciences) using FACSCalibur™ flow cytometer (BD Biosciences). Dead (7–AAD$^+$) cells were excluded from analysis.

Bimolecular fluorescence complementation (BiFC)

BiFC assays were performed as we described[2]. Briefly, EYFP was split into two complementary moieties: the N-terminal 154 amino acids (EYFP1–154) and the C-terminal 84 amino acids

(EYFP155–238). EYFP1–154 was fused with Flag–tagged AID or AID mutants, PKA-Cα, PKA-RIα, RPA1, Ung or Ung mutants, or 14-3-3ζ; EYFP155–238 was fused with influenza hemagglutinin (HA)–tagged 14-3-3β, ε, γ, η, σ, τ or ζ, or Vpr. 5×10^5 HeLa cells cultured in DMEM (Invitrogen) supplemented with FBS, were transfected with 1 μg of plasmid using Lipofectamine™ (Life Technologies). After 24 hours, cells were analyzed for cell viability (7–AAD$^-$) and for EYPF intensity by FACSCalibur™ flow cytometer (BD Biosciences); after 36 hours, cells were imaged for cell viability (ProLong Gold Antifade Reagent with 4',6'-diamidino-2-phenylindole, DAPI, Invitrogen) and for EYFP intensity by an Olympus FluoView 1000 confocal microscope.

Chromatin immunoprecipitation (ChIP)

ChIP assays were performed as we described[2]. B cells were treated with 1% (v/v) formaldehyde for 10 min at 25 °C to crosslink chromatin before being washed with cold PBS containing protease inhibitors (Roche) and resuspended in lysis buffer (20 mM Tris-HCl, 200 mM NaCl, 2 mM EDTA, 0.1% w/v SDS and protease inhibitors, pH 8.0). Chromatin was sonicated to yield DNA fragments (about 200 to 600 bps), pre-cleared with protein A agarose beads (Pierce) and then incubated with rabbit anti–14-3-3γ Ab (catalog # 18647, IBL, Inc.) or mouse anti–AID mAb (catalog # 39-2500, Invitrogen) overnight at 4 °C. Immune complexes were precipitated by Protein A agarose beads, washed and then eluted with elution buffer (50 mM Tris-HCl, 0.5% SDS, 200 mM NaCl, 100 μg/ml proteinase K, pH 8.0), followed by incubation at 65°C for 4 hours to reverse formaldehyde cross-links and digest proteins. DNA in the supernatant was purified using a QIAquick PCR purification kit (Qiagen). Recovered DNA was specified by PCR using the following oligonucleotide primers: Sμ, forward

5'-GCTAAACTGAGGTGATTACTCTGAGGTAAG-3' and reverse 5'-GTTTAGCTTAGCGGCCCAGCTCATTCCAGT-3'; Sγ1, forward 5'-ATAAGTAGTAGTTGGGGATTC-3' and reverse 5'-CTCAGCCTGGTACCTTATACA-3'. Data were normalized to input chromatin DNA and depicted as enrichment of each amplicon DNA relative to baseline value obtained using an irrelevant mAb.

Aicda and IgH locus germline I_H-C_H, circle Iγ1- Cμ and post-recombination Iμ-C_H transcripts

RNA was extracted from 2 x 10^6 cells using the RNeasy Mini Kit (Qiagen) according to the manufacturer's protocol. Levels of *Aicda* transcripts, germline Iμ-Cμ and Iγ1-Cγ1 transcripts, circle Iγ1- Cμ transcripts and post-recombination Iμ-Cγ1 transcripts were quantified by reverse transcription (RT) and real-time quantitative PCR (qPCR). First-strand cDNAs were synthesized from equal amounts of total RNAs (2 μg) using the SuperScript™ III First-Strand Synthesis System (Invitrogen). Real-time qPCR analysis was performed using the DNA Engine Opticon Real-Time PCR Detection System (Bio-Rad Laboratories) to measure SYBR-green (DyNAmo HS SYBR Green) incorporation with the following protocol: 50 °C for 2 min, 95 °C for 10 min, 40 cycles of 95 °C for 10 sec, 60 °C for 20 sec, 72 °C for 30 sec, 80 °C for 1 sec, and data acquisition at 80 °C, and 72 °C for 10 min. Melting curve analysis was performed from 72°-95 °C and samples were incubated for another 5 min at 72 °C. The ΔΔCt method was used to analyze levels of transcripts and data were normalized to levels of *Gapdh* transcripts. For qPCR, the following primers were used: *Aicda* transcripts, forward 5'-TGCTACGTGGTGAAGAGGAG -3' and reverse 5'-TCCCAGTCTGAGATGTAGCG-3'; germline Iμ-Cμ transcripts, forward 5'-ACCTGGGAATGTATGGTTGTGGCTT-3' and reverse 5'- TCTGAACCTTCAAGGATGCTCTTG -3'; germline Iγ1-Cγ1 transcripts, forward 5'-

TCGAGAAGCCTGAGGAATGTG -3' and reverse 5'-ATGGAGTTAGTTTGGGCAGCA-3'; circle Iγ1- Cμ transcripts, forward 5'-GGCCCTTCCAGATCTTTGAG-3' and reverse 5'-ACCTGGGAATGTATGGTTGTGGCTT-3'; post-recombined Iμ-Cγ1 transcripts, forward 5'-ACCTGGGAATGTATGGTTGTGGCTT -3' and reverse 5'-ATGGAGTTAGTTTGGGCAGCA-3'; *Gapdh* transcripts, forward 5'-TTCACCACCATGGAGAAGGC-3' and reverse 5'-GGCATGGACTGTGGTCATGA-3'.

GST pull-down assays

Spleen B cells (10^7) were stimulated with LPS plus mIL-4 for 48 hours. Cells were collected and resuspended in lysis buffer (20 mM of Tris-Cl, pH 7.5, 150 mM of NaCl, 0.5 mM of EDTA, 0.25% (v/v) of NP-40) supplemented with phosphatase inhibitors $Na_4P_2O_7$ (1 mM), NaF (10 mM) and $NaVO_3$ (1 mM) and a cocktail of protease inhibitors (Sigma). After sonication and centrifugation, protein lysates were precleared with immobilized Glutathione Magnetic Beads (Pierce) bound to glutathione S-transferase (GST) for 1 hour at 4 °C. Precleared whole cell lysates were then probed with immobilized Glutathione Magnetic Beads bound to either GST or GST–14-3-3γ for 1 hour at 4 °C. After three times of washing with lysis buffer, protein complexes were eluted in the SDS sample buffer and fractionated by SDS-PAGE.

Immunoblotting

Fractionated protein complexes were transferred onto polyvinylidene difluoride (PVDF) membranes (Thermo Scientific) at 4 ^oC. After blocking and overnight incubation with rabbit anti–14-3-3γ Ab (catalog # 18647, IBL, Inc.), mouse anti–AID mAb (catalog # 39-2500, Invitrogen), rabbit anti–PKAα cat Ab (catalog # 903, Santa Cruz Biotechnology), rabbit anti–

Ung Ab (catalog # 103236, GeneTex), mouse anti–GAPDH mAb (catalog # 239, GeneTex), mouse anti–Flag mAb (catalog # F3165, Sigma) or mouse anti–β-actin mAb (catalog # A5441, Sigma) the membranes were incubated with horseradish peroxidase (HRP)-conjugated secondary Abs. After washing with 0.05% PBS-Tween 20, bound HRP-conjugated Abs were detected using Amersham ECL Plus Western Blotting Detecting Reagents (GE Healthcare).

Image analysis

To detect codistributing molecules, human B cells were spun onto cover slips pre-coated with 10 μg/ml poly-D-lysine (Sigma-Aldrich), fixed with 2% paraformaldehyde and permeabilized with 0.25% Triton X-100. After blocking with 1% BSA, cells were stained with a rabbit anti–14-3-3 Ab (catalog # ab6081, Abcam) and a mouse anti–AID mAb (catalog # 39-2500, Invitrogen) or a mouse anti–RPA/p34 mAb (catalog # MS-691-P1, NeoMarkers), followed by staining with FITC-conjugated goat anti–rabbit and TRITC-conjugated goat anti–mouse IgG Ab. Confocal microscopy images of spontaneously switching 4B6 B cells cultured at 5×10^4 cell/ml in (FBS-RPMI) and human 2E2 B cells stimulated with nil or anti–hCD40 mAb plus hIL-4 were captured by an LSM510-META NLO multi-photon confocal microscope and analyzed using the laser scanning microscope (LSM) Image Examiner software (Carl Zeiss Microimaging, Inc.). Each pixel in individual cells was analyzed for intensity in green (14-3-3) and red (AID or RPA). The ratio of the number of yellow pixels, to the total number of yellow and green pixels was used to quantify the percentage of 14-3-3 molecules codistributing with AID or RPA.

To detect nuclear foci, spontaneously switching human 4B6 B cells or primary mouse B cells stimulated with LPS plus mIL-4 were washed and then extracted in cytoskeletal (CSK) buffer to

deplete soluble cytoplasmic and nuclear components before resuspended in 4% paraformaldehyde in PBS to crosslink chromosomal DNA and bound proteins. Cells were then processed, stained and immunofluorescence images were taken at multiple confocal planes. Such *z*-stacked images were de-convoluted to generate high-resolution images. All images were pseudo-colored for presentation. B cells were scored as positive for colocalization of 14-3-3 nuclear foci with AID nuclear foci or RPA nuclear foci when showing at least two colocalizing foci, defined as spots within the top 75% pixel intensity of each fluorescence on the pixel intensity map by the Autoquant® X software (Media Cybernetics, Inc.). The percentages of positive cells at 0 hour, 24 hours and 48 hours of stimulation were plotted against time points and the Mander's overlapping coefficiency were calculated to be between 0.91-0.99 (maximum is 1.0), thereby reflecting a time-dependent increase of colocalization. Processing and staining of mouse primary B cells or human 4B6 B cells were performed following a protocol for foci formation analysis[51].

Retroviral transduction

The coding sequence of GFP-Vpr (originally from the pGFP-Vpr plasmid, catalog # 11386, *The NIH AIDS Research and Reference Reagents Program*) was cloned into the retroviral vector pCSretTAC to generate pTAC-GFP-Vpr (generation of pTAC-GFP was described before[2]). Retroviral constructs were transfected along with the pCL–Eco retrovirus–packaging vector into HEK293T cells using the ProFection Mammalian Transfection System® (Promega). Transfected cells were cultured in FBS-RPMI in the presence of chloroquine (25 μM) for 8 hours. After the removal of chloroquine, retrovirus-containing culture supernatants were harvested every 12 hours for 48 hours. For transduction and CSR analysis, mouse B cells were activated with LPS

for 24 hours and then centrifuged at 500 *g* together with viral particles in the presence of 6 μg/ml polybrene (Sigma-Aldrich) for 90 min at 25°C. Transduced B cells were then cultured in virus-free FBS-RPMI in the presence of LPS plus mIL-4 for 48 hours for transcript analysis, or for 72 hours for flow cytometry analysis of surface IgG1 and B220 expression in GFP^+ B cells.

HIV-1 Vpr (15-mer) peptides

Twenty-two Vpr peptides, each of 15–amino acids in length and each with a sequential 11–amino acid overlap, covering the entire 96–amino acid viral protein, was provided by *The NIH AIDS Research and Reference Reagents Program* (catalog # 6447). Vpr peptides were dissolved in DMSO and then added to LPS-activated B cell cultures for 24 hours, after which B cells were stimulated with LPS plus mIL-4 for 72 hours to induce CSR from IgM to IgG1.

Detection of Vpr in human B lymphocytes

Tonsils from HIV-1^- subjects and lymph nodes from HIV-1^+ patients (UC Irvine Medical Center) were sectioned (7 μm) onto glass slides and stained with Abs specific to human using rabbit anti–Vpr Ab (catalog #11836, *NIH AIDS Research and Reference Reagents Program*) alone, or with mouse anti–human CD20 Ab (clone 2H7, eBioscience) or with mouse anti–AID mAb (catalog # 39-2500, Invitrogen). Color was development by DAB+ chromogen (Dako) and slides were dehydrated and counterstained with hematoxylin. Images were captured at 40X magnification using Nikon Eclipse E400. To detect B cell uptake of Vpr, human 4B6 B cells were cocultured for 7 days with human CEM.NK^R-CCR5 T cells infected with nil or HIV-192US657 (a clinical isolate of the primary R5 HIV-1 strain[20, 21, 22]), fixed with 2% paraformaldehyde and permeabilized with 0.25% Triton X-100 (Sigma-Aldrich). After blocking

with 1% BSA, cells were stained with FITC-conjugated anti–μ mAb or FITC-conjugated anti–CD4 mAb to identify $sIg\mu^+$ 4B6 cells or $CD4^+$ $CEM.NK^R$-CCR5 T cells, respectively and rabbit anti–Vpr Ab (catalog # 11836, *NIH AIDS Research and Reference Reagents Program*) and Alexa 594-conjugated goat anti–rabbit IgG Ab to identify Vpr uptake for 1 hour. DAPI was used to stain the nucleus. Fluorescence images were captured at 100X magnification. All experiments involving HIV-192US657 were performed in a dedicated Biosafety Level III facility.

Ethics Statement

Human materials. All human subject materials were surgical remnants collected and maintained for research purposes by the School of Medicine Department of Pathology, University of California, Irvine, CA 92697 – under patient privacy rule, no information was disclosed on age, sex and identity of the patient sources of the surgical materials. The use of these materials for research associated with this study was specifically approved by the Institutional Review Board of the University of California, Irvine.

Mice. C57BL/6 mice 8-12 weeks old were housed in a pathogen-free facility and provided with autoclaved food and deionized water. The Institutional Animal Care and Use Committee of the University of California, Irvine, CA 92697, specifically approved the use of mice for the isolation of primary murine B cells for research associated with this study.

Statistical analysis

Statistic analysis was performed using Excel® software (Microsoft) to determine *P* values by two-tailed paired student's *t*-test. *P* values less than 0.05 were considered significant.

2.7 REFERENCES

1. Fu H, Subramanian RR, Masters SC. 14-3-3 proteins: structure, function, and regulation. *Annu Rev Pharmacol Toxicol* 2000, **40:** 617-647.

2. Xu Z, Fulop Z, Wu G, Pone EJ, Zhang J, Mai T*, et al.* 14-3-3 adaptor proteins recruit AID to 5'-AGCT-3'-rich switch regions for class switch recombination. *Nat Struct Mol Biol* 2010, **17**(9)**:** 1124-1135.

3. Li G, White CA, Lam T, Pone EJ, Tran DC, Hayama KL*, et al.* Combinatorial H3K9acS10ph histone modifications in IgH locus S regions target 14-3-3 adaptors and AID to specify antibody class-switch DNA recombination. *Cell Rep* 2013, **5:** D.O.I 10.1016/j.cellrep.2013.1009.1031.

4. Morrison DK. The 14-3-3 proteins: integrators of diverse signaling cues that impact cell fate and cancer development. *Trends Cell Biol* 2009, **19:** 16-23.

5. Chaudhuri J, Khuong C, Alt FW. Replication protein A interacts with AID to promote deamination of somatic hypermutation targets. *Nature* 2004, **430**(7003)**:** 992-998.

6. Kerppola TK. Design and implementation of bimolecular fluorescence complementation (BiFC) assays for the visualization of protein interactions in living cells. *Nat Protoc* 2006, **1**(3)**:** 1278-1286.

7. Barreto V, Reina-San-Martin B, Ramiro AR, McBride KM, Nussenzweig MC. C-terminal deletion of AID uncouples class switch recombination from somatic hypermutation and gene conversion. *Mol Cell* 2003, **12**(2)**:** 501-508.

8. Geisberger R, Rada C, Neuberger MS. The stability of AID and its function in class-switching are critically sensitive to the identity of its nuclear-export sequence. *Proc Natl Acad Sci USA* 2009, **106**(16)**:** 6736-6741.

9. Cheng HL, Vuong BQ, Basu U, Franklin A, Schwer B, Astarita J*, et al.* Integrity of the AID serine-38 phosphorylation site is critical for class switch recombination and somatic hypermutation in mice. *Proc Natl Acad Sci USA* 2009, **106**(8)**:** 2717-2722.

10. Vuong BQ, Lee M, Kabir S, Irimia C, Macchiarulo S, McKnight GS*, et al.* Specific recruitment of protein kinase A to the immunoglobulin locus regulates class-switch recombination. *Nat Immunol* 2009, **10**(4)**:** 420-426.

11. Pasqualucci L, Kitaura Y, Gu H, Dalla-Favera R. PKA-mediated phosphorylation regulates the function of activation-induced deaminase (AID) in B cells. *Proc Natl Acad Sci USA* 2006, **103**(2)**:** 395-400.

12. Zan H, White CA, Thomas LM, Mai T, Li G, Xu Z*, et al.* Rev1 recruits Ung to switch regions and enhances dU glycosylation for immunoglobulin class switch DNA recombination. *Cell Rep* 2012, **2**(5)**:** 1220-1232.

13. Begum NA, Izumi N, Nishikori M, Nagaoka H, Shinkura R, Honjo T. Requirement of non-canonical activity of uracil DNA glycosylase for class switch recombination. *J Biol Chem* 2007, **282**(1)**:** 731-742.

14. Begum NA, Stanlie A, Doi T, Sasaki Y, Jin HW, Kim YS*, et al.* Further evidence for involvement of a noncanonical function of uracil DNA glycosylase in class switch recombination. *Proc Natl Acad Sci USA* 2009, **106**(8)**:** 2752-2757.

15. Kim EC, Edmonston CR, Wu X, Schaffer A, Casali P. The HoxC4 homeodomain protein mediates activation of the immunoglobulin heavy chain 3' hs1,2 enhancer in human B cells. Relevance to class switch DNA recombination. *J Biol Chem* 2004, **279:** 42258-42269.

16. Kino T, De Martino MU, Charmandari E, Ichijo T, Outas T, Chrousos GP. HIV-1 accessory protein Vpr inhibits the effect of insulin on the Foxo subfamily of forkhead transcription factors by interfering with their binding to 14-3-3 proteins: potential clinical implications regarding the insulin resistance of HIV-1-infected patients. *Diabetes* 2005, **54**(1)**:** 23-31.

17. Barnitz RA, Wan F, Tripuraneni V, Bolton DL, Lenardo MJ. Protein Kinase A phosphorylation activates Vpr-induced cell cycle arrest during Human Immunodeficiency Virus Type-1 infection. *J Virol* 2010, **In press**.

18. Wecker K, Morellet N, Bouaziz S, Roques BP. NMR structure of the HIV-1 regulatory protein Vpr in H2O/trifluoroethanol. *Eur J Biochem* 2002, **269**(15)**:** 3779-3788.

19. Xu W, Santini PA, Sullivan JS, He B, Shan M, Ball SC*, et al.* HIV-1 evades virus-specific IgG2 and IgA responses by targeting systemic and intestinal B cells via long-range intercellular conduits. *Nat Immunol* 2009, **10**(9)**:** 1008-1017.

20. Forthal DN, Gilbert PB, Landucci G, Phan T. Recombinant gp120 vaccine-induced antibodies inhibit clinical strains of HIV-1 in the presence of Fc receptor-bearing effector cells and correlate inversely with HIV infection rate. *J Immunol* 2007, **178**(10)**:** 6596-6603.

21. Forthal DN, Landucci G, Phan TB, Becerra J. Interactions between natural killer cells and antibody Fc result in enhanced antibody neutralization of human immunodeficiency virus type 1. *J Virol* 2005, **79**(4)**:** 2042-2049.

22. Hessell AJ, Hangartner L, Hunter M, Havenith CE, Beurskens FJ, Bakker JM*, et al.* Fc receptor but not complement binding is important in antibody protection against HIV. *Nature* 2007, **449**(7158)**:** 101-104.

23. Doi T, Kato L, Ito S, Shinkura R, Wei M, Nagaoka H*, et al.* The C-terminal region of activation-induced cytidine deaminase is responsible for a recombination function other than DNA cleavage in class switch recombination. *Proc Natl Acad Sci USA* 2009, **106**(8)**:** 2758-2763.

24. Kellner WA, Ramos E, Van Bortle K, Takenaka N, Corces VG. Genome-wide phosphoacetylation of histone H3 at Drosophila enhancers and promoters. *Genome Res* 2012, **22**(6)**:** 1081-1088.

25. Liu M, Duke JL, Richter DJ, Vinuesa CG, Goodnow CC, Kleinstein SH*, et al.* Two levels of protection for the B cell genome during somatic hypermutation. *Nature* 2008, **451**(7180)**:** 841-845.

26. Yamane A, Resch W, Kuo N, Kuchen S, Li Z, Sun HW*, et al.* Deep-sequencing identification of the genomic targets of the cytidine deaminase AID and its cofactor RPA in B lymphocytes. *Nat Immunol* 2011, **12**(1)**:** 62-69.

27. Staszewski O, Baker RE, Ucher AJ, Martier R, Stavnezer J, Guikema JE. Activation-induced cytidine deaminase induces reproducible DNA breaks at many non-Ig Loci in activated B cells. *Mol Cell* 2011, **41**(2)**:** 232-242.

28. Pavri R, Gazumyan A, Jankovic M, Di Virgilio M, Klein I, Ansarah-Sobrinho C*, et al.* Activation-induced cytidine deaminase targets DNA at sites of RNA polymerase II stalling by interaction with Spt5. *Cell* 2010, **143**(1)**:** 122-133.

29. Kenter AL. AID targeting is dependent on RNA polymerase II pausing. *Semin Immunol* 2012, **24**(4)**:** 281-286.

30. Xu Z, Zan H, Pone EJ, Mai T, Casali P. Immunoglobulin class-switch DNA recombination: induction, targeting and beyond. *Nat Rev Immunol* 2012, **12**(7)**:** 517-531.

31. Masani S, Han L, Yu K. Apurinic/apyrimidinic endonuclease 1 is the essential nuclease during immunoglobulin class switch recombination. *Mol Cell Biol* 2013, **33**(7)**:** 1468-1473.

32. Ranjit S, Khair L, Linehan EK, Ucher AJ, Chakrabarti M, Schrader CE*, et al.* AID binds cooperatively with UNG and Msh2-Msh6 to Ig switch regions dependent upon the AID C terminus. *J Immunol* 2011, **187**(5)**:** 2464-2475.

33. Rada C, Di Noia JM, Neuberger MS. Mismatch recognition and uracil excision provide complementary paths to both Ig switching and the A/T-focused phase of somatic mutation. *Mol Cell* 2004, **16**(2)**:** 163-171.

34. Andersen SD, Keijzers G, Rampakakis E, Engels K, Luhn P, El-Shemerly M*, et al.* 14-3-3 checkpoint regulatory proteins interact specifically with DNA repair protein human exonuclease 1 (hEXO1) via a semi-conserved motif. *DNA Repair* 2012, **11**(3)**:** 267-277.

35. Yamane A, Robbiani DF, Resch W, Bothmer A, Nakahashi H, Oliveira T*, et al.* RPA accumulation during class switch recombination represents 5'-3' DNA-end resection during the S-G2/M phase of the cell cycle. *Cell Rep* 2013, **3**(1)**:** 138-147.

36. Otterlei M, Warbrick E, Nagelhus TA, Haug T, Slupphaug G, Akbari M*, et al.* Post-replicative base excision repair in replication foci. *EMBO J* 1999, **18:** 3834-3844.

37. Guo S, Zhang Y, Yuan F, Gao Y, Gu L, Wong I*, et al.* Regulation of replication protein A functions in DNA mismatch repair by phosphorylation. *J Biol Chem* 2006, **281:** 21607-21616.

38. Oakley GG, Tillison K, Opiyo SA, Glanzer JG, Horn JM, Patrick SM. Physical interaction between replication protein A (RPA) and MRN: involvement of RPA2 phosphorylation and the N-terminus of RPA1. *Biochemistry* 2009, **48:** 7473-7481.

39. Selig L, Benichou S, Rogel ME, Wu LI, Vodicka MA, Sire J*, et al.* Uracil DNA glycosylase specifically interacts with Vpr of both human immunodeficiency virus type 1 and simian immunodeficiency virus of sooty mangabeys, but binding does not correlate with cell cycle arrest. *J Virol* 1997, **71**(6)**:** 4842-4826.

40. Kino T, Gragerov A, Valentin A, Tsopanomihalou M, Ilyina-Gragerova G, Erwin-Cohen R*, et al.* Vpr protein of human immunodeficiency virus type 1 binds to 14-3-3 proteins and facilitates complex formation with Cdc25C: implications for cell cycle arrest. *J Virol* 2005, **79**(5)**:** 2780-2787.

41. Qiao X, He B, Chiu A, Knowles DM, Chadburn A, Cerutti A. Human immunodeficiency virus 1 Nef suppresses CD40-dependent immunoglobulin class switching in bystander B cells. *Nat Immunol* 2006, **7**(3)**:** 302-310.

42. Bolton DL, Barnitz RA, Sakai K, Lenardo MJ. 14-3-3 theta binding to cell cycle regulatory factors is enhanced by HIV-1 Vpr. *Biol Direct* 2008, **3:** 17.

43. Moir S, Malaspina A, Li Y, Chun TW, Lowe T, Adelsberger J*, et al.* B cells of HIV-1-infected patients bind virions through CD21-complement interactions and transmit infectious virus to activated T cells. *J Exp Med* 2000, **192**(5)**:** 637-646.

44. Stoiber H, Speth C, Dierich MP. Role of complement in the control of HIV dynamics and pathogenesis. *Vaccine* 2003, **21 Suppl 2:** S77-82.

45. Tungaturthi PK, Sawaya BE, Singh SP, Tomkowicz B, Ayyavoo V, Khalili K*, et al.* Role of HIV-1 Vpr in AIDS pathogenesis: relevance and implications of intravirion, intracellular and free Vpr. *Biomed Pharmacother* 2003, **57**(1)**:** 20-24.

46. Sherman MP, Schubert U, Williams SA, de Noronha CM, Kreisberg JF, Henklein P*, et al.* HIV-1 Vpr displays natural protein-transducing properties: implications for viral pathogenesis. *Virology* 2002, **302**(1)**:** 95-105.

47. Zhao J, Du Y, Horton JR, Upadhyay AK, Lou B, Bai Y*, et al.* Discovery and structural characterization of a small molecule 14-3-3 protein-protein interaction inhibitor. *Proc Natl Acad Sci USA* 2011, **108**(39)**:** 16212-16216.

48. Zhao J, Meyerkord CL, Du Y, Khuri FR, Fu H. 14-3-3 proteins as potential therapeutic targets. *Semin Cell Dev Biol* 2011, **22**(7)**:** 705-712.

49. Park SR, Zan H, Pal Z, Zhang J, Al-Qahtani A, Pone EJ*, et al.* HoxC4 binds to the promoter of the cytidine deaminase AID gene to induce AID expression, class-switch DNA recombination and somatic hypermutation. *Nat Immunol* 2009, **10**(5)**:** 540-550.

50. Pone EJ, Zhang J, Mai T, White CA, Li G, Sakakura J*, et al.* BCR-signalling synergizes with TLR-signalling for induction of AID and immunoglobulin class-switching through the non-canonical NF- κB pathway. *Nat Commun* 2012**:** doi: 10.1038/ncomms1769.

51. Wu G, Lin YT, Wei R, Chen Y, Shan Z, Lee WH. Hice1, a novel microtubule-associated protein required for maintenance of spindle integrity and chromosomal stability in human cells. *Mol Cell Biol* 2008, **28**(11)**:** 3652-3662.

CHAPTER 3

THE ROLE OF B CELL RAB7 IN T-DEPENDENT AND T-INDEPENDENT ANTIBODY RESPONSES

3.1 THE ROLE OF RAB7 IN B LYMPHOCYTES: ENGINEERING OF *Igh*$^{+/C}\gamma^{1\text{-}cre}$ *Rab7*$^{fl/fl}$ MICE

Autophagy-related double-membrane structures, which originate from the ER or mitochondrial membranes, play a role in MAPK p38 activation that is triggered by BCR and TLR9[1]. A role of intracellular membranes in B cell signal transduction is suggested by the regulation of CD40 and BCR signaling in immunity and inflammation by autophagy-related (Atg) factors, including Atg5[1, 2, 3, 4]. Rab7 small GTPase mediates the maturation of endosomes, intracellular membrane compartments in eukaryotes that have switched their bound Rab5 to Rab7, conversion of endosomes to lysosomes, and/or fusion of endosomes with autophagosomes to form amphisomes in different cell types[5]. In stressed cells, such as those having phagocytosed large extracellular components or having engulfed cytoplasmic components in response to challenging metabolic conditions, Rab7 mediates the fusion of autophagosomes or amphisomes with lysosomes to form autolysomes, in which cargo is degraded. Rab7 also promotes cell death induced by growth factor withdrawal and clearance of apoptotic bodies[6, 7, 8, 9]. It has been suggested that Rab7 may play critical roles in proliferating and differentiation of immune cells, which are not restricted under starving conditions.

The role or Rab7 has been described in T cells, but its role in B cells was unknown. Therefore, we wanted to address the role of **Rab7 in B cells**, specifically in B cells that are induced to class-switch. We constructed conditional *Igh*$^{+/C}\gamma^{1\text{-}cre}$ *Rab7*$^{fl/fl}$ mice, in which Rab7 expression is abrogated only in B cells undergoing *Igh*$^{C}\gamma^{1\text{-}cre}$ Iγ1-Sγ1-Cγ1-*cre* transcription, as induced by IL-4 together with a primary stimulus.

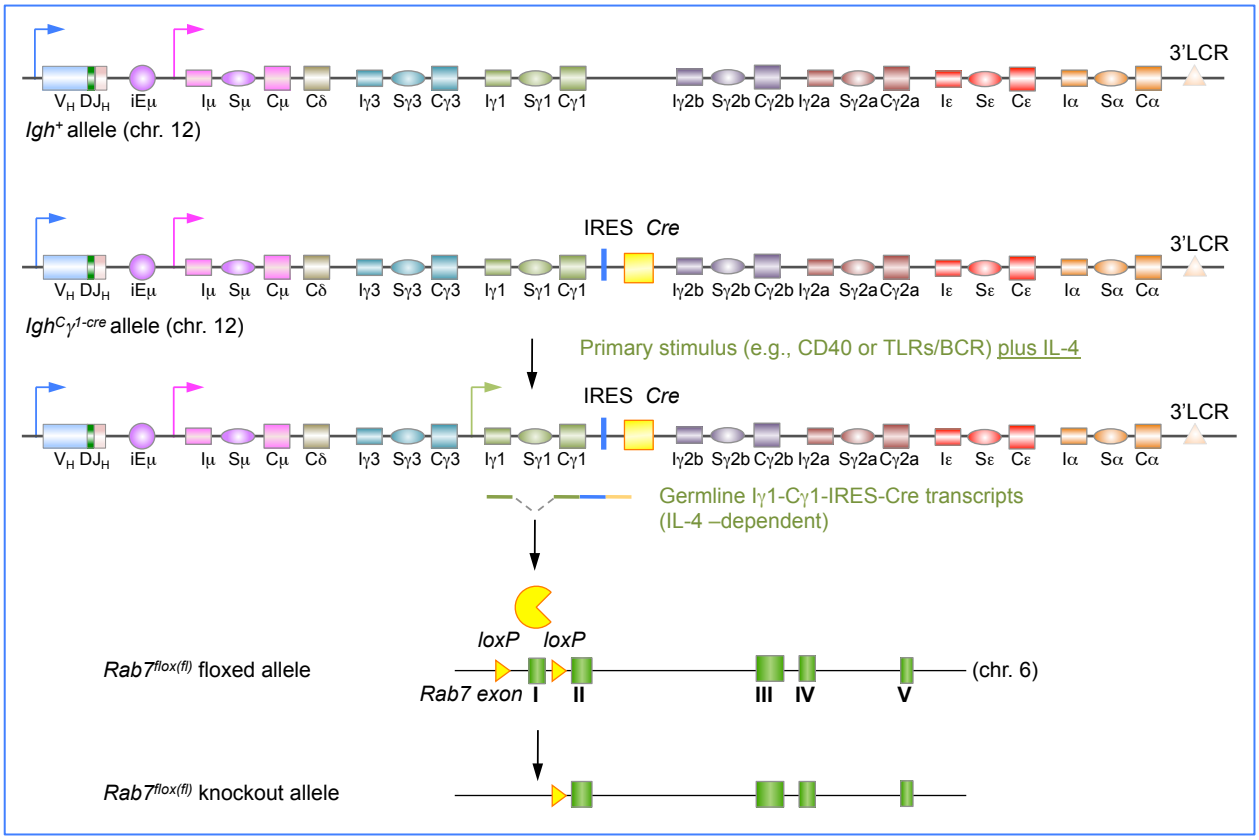

Figure 3.1 Engineering of $Igh^{+/C}\gamma^{1\text{-}cre}$ $Rab7^{flox/flox}$ mice (*Cγ1-Rab7KO*). The Cre recombinase is expressed only in B cells activated to undergo high levels of *IgH* **germline Iγ1-Sγ1-Cγ1 transcription.** *Cγ1-Rab7KO* mice will express germline Iγ1-Sγ1-Cγ1 transcripts from the Igh^{+} allele and germline Iγ1-Sγ1-Cγ1-cre transcripts from the $Igh^{+/C}\gamma^{1\text{-}cre}$ allele, as induced by **IL-4** (a "**secondary**" CSR-inducing stimulus; the other secondary stimuli include TGFβ and IFNγ) together with a "**primary" stimulus**" (e.g., CD40 or TLR/BCR engagement) during immune responses - IL-4 specifies CSR to IgG1 and IgE, but not to other IgG isotypes or IgA; Cre expression results in *Rab7* deletion of the first *Rab7* exon (total of five exons) flanked by loxP sites, as constructed by our collaborator Dr. A.L. Edinger. (back-crossed onto the C57BL/6 background for 9 generations). In all of our experiments, $Igh^{+/C}\gamma^{1\text{-}cre}$ $Rab7^{fl/fl}$ mice were used as conditional knockout mice and $Igh^{+/C}\gamma^{1\text{-}cre}$ $Rab7^{+/fl}$ mice were used as their "wildtype" littermate controls, as these mice did not display hypomorphism in the Rab7 protein expression. $Igh^{+/+}$ $Rab7^{fl/fl}$ mice were not chosen as "wildtype" controls because they have two Igh^{+} alleles capable of encoding IgG1, while $Igh^{+/C}\gamma^{1\text{-}cre}$ $Rab7^{fl/fl}$ mice had only one.

Unlike mice with *Rab7* deletion in germ cells[9, 10], $Igh^{+/C}\gamma^{1\text{-}cre}$ $Rab7^{fl/fl}$ mice were born at Mendelian ratio due to their intact *Rab7* locus throughout embryogenesis. They were indistinguishable from their $Igh^{+/+}$ $Rab7^{+/fl}$, $Igh^{+/+}$ $Rab7^{fl/fl}$ and $Igh^{+/C}\gamma^{1\text{-}cre}$ $Rab7^{+/fl}$ littermates in the size, fertility and organ morphology during development and maturation. This was expected, as in $Igh^{+/C}\gamma^{1\text{-}cre}$ $Rab7^{fl/fl}$ mice, efficient Cre recombinase expression and Cre-mediated *Rab7* KO occurred exclusively in B cells activated to undergo germline Iγ1-Sγ1-Cγ1-*cre* transcription in the $Igh^{C}\gamma^{1\text{-}cre}$ allele (**Figure 3.1**). This transcription process, like *IgH* germline Iγ1-Sγ1-Cγ1 transcription, was induced by IL-4 in the presence of a primary stimulus, such as CD154, LPS or CpG ODN plus anti–δ mAb/dex, leading to a virtual abrogation of Rab7 protein expression and its cytoplasmic localization in B cells (**Figure 3.2**).

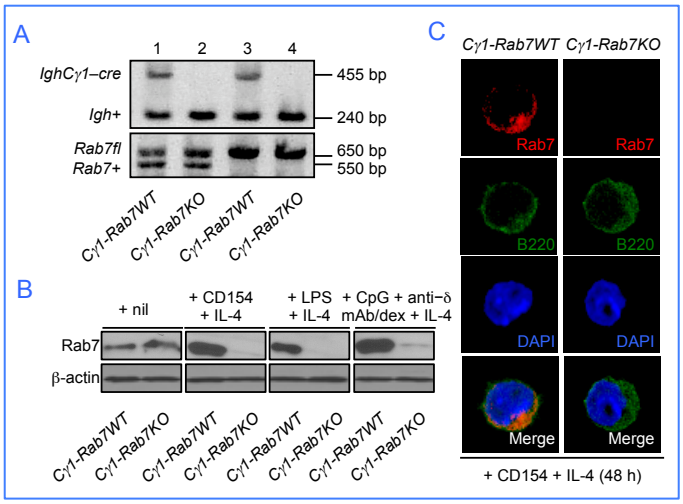

Figure 3.2 Abrogation of Rab7 protein expression in *Cγ1-Rab7KO* B cells stimulated by a primary stimulus plus IL-4. (**A**) DNA electrophoresis of PCR products from the genotyping of four littermates born from breeding of an *Cγ1-Rab7WT* mouse with an *Cγ1-Rab7KO* mouse. (**B**) Immunoblotting analysis of Rab7 expression in *Cγ1-Rab7KO* B cells stimulated with CD154, LPS, or CpG plus anti–δ/dex (as indicated) plus IL-4 for 48 h and their *Cγ1-Rab7WT* B cell counterparts. (**C**) Immunofluorescence staining and confocal microscopy analysis of Rab7 and B220 expression (pseudo-colored) in *Cγ1-Rab7KO* B cells stimulated with CD154 plus IL-4 for 48 h and their *Cγ1-Rab7WT* B cell counterparts. Data are representative of three independent experiments.

Consistent with the lack of $Igh^{C}\gamma^{1\text{-}cre}$ germline Iγ1-Sγ1-Cγ1-*cre* transcription in B cells and T cells during their development and maturation, $Igh^{+/C}\gamma^{1\text{-}cre}$ $Rab7^{fl/fl}$ mice displayed normal frequencies, cellularity and viability of B and T cells at different developmental stages in central and peripheral lymphoid organs, including B1 cells in the peritoneal cavity (**Figure 3.3**). Thus, $Igh^{+/C}\gamma^{1\text{-}cre}$ $Rab7^{fl/fl}$ mice show normal B and T cell development and maturation; $Igh^{+/C}\gamma^{1\text{-}cre}$ $Rab7^{fl/fl}$ B cells show abrogated Rab7 expression upon stimulation by a primary CSR-inducing stimulus plus IL-4.

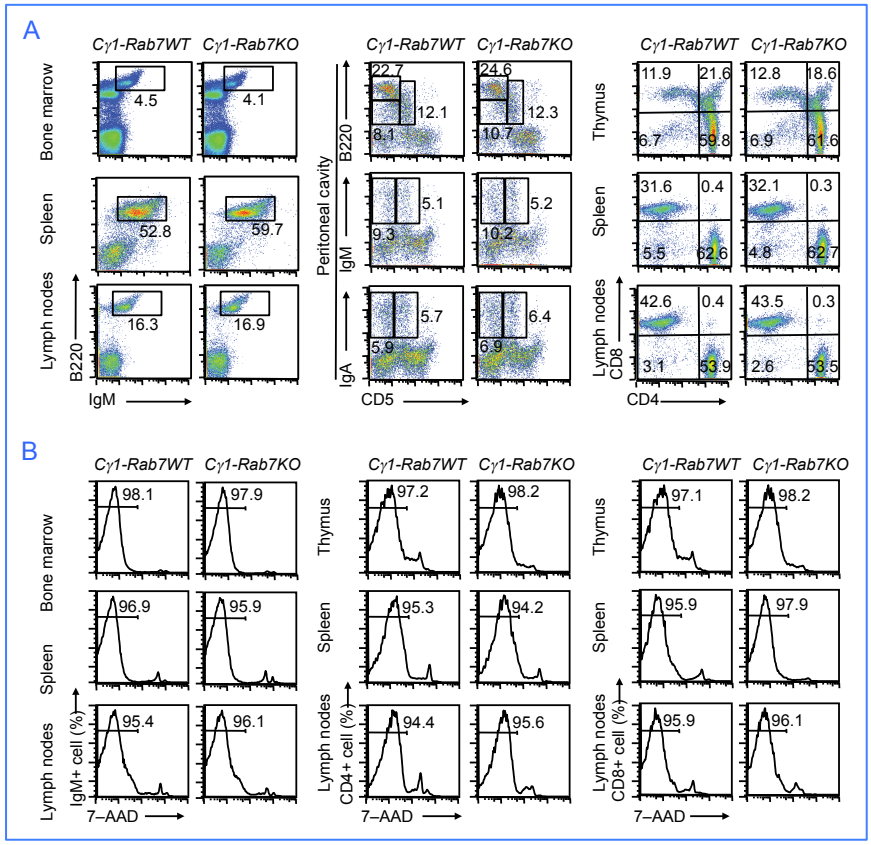

Figure 3.3 *Cγ1-Rab7KO* mice show normal B and T cell development and survival. (**A**) Flow cytometry analysis of expression of B220 and IgM in bone marrow, spleen and lymph node cells (left panels), expression of CD5, a B1 cell marker in humans and mice[11], and B220 in peritoneal cavity cells (B2 cells were $CD5^{-}$ $B220^{hi}$, B1a cells were $CD5^{+}$ $B220^{+}$ and B1b cells were $CD5^{-}$ $B220^{+}$) as well as that of CD5 and IgM or IgA (middle panels), and expression of CD4 and CD8 in thymus, spleen and lymph node cells (right panels) in *Cγ1-Rab7KO* mice and their *Cγ1-Rab7WT* littermates. (**B**) Flow cytometry analysis of the viability ($7\text{–}AAD^{-}$) of IgM^{+} B cells in the bone marrow, spleen and lymph nodes (left panels), as well as that of $CD4^{+}$ (middle panels) and $CD8^{+}$ (right panels) T cells in the thymus, spleen and lymph nodes in *Cγ1-Rab7KO* mice and their *Cγ1-Rab7WT* littermates. Data are representative of three independent experiments.

3.2 ABROGATION OF CSR: B CELL RAB7 IN ANTIBODY RESPONSES

In *Igh*$^{+/C}$*γ1*$^{-cre}$ *Rab7*$^{fl/fl}$ mice and their *Igh*$^{+/C}$*γ1*$^{-cre}$ *Rab7*$^{+/fl}$ littermate controls (which showed phenotypes comparable to those of *Igh*$^{+/C}$*γ1*$^{-cre}$ *Rab7*$^{+/+}$), IgG1expression was driven solely by the *Igh*$^{+}$ allele that had undergone a productive V_HDJ_H recombination and then CSR from Igμ to Igγ1, as the *Cre* sequence would interfere with the expression of *V_HDJ_H–Cγ1* in the *Igh*^{C}*γ1*$^{-cre}$ allele[12]. As compared to their *Igh*$^{+/C}$*γ1*$^{-cre}$ *Rab7*$^{+/fl}$ littermates, *Igh*$^{+/C}$*γ1*$^{-cre}$ *Rab7*$^{fl/fl}$ mice showed normal titers of serum IgM, but much reduced (by 85%) titers of IgG1 (**Figure 3.4A**).

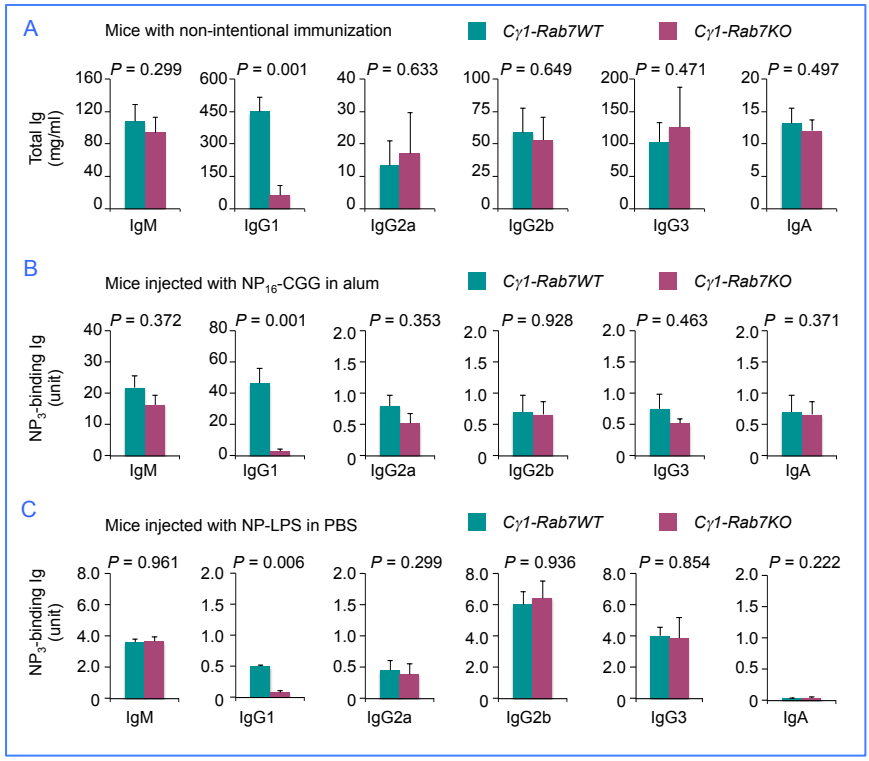

Figure 3.4 *Cγ1-Rab7KO* mice display reduced titers of overall IgG1 and antigen-specific IgG1. (**A**) ELISA of serum titers of IgM, IgG1, IgG2a, IgG2b, IgG3 and IgA in *Cγ1-Rab7KO* mice and their *Cγ1-Rab7WT* littermates (mean and s.e.m. of data from five pairs of mice). (**B**) ELISA of serum titers of high-affinity NP-specific (NP_3-binding) IgG1, IgG2a, IgG2b, IgG3 and IgA as well as NP_3-binding IgM (due to the high-avidity) in *Cγ1-Rab7KO* mice and their *Cγ1-Rab7WT* littermates 9 d after injection with NP-CGG (mean and s.e.m. of data from five pairs of mice). (**C**) ELISA of serum titers of NP_3-binding IgM, IgG1, IgG2a, IgG2b, IgG3 and IgA in *Cγ1-Rab7KO* mice and their *Cγ1-Rab7WT* littermates 9 d after injection with NP-LPS (mean and s.e.m. of data from three pairs of mice). *P* values, as calculated by paired student *t* test, less than 0.05 were considered significant.

We next addressed the role of Rab7 in a specific T-dependent response by injecting mice with NP-CGG, which elicits predominantly NP-binding IgM and IgG1. *Igh*$^{+/C}$*γ1*$^{-cre}$ *Rab7*$^{fl/fl}$ mice showed a severe defect (over 96% reduction) in generation of (high-affinity) NP-specific IgG1, but normal levels of NP-specific IgM and other IgG isotypes (IgG2a, IgG2b, IgG3) and IgA (**Figure 3.4B**). Likewise, *Igh*$^{+/C}$*γ1*$^{-cre}$ *Rab7*$^{fl/fl}$ mice could not produce T-independent NP-specific IgG1 response to NP-LPS (90% reduction), but were fully competent in generating NP-specific IgM, IgG2a, IgG2b and IgG3 (**Figure 3.4C**) – class-switching to IgG2b and IgG3 are induced by LPS alone. They had normal titers of other switched IgG isotypes (IgG2a, IgG2b, IgG3) and IgA, consistent with our prediction that B cells that were set to switch to these Ig isotypes maintained an intact *Rab7* locus due to their germline Iγ2a-Sγ2a-Cγ2a, Iγ2b-Sγ2b-Cγ2b or Iγ3-Sγ3-Cγ3 transcription and lack of Iγ1-Sγ1-Cγ1-*cre* transcription.

In *Igh*$^{+/C}$*γ1*$^{-cre}$ *Rab7*$^{fl/fl}$ mice injected with OVA, the levels of OVA-specific IgE and IgG1 as well as total IgE and IgG1 were significantly reduced, as compared to those in *Igh*$^{+/C}$*γ1*$^{-cre}$ *Rab7*$^{+/fl}$ littermates, while IgM levels were normal (**Figure 3.5**).

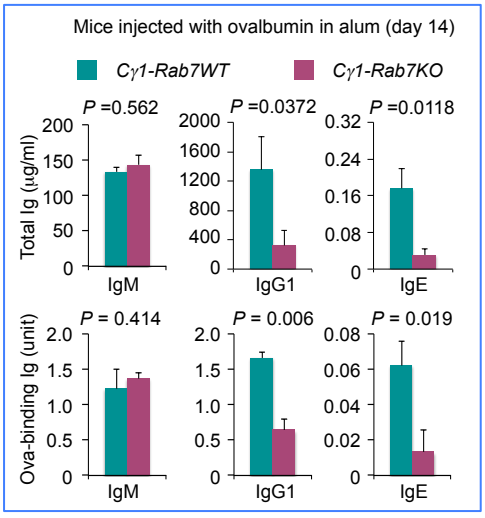

Figure 3.5 ***Cγ1-Rab7KO*** **B cells display impairment in CSR to IgE** ***in vivo.*** ELISA of titers of total (top panels) and ovalbumin-binding (bottom panels) IgM, IgG1 and IgE in *Cγ1-Rab7KO* mice (plum) and their *Cγ1-Rab7WT* littermates (teal) 14 d after injection with ovalbumin (mean and s.e.m. of data from three pairs of mice).

Our data further shows that Rab7 plays an important role in mediating CSR. Such a role is induced by all the T-dependent and T-independent stimuli.

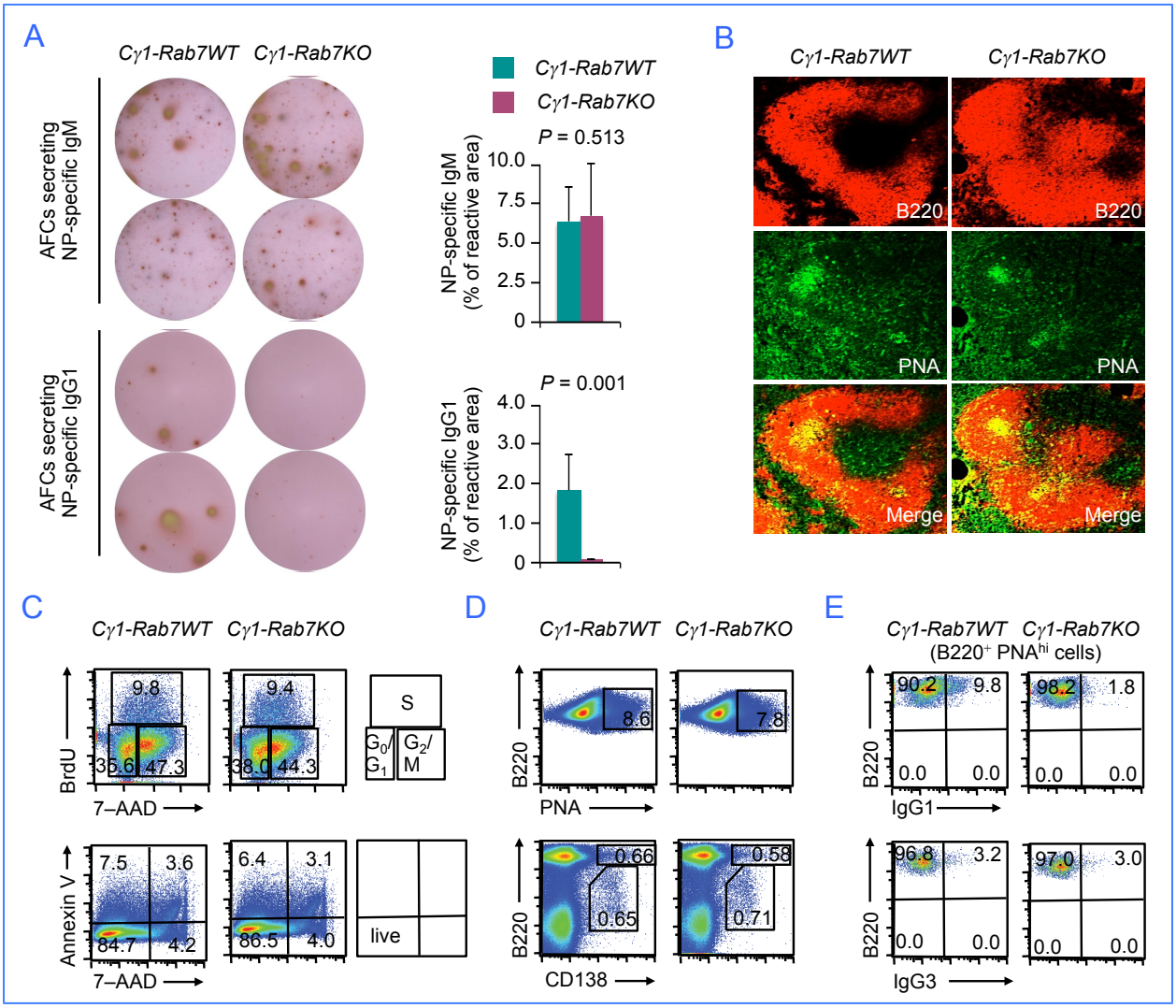

Figure 3.6 ***Cγ1-Rab7KO*** **mice show decreased IgG1$^+$ B cells and IgG1-secreting AFCs.** (**A**) ELISPOT analysis and quantification of AFCs that produced NP-specific IgM or IgG1 in spleens of *Cγ1-Rab7KO* mice (plum) and their *Cγ1-Rab7WT* littermates (teal) 9 d after injection with NP-CGG. (**B**) Immunofluorescence staining and confocal microscopy analysis of germinal centers (PNA^{hi}) within B220$^+$ follicles in spleens of *Cγ1-Rab7KO* mice (plum) and their *Cγ1-Rab7WT* littermates mice 9 d after injection with NP-CGG. (**C**) Cell cycle analysis (top panels; the quadrant corresponding to the G0/G1, S or G2/M phase of the cell cycle was also depicted) and viability analysis (bottom panels; live cells were Annexin V$^-$ 7–AAD$^-$) of spleen B cells isolated *ex vivo* from *Cγ1-Rab7KO* mice (plum) and their *Cγ1-Rab7WT* littermates 9 d after injection with NP-CGG. (**D**) Proportion of germinal centers (PNA^{hi}) cells among (B220$^+$) B cells (top panels) and proportion of (CD138$^+$ B220^{hi}) plasmablasts and (CD138$^+$ B220^{lo}) plasma cells in spleens of *Cγ1-Rab7KO* mice (plum) and their *Cγ1-Rab7WT* littermates 9 d after injection with NP-CGG. (**E**) Proportion of IgG1$^+$ (top panels) and IgG3$^+$ (bottom panels) cells among (B220$^+$ PNA^{hi}) germinal center B cells in spleens of *Cγ1-Rab7KO* mice (plum) and their *Cγ1-Rab7WT* littermates 9 d after injection with NP-CGG. Data are representative of three independent experiments.

3.3 MODULATION OF CSR: RAB7 MEDIATES AID EXPRESSION

Our studies strongly suggested that Rab7 mediated processes that were induced mainly by primary CSR-inducing stimuli, but not secondary stimuli (which specify the isotype that a B cell will switch to). Indeed, $Igh^{+/C}\gamma^{1\text{-}cre}$ $Rab7^{fl/fl}$ B cells underwent normal germline Iγ1-Sγ1-Cγ1 and Iε-Sε-Cε transcription, when induced *in vivo* and *in vitro* by IL-4 plus a primary stimulus (**Figure 3.7A-C**). They, however, showed significantly reduced expression of the *Aicda* transcripts and protein (**Figure 3.7A-C**) as well as reduced levels of circle Iγ1-Cμ and Iε-Cμ transcripts and post-recombination Iμ-Cγ1 and Iμ-Cε transcripts.

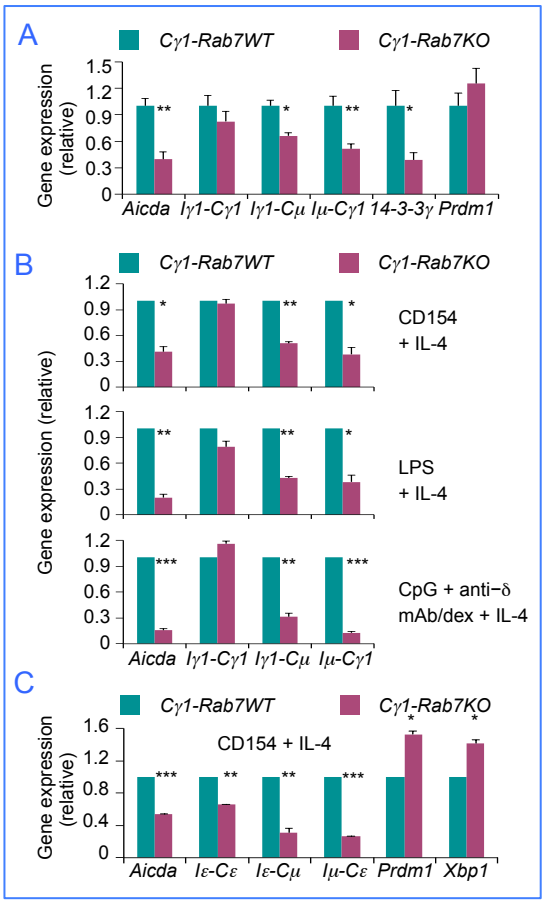

Figure 3.7 *Cγ1-Rab7KO* B cells are defective in the induction of AID *in vivo* and *in vitro*. (**A**) qRT-PCR analysis of levels of *Aicda*, IgH germline Iγ1-Sγ1-Cγ1 transcripts, circle Iγ1-Cμ transcript, post-recombination Iμ-Cγ1 transcripts, *14-3-3γ* transcripts and *Pdrm1* transcripts in B cells isolated *ex vivo* from *Cγ1-Rab7KO* mice (plum) and their *Cγ1-Rab7WT* littermates (teal) 9 d after injection with NP-CGG. Data were normalized to the level of *Cd79b* and are expressed as ratios of values in *Cγ1-Rab7WT* B cells to those in *Cγ1-Rab7KO* B cells (mean and s.e.m. of data from three pairs of mice). (**B**) qRT-PCR analysis of levels of *Aicda* transcripts, *IgH* germline *Iγ1-Cγ1* transcripts, circle *Iγ1-Cμ* transcripts and post-recombination *Iμ-Cγ1* transcripts in *Cγ1-Rab7KO* B cells stimulated by CD154, LPS or CpG plus anti–δ mAb/dex in the presence of IL-4 for 48 h and in their *Cγ1-Rab7WT* B cell counterparts. Data were normalized to the level of *Cd79b* transcripts and are expressed as ratios of values in *Cγ1-Rab7WT* B cells to those in *Cγ1-Rab7KO* B cells (mean and s.e.m. of data from three independent experiments). (**C**) qRT-PCR analysis of levels of *Aicda* transcripts, *IgH* germline *Iε-Cε* transcripts, circle *Iε-Cμ* transcripts and post-recombination Iμ-Cε transcripts as well as those of *Prdm1* and *Xbp1* transcripts in *Cγ1-Rab7KO* B cells stimulated by CD154 plus IL-4 for 48 h and in their *Cγ1-Rab7WT* B cell counterparts. Data were normalized

to the level of *Cd79b* transcripts and are expressed as ratios of values in *Cγ1-Rab7WT* B cells to those in *Cγ1-Rab7KO* B cells (mean and s.e.m. of data from three independent experiments).

Rab7 deficiency also decreased the expression of 14-3-3γ adaptor molecules, which stabilize AID and other CSR factors on the donor and receptor S region DNA for CSR to unfold[13].

Thus, Rab7 is important in mediating induction of AID expression, as triggered by primary CSR-inducing stimuli. Rab7, however, is dispensable for induction of germline I_H-S-C_H transcription and expression of Blimp-1 and Xbp-1, consistent with the normal differentiation of $Igh^{+/C}\gamma^{1\text{-}cre}$ $Rab7^{fl/fl}$ B cells into plasma cells.

3.4 THERAPEUTICS USING RAB7 SPECIFIC INHIBITOR (CID 1067700) TO PREVENT UNWANTED ANTIBODY CLASS-SWITCHING

As we have shown that Rab7 is critical for CSR, we next sought to disrupt Rab7 function by utilizing a small molecule compound. We treated C57BL/6 mice with CID 1067700, a recently identified (and the only known) specific inhibitor of Rab7[14] (**Figure 3.8**). CID 1067700 (EC_{50} = 11-21 nM) fits into the narrow Rab7 GTP-binding pocket (PDB ID 1T91) and the more open GDP-binding pocket, thereby inhibiting Rab7 GTPase switch.

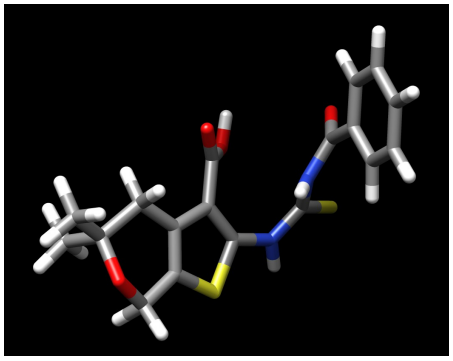

Figure 3.8 Chemical structural model of Rab7 inhibitor: CID 1067700. CID 1067700 is one of the first identified competitive inhibitors of nucleotide binding by Ras-related GTPases. CID 1067700 competes for the GTP- and GDP-binding pocket of Rab7 small GTPase with a K_i value of 13 nM, thereby preventing BODIPY-linked GTP- and GDP-binding with EC_{50} values of 11.2 and 21 nM, respectively[14]. Rab7-GDP remains in the cytoplasm, while Rab7-GTP is membrane bound.

In mice (n = 3) that were injected with NP-LPS, the generations of NP-specific IgG3 and IgG2b class-switched antibodies are virtually abrogated, except for IgM (**Figure 3.9**). CID 1067700 reduced, in a dose-dependent manner, switched (IgG3 and IgG2b) specific antibodies to a T-independent antigen NP-LPS in normal C57BL/6 mice and did so without affecting NP-specific IgM antibodies. These *in vivo* findings echo our findings in Rab7 B cell-specific KO mice/B cells *in vivo* and *in vitro,* and point to a B cell-intrinsic action of CID 1067700 and other Rab7-specific inhibitors to be identified by us to blunt class-switched antibody and autoantibody responses.

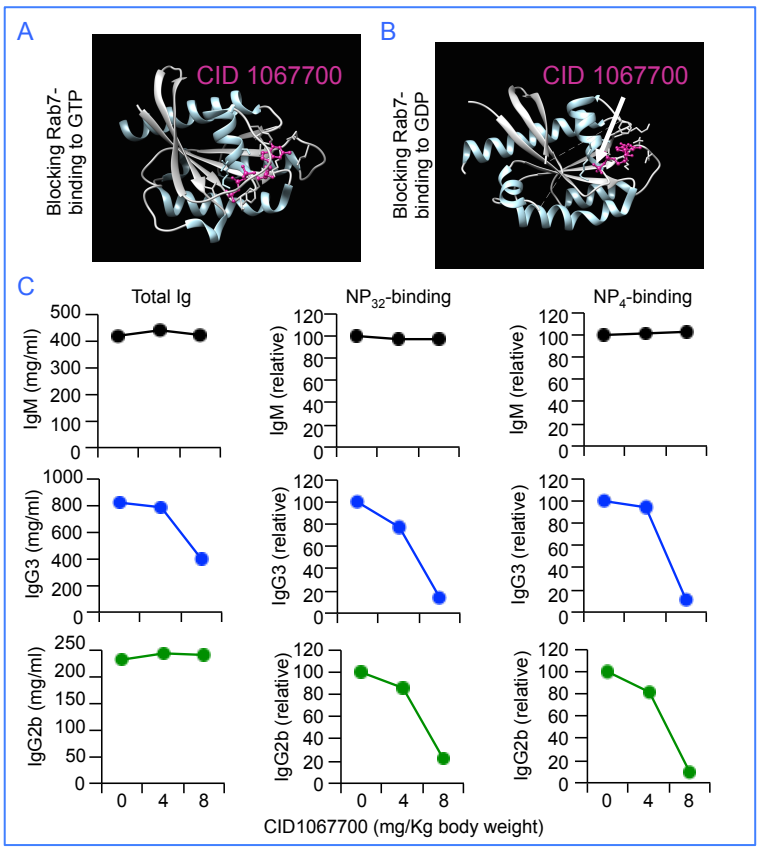

Figure 3.9 Rab7 inhibitor, CID 1067700, inhibits class-switched antibody responses without affecting IgM. (**A, B**) Model of CID 1067700 (**magenta**) docking into the nucleotide-binding pocket of Rab7 in (**A**) GTP-bound and (**B**) GDP-bound conformations. CID 1067700 inhibits Rab7 GTPase activity by fitting into both the Rab7 GTP-binding pocket (PDB ID 1T91) and the GDP-binding pocket (PDB ID 1VG1), of Rab7, thereby inhibiting Rab7 GTPase function, but not Rab7 expression. (**C**) CID 1067700 reduces total NP_{32}-specific IgG3 and NP_4-specific IgG3 and IgG2b, but not IgM, in C57BL/6 mice that were injected i.p. with NP_{17}-LPS (d 6), as compared to those in untreated (0 mg) mice (set as 100 for NP_{32}- and NP_4-binding Ig).

Having shown that Rab7-specific inhibitor CID 1067700 can blunt the generation of IgG3 and IgG2b in T-independent antibody responses; we next set to design double-blind therapeutic treatment studies to blunt the generation of pathogenic autoantibodies in autoimmune mice. In Chapter 4, we describe our therapeutic treatment studies using CID 1067700 on autoimmune MRL/*Fas*$^{lpr/lpr}$ lupus mice. Such therapeutics would preferentially target lupus B cells, in which Rab7 is highly expressed.

3.5 SUMMARY TO CHAPTER 3

In this study, we have unveiled an important B cell-intrinsic role of Rab7 in the antibody response by constructing conditional KO mice that lack Rab7 only in B cells induced to undergo Iγ1-Sγ1-Cγ1 transcription. As validated by our data, this design has circumvented any complications potentially arising from possible roles of Rab7 in B cell and T cell development. It has also allowed us to outline an important role of Rab7 in CSR, through activation of the canonical NF-κB pathway and induction of AID expression. The role of Rab7 in the generation of class-switched B cells and AFCs, but not plasma cells, contrasts the role of Atg5 in mediating the development of peritoneal B1 cells and generation/function of plasma cells, but not CSR[15, 16, 17]. Rab7 may play a role in the bone marrow homing of plasma cells originating in secondary lymphoid organs, as suggested by our unpublished observations in $Igh^{+/C}\gamma^{1\text{-}cre}$ $Rab7^{fl/fl}$ mice; it might also mediate the differentiation of IgM^+ and residual class-switched B cell into memory B cells and the maintenance/function of memory B cells – the Atg7 autophagic protein has been shown to play such a role[18]. Finally, the normal IgM expression, proliferation and survival of $Igh^{+/C}\gamma^{1\text{-}cre}$ $Rab7^{fl/fl}$ B cells suggests that the role of Rab7 is redundant with that of other small GTPases in mediating basal membrane functions and maintaining B cell homeostasis.

The role of Rab7 in induction of AID expression and CSR was intrinsic to B cells, as shown by the failure of $Igh^{+/C}\gamma^{1\text{-}cre}$ $Rab7^{fl/fl}$ B cells to undergo T-independent antibody response *in vivo* and CSR *in vitro*. In T-dependent antibody responses, Rab7 might mediate, in addition to CSR, autophagy in B cells for antigen presentation[19, 20, 21, 22], thereby activating T_H cells, which, in turn, induce further B cell activation and differentiation. In $Igh^{+/C}\gamma^{1\text{-}cre}$ $Rab7^{fl/fl}$ mice injected

with (T-dependent) NP-CGG, however, B cells displayed normal proliferation, survival, germinal center reaction, IgM production and plasma cell differentiation, suggesting that Rab7-deficient B cells were competent in activating T_H cells, possibly by using a different Rab GTPase (e.g., Rab9) for autophagy-mediated antigen-presentation, thereby receiving full T_H cell help. *Igh*$^{+/C}\gamma^{1\text{-}cre}$ *Rab7*$^{fl/fl}$ B cells showed impaired CSR to not only IgG1, but also IgE *in vivo* and *in vitro* despite normal *Igh*$^{+}$ germline Iε-Sε-Cε transcription, further suggesting that mediating induction of AID expression is the mechanism by which Rab7 plays a role in CSR. Decreased AID expression in these B cells would impair direct Sμ→Sε (IgM→IgE) switching and sequential Sμ→Sγ1→Sε (IgM→IgG1 and then →IgE) switching (**Figure 3.10**).

To further investigate the importance of Rab7 in modulating CSR, we treated C57BL/6 mice with a Rab7-specific inhibitor, CID 1067700, to disrupt Rab7 function. In mice that were injected with NP-LPS, the generations of NP-specific IgG3 and IgG2b class-switched antibodies, but not IgM are virtually abrogated. Our data shows that CID 1067700 can be used dampen the antibody response and suggests that this small molecule compound can be used as a therapeutic treatment for unwanted CSR, such as in the generation of autoantibodies in autoimmune disease.

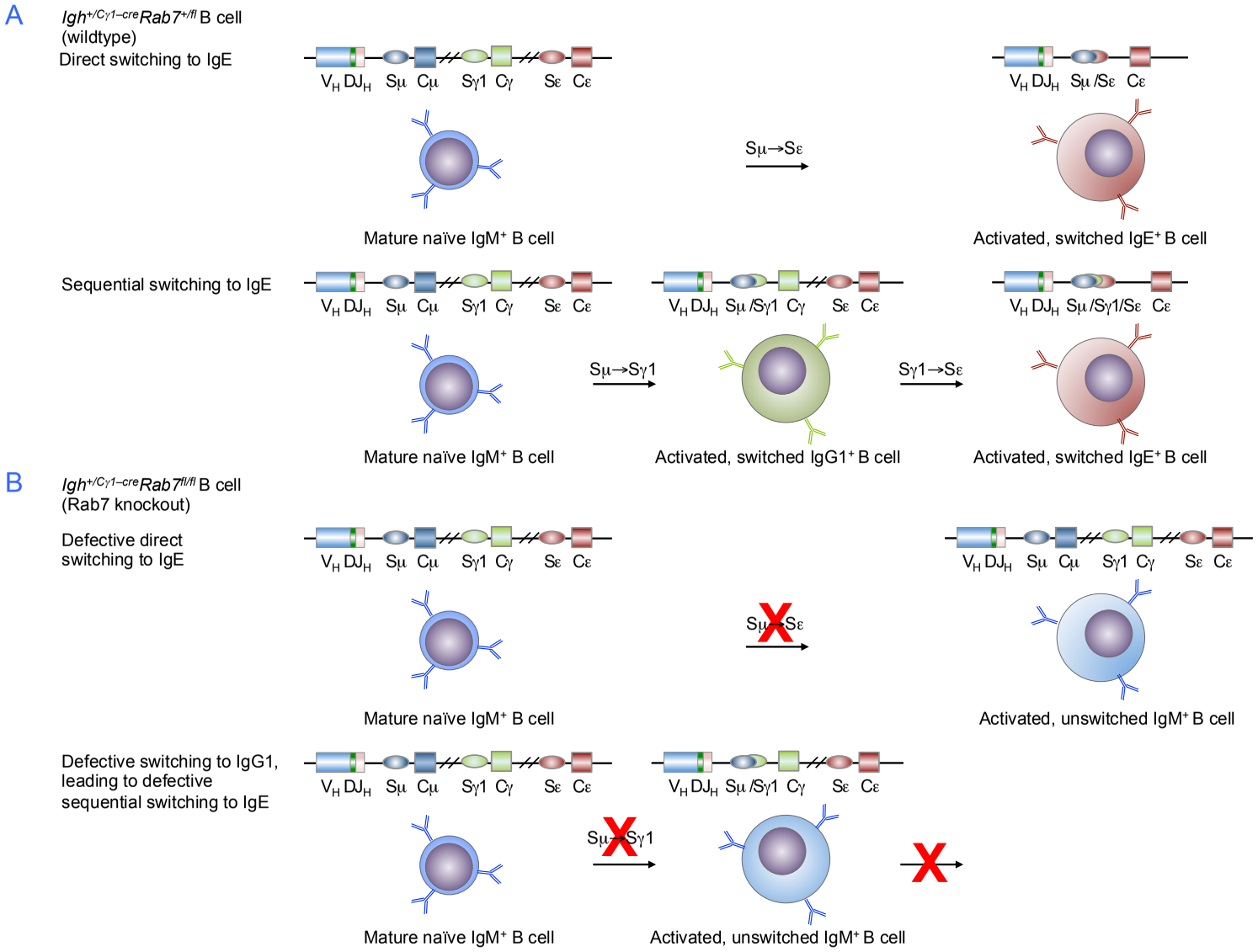

Figure 3.10 Schematic depiction of defective switching to IgE. (A) Depiction of direct switching from IgM to IgE (top) and sequential switching from IgM to IgG1 and then IgE in *Igh*$^{+/C\gamma1-cre}$*Rab7*$^{+/fl}$ (wildtype) B cells. (B) Depiction of defective direct switching from IgM to IgE in *Igh*$^{+/C\gamma1-cre}$*Rab7*$^{fl/fl}$ (Rab7 knockout) B cells due to impairment in the induction of AID expression (top). As the generation of IgG1+ B cells is also impaired (bottom) due to defective CSR from IgM to IgG1, sequential switching from IgM to IgG1 and then IgE is also blocked in these B cells.

3.6 MATERIALS AND METHODS

Mice and Immunization

Igh$^{+/C}\gamma^{1\text{-}cre}$ *Rab7*$^{fl/fl}$ mice and their *Igh*$^{+/C}\gamma^{1\text{-}cre}$ *Rab7*$^{+/fl}$ littermate controls (**Figure 3.1, 3.2A**) were generated by the breeding of *Igh*$^{+/C}\gamma^{1\text{-}cre}$ mice[12], (JAX stock number 010611) with *Rab7*$^{fl/fl}$ mice[9], (JAX stock number 021589), both of which had been backcrossed onto the C57BL/6 background for at least 9 generations. Mice were maintained in pathogen-free vivaria, and were used for experiments at 8-12 weeks of age and without any apparent infection or disease. For immunization, mice were injected intraperitoneally (i.p.) with 100 μg of NP-CGG (average of 16 molecules of 4-hydroxy-3-nitrophenyl acetyl coupled to 1 molecule of chicken γ-globulin; Biosearch Technologies) in 100 μl of alum (Imject® Alum, Pierce), 100 μg of ovalbumin (OVA) in 100 μl of alum, or 25 μg of NP-conjugated LPS (NP-LPS; average 0.2 NP molecule conjugated with one LPS molecule; Biosearch Technologies) in 100 μl of PBS. All protocols were in accordance with the rules and regulations of the Institutional Animal Care and Use Committee (IACUC) of the University of Texas Health Science Center at San Antonio and those of IACUC of the University of California, Irvine.

B cells and CSR

Single B cell suspensions were prepared from spleens or pooled axillary, inguinal and cervical lymph nodes using a 70-μm cell strainer. Spleen B cells were resuspended in ACK Lysis Buffer (Lonza) to lyse red blood cells and, after quenching with RPMI-1640 medium (Invitrogen) supplemented with FBS (10% v/v, Hyclone), penicillin-streptomycin (1% v/v, Invitrogen) and amphotericin B (1% v/v, Invitrogen) (RPMI-FBS), were resuspended in RPMI-FBS before

purification of B cells. Lymph node cells were directly resuspended in RPMI-FBS before purification. B cells were purified by depletion of cells expressing CD43, CD4, CD8, CD11b, CD 49b, CD90.2, Gr-1 or Ter-119 using the EasySep^{TM} Mouse B cell Isolation kit (Stemcell Technologies) following the manufacturer's protocol, resulting in a preparation of more than 99% B220^{+}Igδ^{hi} B cells. For labeling with carboxyfluorescein diacetate succinimidyl ester (CFSE, Invitrogen), B cells were resuspended in PBS at 10^7 cell/ml and incubated with 4 μM CFSE at 37°C for 5 m and immediately quenched with RPMI-FBS. After pelleting, B cells were resuspended and cultured at 3 x 10^5 cell/ml in RPMI-FBS supplemented with 50 μM β-mercaptoethanol.

For CSR induction, B cells were stimulated with the following primary stimuli: CD154 (3 U/ml, mouse CD154-containing membrane fragments of baculovirus-infected Sf21 insect cells[23]), LPS (3 μg/ml, from *E. coli*, serotype 055:B5, deproteinized by chloroform extraction, Sigma-Aldrich), TLR1/2 ligand Pam_3CSK_4 (100 ng/ml, Invivogen), TLR4 ligand monophophoryl lipid A (lipid A, 1 μg/ml, Sigma-Aldrich), TLR7 ligand R-848 (30 ng/ml, Invivogen) or TLR9 ligand CpG ODN1826 with a phosphorothioate backbone (CpG, 1 μM, sequence 5'–TCCATGACGTTCCTGACGTT–3'; Operon). Anti–Igδ mAb (clone 11-26c) conjugated to dextran (anti–δ mAb/dex; Fina Biosolutions) was added, as indicated, to crosslink BCRs. Recombinant IL-4 (4 ng/ml) was added for CSR to IgG1 and IgE, IFN-γ (50 ng/ml) for CSR to IgG2a, and TGF-β (2 ng/ml) for CSR to IgG2b (all from R&D Systems). After stimulation, B cells were harvested, stained with fluorochrome-conjugated mAbs in Hank's Buffered Salt Solution (HBSS) for 15 m and analyzed by flow cytometry for Igγ3, Igγ1, Igγ2b and Igγ2a expression (CSR to IgG3, IgG1, IgG2b and IgG2a) and other B cell surface molecules. For intracellular Igε analysis, B cells (2 x 10^6) stimulated by CD154 or LPS plus IL-4 were

harvested and treated with 200 μl of trypsin for 2 m to cleave off FcεRI, as described[24], followed by quenching with 1 ml RMPI-FBS. Cells were then fixed in 200 μl of formaldehyde (3.7% v/v) at 25°C for 10 m and, after quenching with 22 μl 1 M glycine (pH 7.0), were permeabilized in 500 μl 90% cold methanol on ice for 30 m before staining with fluorochrome-conjugated Abs and flow cytometry analysis. FACS data were analyzed by the FlowJo® software (Tree Star).

B cell proliferation and survival

For analysis of B cell proliferation *in vivo* in mice immunized with NP-CGG, mice were injected i.p. with bromodeoxyuridine (BrdU) twice, 2 mg (in 200 μl PBS) each time, within a 20-h interval and sacrificed 4 h after the second injection. B cells were analyzed by flow cytometry for BrdU incorporation and DNA contents in spleen B cells using a BrdU Flow Kit (BD Biosciences), following the manufacturer's instructions. Briefly, spleen cells were stained with fluorochrome-conjugated anti–B220 mAb and, after washing, resuspended in the BD Cytofix/Cytoperm™ buffer for 15 m on ice. After washing, cells were incubated with APC-conjugated anti–BrdU mAb and 7–AAD for staining of incorporated BrdU and DNA, respectively, and then analyzed by flow cytometry. For analysis of B cell proliferation *in vitro*, purified CFSE-labeled naïve B cells were cultured for 96 h in the presence of appropriate stimuli and then analyzed by flow cytometry for CFSE intensity (CFSE distributes equally into the two daughter cells when a cell divides). The number of B cell divisions was determined by the "Proliferation Platform" of the FlowJo® software. CSR as a function of the cell division number was the ratio of class-switched B cells in each division over the total number of B cells in that division. For analysis of B cell viability, cells were stained with 7–AAD and/or fluorochrome-conjugated Annexin V in HBSS and analyzed by flow cytometry.

Secreted Ig

To determine titers of total IgM, IgG1, IgG2a, IgG2b, IgG3, IgA or IgE, sera and culture supernatants were first diluted 4 – 100-fold and 10-fold, respectively, with PBS (pH 7.4) plus 0.05% (v/v) Tween-20 (PBST). Two-fold serially diluted samples and standards for each Ig isotypes were incubated in 96-well plates coated with pre-adsorbed goat anti–IgM, –IgG (to capture IgG1, IgG2a, IgG2b and IgG3), –IgA or –IgE Abs. After washing with PBST, captured Igs were detected with biotinylated anti–IgM, –IgG1, –IgG2a, –IgG2b, –IgG3, –IgA or –IgE Abs, followed by reaction with horseradish peroxidase (HRP)-labeled streptavidin (Sigma-Aldrich), development with o-phenylenediamine and measurement of absorbance at 492 nm. Ig concentrations were determined using Prism® (GraphPad Software) or Excel® (Microsoft) software.

To analyze titers of high-affinity NP-specific Abs, sera were diluted 1,000-fold in PBST. Two-fold serially diluted samples were incubated in a 96-well plate pre-blocked with BSA and coated with NP_3-BSA (average 3 NP molecules on one BSA molecule). Captured Igs were detected with biotinylated Ab to IgM, IgG1, IgG2a, IgG2b, IgG3 or IgA. To analyze titers of OVA-specific IgG1 and IgE, serum samples were diluted 100-fold and incubated in plates coated with anti–IgG1 or anti–IgE. Captured IgG1 or IgE were detected with biotinylated OVA. Data are expressed as relative values based on end-point dilution factors.

ELISPOT

MultiScreen® filter plates (Millipore) were activated with 35% ethanol, washed with PBS and coated with with NP_3-BSA. Single B cell suspensions were cultured at 50,000 cells/ml in FBS-RPMI supplemented with 50 μM β-mercaptoethanol at 37°C for 16 h. After supernatants were

removed, plates were incubated with biotinylated goat anti–mouse IgM or anti–IgG1 Ab for 2 h and, after washing, incubated with HRP-conjugated streptavidin. After washing, plates were developed using the Vectastain AEC peroxidase substrate kit (Vector Laboratories) to stain antibody forming cells (AFCs). The stained area in each well was quantified using the CTL Immunospot software (Cellular Technology) and depicted as the percentage of total area of each well. This was used to quantify the production of AFCs.

RNA isolation and qRT–PCR analysis of transcripts

Total RNA was extracted from 5 x 10^6 B cells using the RNeasy Mini Kit (Qiagen). First-strand cDNA was synthesized from 2 μg RNAs using the SuperScript™ III System (Invitrogen) and analyzed by qPCR using SYBR Green (Dynamo HS kit; New England Biolabs) and appropriate primers. PCR was performed in a MyiQ Real-Time PCR System (Bio-Rad Laboratories) according to the following protocol: 95°C for 30 s, 40 cycles of 95°C for 10 s, 60°C for 30 s, 72°C for 30 s. Melting curve analysis was performed at 72°C–95°C. The ΔΔCt method was used to analyze levels of transcripts and data were normalized to the level of *Cd79b*, which encodes the BCR Igβ chain constitutively expressed in B cells.

Immunofluorescence

To visualize germinal centers, spleens from immunized mice were embedded in OCT (Tissue-tek) and snap-frozen on dry ice. Cryostat sections (7 μm) were fixed in pre-chilled acetone at –80°C for 30 m and then air dried at 25°C for 30 m. Sections were stained with PE-conjugated anti–B220 mAb and FITC-conjugated peanut agglutinin (PNA; EY Laboratories) at 25°C for 1 h in a moist chamber. After washing with HBSS, sections were mounted using ProLong® Gold

Antifade Reagent with DAPI (Invitrogen) and examined under an Olympus FluoView 1000 confocal microscope.

To visualize Rab7 expression, B cells were spun onto cover slips pre-coated with poly-D-lysine (10 μg/ml, Sigma-Aldrich) and fixed with 2% paraformaldehyde for 10 m. After blocking with 1% BSA, cells were stained with FITC-conjugated anti–B220 mAb. After washing with HBSS and permeabilization with 0.5% Triton X-100 for 10 m, cells were stained with a rabbit anti–Rab7 mAb at 25°C for 1 h, followed by staining with Alexa Fluor647-conjugated goat anti–rabbit Ab. After washing, cells were mounted using ProLong® Gold with DAPI for confocal microscopic analysis.

3.7 REFERENCES

1. McLeod IX, Jia W, He YW. The contribution of autophagy to lymphocyte survival and homeostasis. *Immunol Rev* 2012, **249**(1)**:** 195-204.

2. Deretic V, Saitoh T, Akira S. Autophagy in infection, inflammation and immunity. *Nat Rev Immunol* 2013, **13**(10)**:** 722-737.

3. Levine B, Mizushima N, Virgin HW. Autophagy in immunity and inflammation. *Nature* 2011, **469**(7330)**:** 323-335.

4. Virgin HW, Levine B. Autophagy genes in immunity. *Nat Immunol* 2009, **10**(5)**:** 461-470.

5. Zerial M, McBride H. Rab proteins as membrane organizers. *Nat Rev Mol Cell Biol* 2001, **2**(2)**:** 107-117.

6. Edinger AL, Cinalli RM, Thompson CB. Rab7 prevents growth factor-independent survival by inhibiting cell-autonomous nutrient transporter expression. *Dev Cell* 2003, **5**(4)**:** 571-582.

7. Kinchen JM, Doukoumetzidis K, Almendinger J, Stergiou L, Tosello-Trampont A, Sifri CD*, et al.* A pathway for phagosome maturation during engulfment of apoptotic cells. *Nat Cell Biol* 2008, **10**(5)**:** 556-566.

8. Romero Rosales K, Peralta ER, Guenther GG, Wong SY, Edinger AL. Rab7 activation by growth factor withdrawal contributes to the induction of apoptosis. *Mol Biol Cell* 2009, **20**(12)**:** 2831-2840.

9. Roy SG, Stevens MW, So L, Edinger AL. Reciprocal effects of rab7 deletion in activated and neglected T cells. *Autophagy* 2013, **9**(7)**:** 1009-1023.

10. Kawamura N, Sun-Wada G, Aoyama M, Harada A, Takasuga S, Sasaki T*, et al.* Delivery of endosomes to lysosomes via microautophagy in the visceral endoderm of mouse embryos. *Nat Commun* 2012, **3 (1071):** 1-10.

11. Kasaian MT, Ikematsu H, Casali P. Identification and analysis of a novel human surface CD5- B lymphocyte subset producing natural antibodies. *J Immunol* 1992, **148**(9)**:** 2690-2702.

12. Casola S, Cattoretti G, Uyttersprot N, Koralov SB, Seagal J, Hao Z*, et al.* Tracking germinal center B cells expressing germ-line immunoglobulin gamma1 transcripts by conditional gene targeting. *Proc Natl Acad Sci USA* 2006, **103**(19)**:** 7396-7401.

13. Lam T, Thomas LM, White CA, Li G, Pone EJ, Xu Z*, et al.* Scaffold functions of 14-3-3 adaptors in B cell immunoglobulin class switch DNA recombination. *PLoS One* 2013, **8**(11)**:** e80414.

14. Agola JO, Hong L, Surviladze Z, Ursu O, Waller A, Strouse JJ*, et al.* A competitive nucleotide binding inhibitor: in vitro characterization of Rab7 GTPase inhibition. *ACS chemical biology* 2012, **7**(6)**:** 1095-1108.

15. Conway KL, Kuballa P, Khor B, Zhang M, Shi HN, Virgin HW*, et al.* ATG5 regulates plasma cell differentiation. *Autophagy* 2013, **9**(4).

16. Miller BC, Zhao Z, Stephenson LM, Cadwell K, Pua HH, Lee HK*, et al.* The autophagy gene ATG5 plays an essential role in B lymphocyte development. *Autophagy* 2008, **4**(3)**:** 309-314.

17. Pengo N, Scolari M, Oliva L, Milan E, Mainoldi F, Raimondi A*, et al.* Plasma cells require autophagy for sustainable immunoglobulin production. *Nat Immunol* 2013, **14**(3)**:** 298-305.

18. Chen M, Hong MJ, Sun H, Wang L, Shi X, Gilbert BE*, et al.* Essential role for autophagy in the maintenance of immunological memory against influenza infection. *Nat Med* 2014, **20**(5)**:** 503-510.

19. Ireland JM, Unanue ER. Autophagy in antigen-presenting cells results in presentation of citrullinated peptides to CD4 T cells. *J Exp Med* 2011, **208**(13)**:** 2625-2632.

20. Kuballa P, Nolte WM, Castoreno AB, Xavier RJ. Autophagy and the immune system. *Annu Rev Immunol* 2012, **30**(1)**:** 611-646.

21. Lee HK, Mattei LM, Steinberg BE, Alberts P, Lee YH, Chervonsky A*, et al.* In Vivo requirement for Atg5 in antigen presentation by dendritic cells. *Immunity* 2010, **32**(2)**:** 227-239.

22. Menendez-Benito V, Neefjes J. Autophagy in MHC class II presentation: sampling from within. *Immunity* 2007, **26**(1)**:** 1-3.

23. Li G, White CA, Lam T, Pone EJ, Tran DC, Hayama KL*, et al.* Combinatorial H3K9acS10ph histone modification in IgH locus S regions targets 14-3-3 adaptors and AID to specify antibody class-switch DNA recombination. *Cell Rep* 2013, **5**(3)**:** 702-714.

24. Wesemann DR, Magee JM, Boboila C, Calado DP, Gallagher MP, Portuguese AJ*, et al.* Immature B cells preferentially switch to IgE with increased direct Sμ to Sε recombination. *J Exp Med* 2011, **208**(13)**:** 2733-2746.

CHAPTER 4

B CELL RAB7 MODULATES AUTOANTIBODY RESPONSES IN AUTOIMMUNE MRL/*Fas*$^{lpr/lpr}$ MICE

4.1 RAB7 EXPRESSION IN LUPUS B LYMPHOCYTES

Systemic lupus erythematosus (SLE) is a complex disease occurring nine times more often then men, with no available cure. Lupus is characterized by life-debilitating systemic damages to multiple organs, including kidney (manifested as nephritis), skin (e.g., "butterfly" rash on the face), brain (e.g., SLE neuropsychiatry, SLENP), heart (e.g., coronary heart disease) and lungs (e.g., pneumonitis, pulmonary hemorrhage and acute respiratory distress syndrome)[1]. It is associated with multiple genetic susceptibilities[2, 3, 4, 5, 6] that, when compounded with epigenetic alterations, mediate dysregulation of different immune compartments, such as B and T lymphocytes, dendritic cells (DCs), neutrophils, and inflammatory cytokines, most of which in turn contribute to the disease onset and progression. Understanding lupus mechanisms will advance our fundamental knowledge in immune regulation/dysregulation, and has obvious translational significance human health.

We set to focus on the B cell-intrinsic mechanisms of lupus. While, B cells play a critical role in host immunity, autoreactive B cells that have broken the tolerance are a central mediator of lupus[7, 8, 9]. These B cells participate in a self-reinforcing cycle involving other immune cells and elements, leading to a cascade of their dysregulation[10, 11]. They also express antibodies recognizing self-antigens, e.g., double-strand DNA (dsDNA)[12] and Ro antigen[13]. Upon activation by appropriate stimuli[14], B cells undergo class-switch DNA recombination (CSR), which underpins autoantibody class-switching from the non-harmful IgM class to the pathogenic IgG and IgA classes, and somatic hypermutation (SHM), which underpins the generation of autoantibody mutants with high affinities to self-antigens. Both CSR and SHM requires, activation-induced cytidine deaminase (AID, as encoded by the *AICDA* gene in humans and

Aicda gene in mice)[14]. AID expression is restricted to B cells activated by the T cell-dependent primary stimulus, namely T cell CD154 that engages CD40 on B cells, or T cell-independent primary stimuli, such as complex antigens that can engage both a Toll-like receptor (TLR) and the B cell receptor (BCR)[15]. Notably, *AICDA* expression is significantly higher in B cells isolated from peripheral blood mononuclear cells (PBMCs) of lupus patients; as compared to those from PBMCs of age- and sex-matched healthy subjects[16].

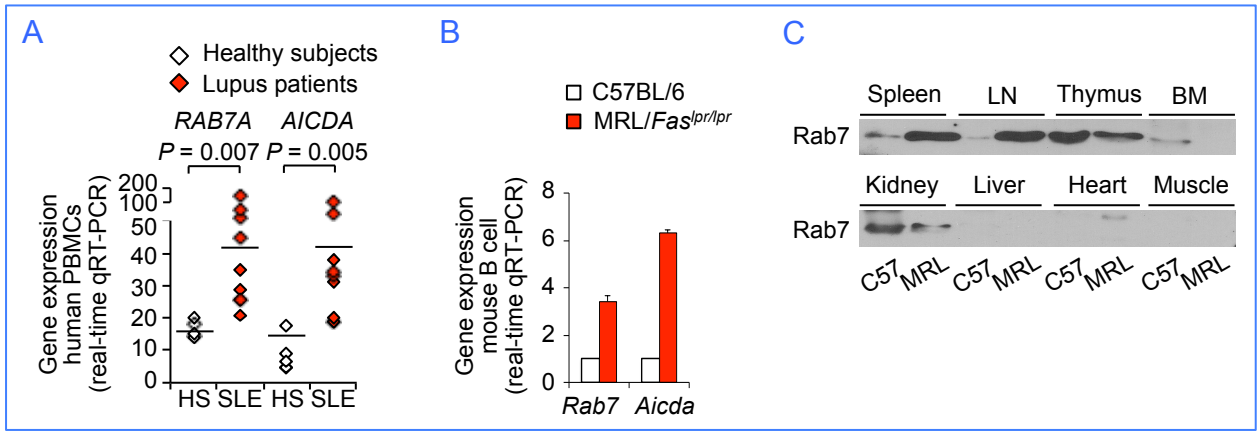

Figure 4.1 Rab7 is highly expressed in lupus B cells. (**A**) qRT-PCR analysis of levels of *RAB7A* and *AICDA* transcripts in PBMCs isolated from lupus patients (n=8) or healthy subjects (n=5). (**B**) qRT-PCR analysis of levels of *Rab7* and *Aicda* transcripts in B cells isolated from C57BL/6 or MRL/*Fas*$^{lpr/lpr}$ mice (12-week-old). (**C**) Immunoblotting analysis of (levels of Rab7 and AID protein in lymphoid organs and non-lymphoid organs (of equal amount, 12 ug, from each tissue/organ) from C57BL/6 or MRL/*Fas*$^{lpr/lpr}$ mice. Modified from our manuscript[17].

Our analysis[17] also showed that *RAB7A* were expressed at higher levels in PBMCs from lupus patients, as compared to their respective counterparts from healthy subjects (**Figure 4.1A**). We also analyzed *Rab7* and *Aicda* in purified B cells (**Figure 4.1B**) from lupus-prone MRL/*Fas*$^{lpr/lpr}$ mice. Further, Rab7 were highly expressed in peripheral lymphoid organs (e.g., spleen, lymph nodes), particularly B cell-containing organs (spleen and lymph nodes), in lupus-prone MRL/*Fas*$^{lpr/lpr}$ mice, as compared to those in age- and sex-matched normal C57BL/6 mice (**Figure 4.1C**).

4.2 RAB7 INHIBITOR (CID 1067700) DAMPENS LUPUS DEVELOPMENT AND INCREASES LIFESPAN OF AUTOIMMUNE MRL/*Fas*$^{lpr/lpr}$ MICE

We proposed that Rab7-dependent mature endosomes in B cells play an important role in mediating signal transduction from CD40 and TLRs, leading to activation of NF-κB to induce AID for CSR and, eventually, generation of class-switched specific antibodies in normal mice and pathogenic autoantibodies in lupus mice, in which Rab7 is upregulated in B cells. Rationale for our hypothesis stems from our preliminary data showing that *Rab7 B-KO* mice/B cells were defective in CSR *in vivo*.

CID 1067700 is a recently identified (and the only known) specific inhibitor of Rab7[18]. We started the CID 1067700 treatment (EC_{50} = 11-21 nM) in seven MRL/*Fas*$^{lpr/lpr}$ mice at 10 weeks of age, when these mice started to show class-switched anti–dsDNA autoantibodies. The treatment prolonged life of mice, all of which (except for one that was sacrificed for experiments) are still alive, beyond 34-week of age, while untreated control mice all died by 22-week of age[17] (P = 0.0002, **Figure 4.2A, B**). The treatment also prevented the appearance of "butterfly rash" on the face and/or skin lesions. These hallmarks of early lupus were readily visible on six out of eight untreated control MRL/*Fas*$^{lpr/lpr}$ mice[17]. Finally, the CID 1067700 treatment reduced proteinuria (by 100-fold), prevented hypercellularity and capillary wall thickening in glomeruli, and prevented splenomegaly and lymphadenopathy (**Figure 4.2C, D,** and not shown). The systemic improvement of lupus-related pathology in CID 1067700-treated mice strongly suggests that generation of class-switched pathogenic autoantibodies, the key mediator of systemic lupus, is blunted by small molecules that target Rab7.

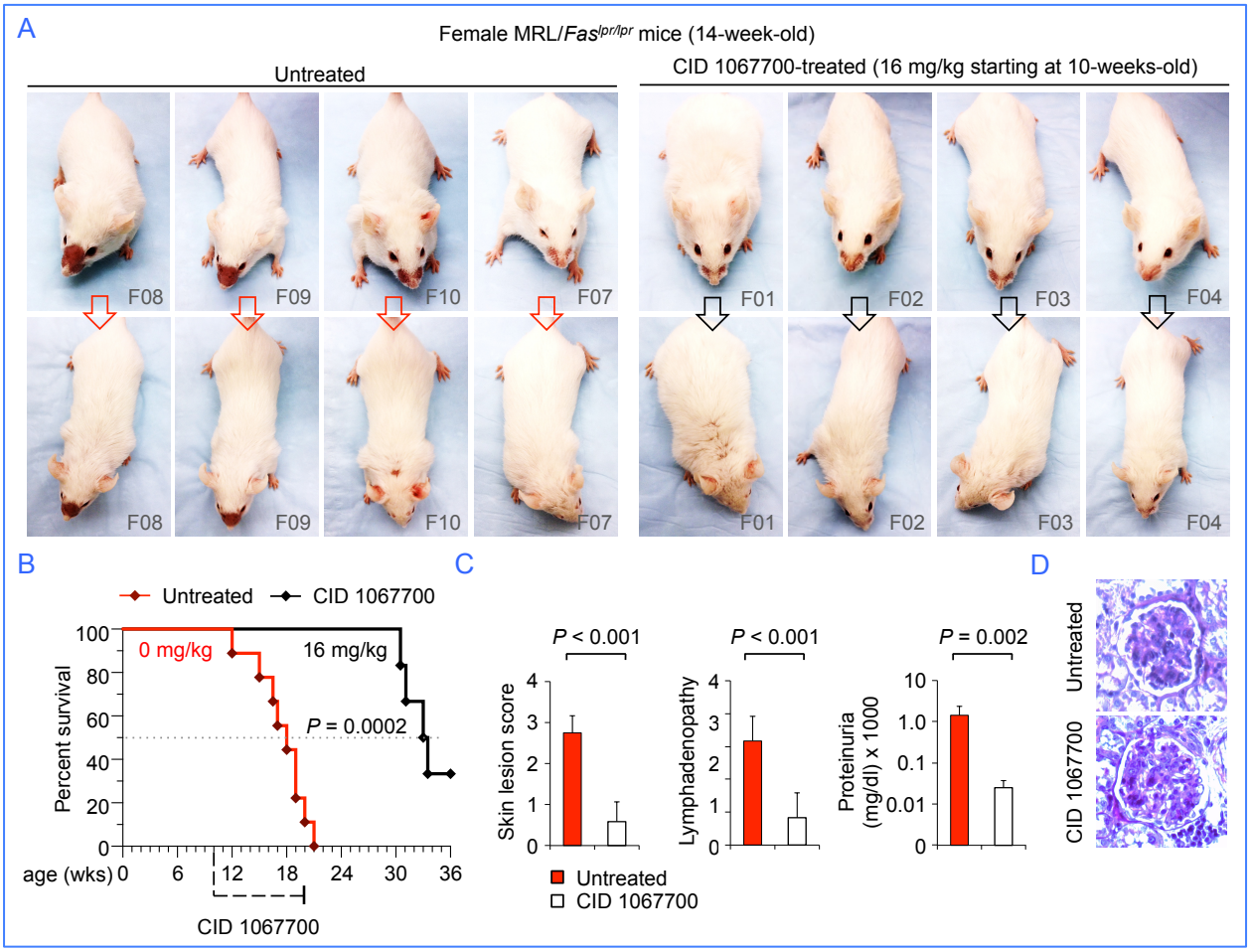

Figure 4.2 Treatment using Rab7 inhibitor (CID 1067700) reduces the clinical incidences of skin lesion, proteinuria and kidney deposition and increases survival in MRL/*Fas*$^{lpr/lpr}$ mice. (A) Image analysis of MRL/*Fas*$^{lpr/lpr}$ mice that were treated with 0 mg/kg or 16 mg/kg of CID 1067700. (B) Survival curve of MRL/*Fas*$^{lpr/lpr}$ mice treated with 0 mg/kg CID 1067700 (red), treated with 16 mg/kg CID 1067700 starting at 10-weeks-old (black). (C) Skin lesion score, lymphadenopathy and proteinuria score of MRL/*Fas*$^{lpr/lpr}$ mice following 7 weeks of treatment with 0 mg/kg or 16 mg/kg of CID 106700, *n=6*. (D) H&E analysis of glomeruli from kidney sections of MRL/*Fas*$^{lpr/lpr}$ mice following 7 weeks of treatment with 0 mg/kg or 16 mg/kg of CID 106700.

Overall, CID 1067700 treatment significantly prolonged the lifespan and survival of CID 1067700-treated MRL/*Fas*$^{lpr/lpr}$ lupus-prone mice, as compared to mice that did not receive treatment. CID 1067700-treated MRL/*Fas*$^{lpr/lpr}$ showed reduced lupus immunopathology, including the prevention of kidney immunopathology.

Having shown that CID 1067700, which potently inhibited Rab7 and effectively prevented development of lupus symptoms, we next wanted to analyze total antibody titers and anti–dsDNA IgG autoantibodies, which are pathogenic and mediate immune complex depositions leading to kidney immunopathology. CID 1067700-treated lupus mice showed significantly reduced levels of autoantibodies that can cause nephritis, e.g., class-switched (IgG2a, IgG1 and IgG2b) anti–dsDNA antibodies (**Figure 4.3**).

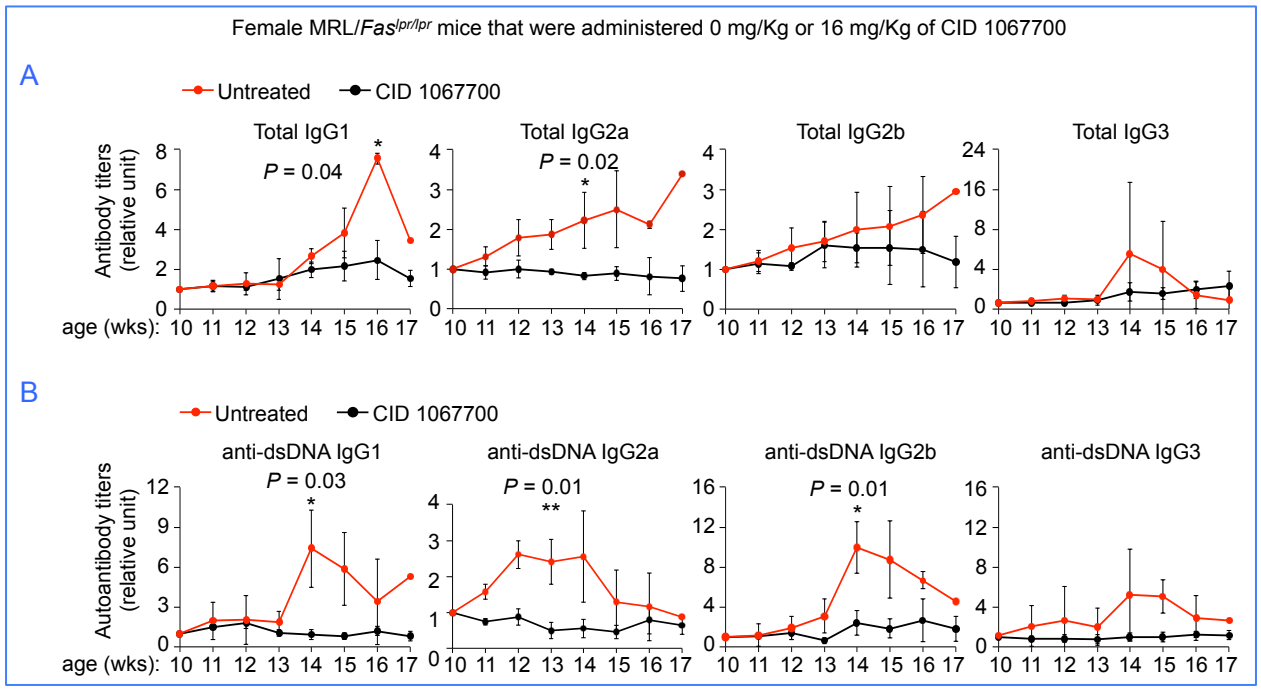

Figure 4.3 Treatment using Rab7 inhibitor (CID 1067700) blunts the generation of pathogenic class-switched anti–dsDNA autoantibodies. (**A**) Titers of circulating total IgG1, IgG2a, IgG2b, IgG3 from MRL/*Fas*$^{lpr/lpr}$ mice that were treated with 0 mg/kg or 16 mg/kg of CID 1067700 (n ≥ mice per group). (**B**) Titers of circulating anti–dsDNA IgG1, IgG2a, IgG2b, IgG3 from MRL/*Fas*$^{lpr/lpr}$ mice that were treated with 0 mg/kg or 16 mg/kg of CID 1067700 (n ≥ 3 mice per group). P values, as calculated by paired student t test, less than 0.05 were considered significant.

The systemic improvement of lupus-related pathology in CID 1067700-treated mice strongly suggests that generation of class-switched pathogenic autoantibodies, the key mediator of systemic lupus, is blunted by small molecules that target Rab7.

4.3 RAB7 INHIBITOR (CID 1067700) INHIBITS THE GENERATION OF CLASS-SWITCHED PLASMABLASTS IN AUTOIMMUNE MRL/*Fas*$^{lpr/lpr}$ MICE

SLE is characterized by the generation of an array of pathogenic autoantibodies – a key mediator of systemic lupus. Having shown that pathogenic anti–dsDNA IgG autoantibodies are involved in systemic lupus, we next to assess the cellular distribution of B cells, T cells, CD138^{+} plasma cells and CD138^{lo} plasmablasts (which produce pathogenic autoantibodies) by comparative FACS analysis.

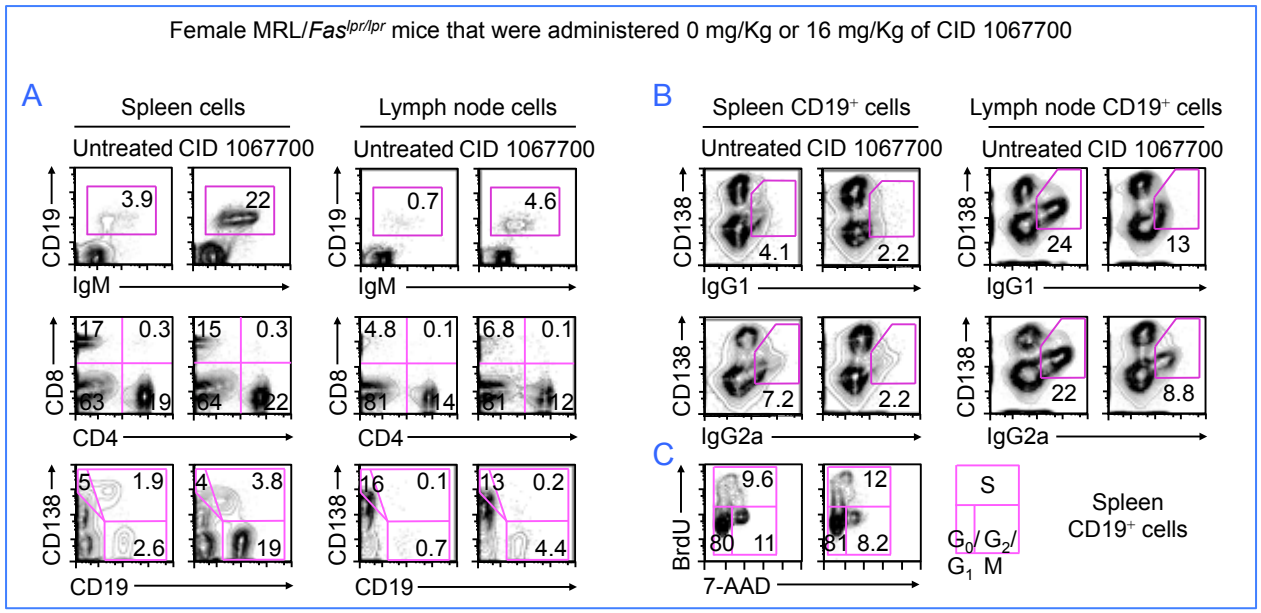

Figure 4.4 Treatment using Rab7 inhibitor (CID 1067700) blunts the generation of class-switched IgG1^{+} and IgG2a^{+} plasmablasts in MRL/*Fas*$^{lpr/lpr}$ mice. (A) Flow cytometry analysis of expression of CD19^{+} IgM^{+} (B cells, top panels), CD8^{+} CD4^{+} (T cells, middle panels) and CD138 and CD19 (for CD138^{+} CD19^{-} plasma cells and for CD138^{+} CD19^{lo} plasmablasts) in spleen cells (left panels) and lymph node cells (right panels) from MRL/*Fas*$^{lpr/lpr}$ mice following 7 weeks of treatment with 0 mg/kg or 16 mg/kg of CID 106700. (B) Flow cytometry analysis of expression of class-switched CD138^{lo} IgG1^{+} plasmablasts and CD138^{lo} IgG2a^{+} plasmablasts from MRL/*Fas*$^{lpr/lpr}$ mice following 7 weeks of treatment with 0 mg/kg or 16 mg/kg of CID 106700. (C) Comparative cell cycle analysis as shown by incorporation of BrdU (a thymidine analogue) and 7-AAD staining (to stain total DNA) of spleen B cells (CD19^{+}) from MRL/*Fas*$^{lpr/lpr}$ mice following 7 weeks of treatment with 0 mg/kg or 16 mg/kg of CID 106700. Data are representative of two independent experiments.

Consistent with reduced lymphadenopathy, CID 1067700-treated mice had lower numbers of total spleen cells, lymph node cells and number of $CD8^+$ $CD4^+$ T cells (not shown). However, there is a dramatic and remarkable difference in the proportions of $CD19^+$ IgM^+ B cells in the spleen (3.9% in untreated and 22% in treated) and lymph nodes (0.7% in untreated and 4.6% in treated) between untreated and CID 1067700-treated mice (**Figure 4.4A**). IgM antibodies play a protective role in lupus[19]. By contrast, untreated mice and treated mice and displayed comparable proportions of $CD8^+$ and $CD4^+$ T cells in both the spleen and lymph nodes (**Figure 4.4A**). In addition, CID 1067700-treatment did not affect $CD138^+$ (a plasma cell marker) proportions, including plasmablasts ($CD138^{lo}$) and plasma cells ($CD138^{hi}$, **Figure 4.4A**).

Further, as Rab7 expression is upregulated in activated B cells, CID 1067700 targeting is specific to B cells induced to undergo CSR *in vivo*, as displayed by the proportions of class-switched $IgG1^+$ $CD138^{lo}$ plasmablasts in the spleen (4.1% in untreated and 2.2% in treated) and in the lymph nodes (24% in untreated and 13% in treated, **Figure 4.4B**). In addition, CID 1067700-treatment significantly impaired the generation of $IgG2a^+$ $CD138^{lo}$ plasmablasts in the spleen (7.2% in untreated and 2.2% in treated) and in the lymph nodes (22% in untreated and 8.8% in treated, **Figure 4.4B**). CID 1067700 treatment did not affect B cell cycle *in vivo*, as shown by incorporation of BrdU (a thymidine analogue) and 7-AAD staining (which stains total DNA) in spleen from MRL/$Fas^{lpr/lpr}$ mice, as compared to untreated mice (**Figure 4.4C**).

Thus, treatment with Rab7 inhibitor blunts the generation of $IgG1^+$ $CD138^{lo}$ plasmablasts and $IgG2a^+$ $CD138^{lo}$ plasmablasts that produce pathogenic autoantibodies, which is consistent with the reduction of circling pathogenic anti–dsDNA IgGs autoantibody titers.

4.4 CID 1067700 IMPAIRS CSR WITHOUT ALTERING B CELL PROLIFERATION

Having shown that CID 1067700 can inhibit the generation of class-switched plasmablasts, we next wanted to address the impact of CID 1067700 on B cells and CSR *in vitro*.

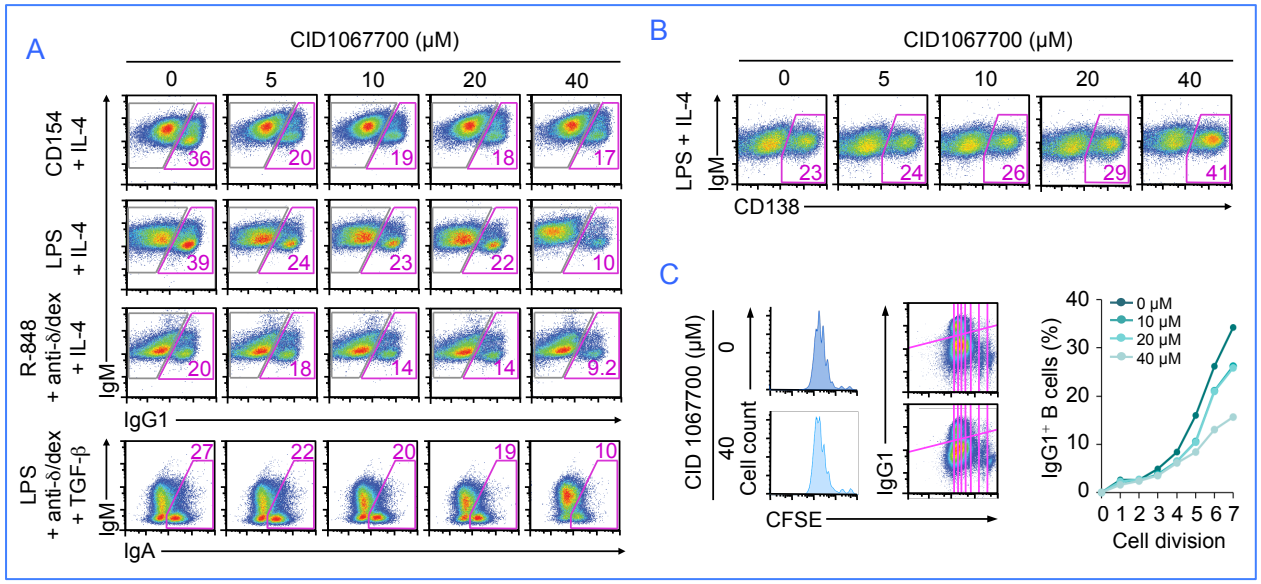

Figure 4.5 CID 1067700 impairs CSR without affecting B cell viability or proliferation. (**A**) Surface expression of IgM and IgG1 or IgA on $CD19^+$ B cells stimulated with T-dependent stimuli, CD154 (3 U/ml, to engage CD40) plus IL-4 (4 ng/ml, for CSR to IgG1) or T-independent stimuli, LPS (3μg/ml, to engage TLR4) plus IL-4 (4 ng/ml, for CSR to IgG1) or R-848 (30 ng/ml, to engage TLR7/8) plus anti–δ/dextran (30 ng/ml) plus IL-4 (4 ng/ml, for CSR to IgG1), or LPS plus anti–δ/dextran (30 ng/ml) plus TGF-β (2 ng/ml, for CSR to IgA) in the presence of nil or increasing doses of CID 1067700 (concentrations lower than CID 1067700 treated mice) for 4 d. (**B**) Surface expression of IgM and CD138 (a plasma cell marker) on B cells stimulated with LPS plus IL-4 in the presence of nil or increasing doses of CID 1067700 for 4 d. (**C**) Proliferation of lymph node $CD19^+$ B cells labeled with CFSE and stimulated for 4 d with LPS plus IL-4 in the presence of 0 or 40 μm of CID 1067700. Progressive left shift of fluorescence intensity indicates $CD19^+$ B cell division (left panels). Cell divisions were plotted as vertical lines versus IgG1 surface density, among $CD19^+$ B cells (middle panels). Percentages of $IgG1^+$ $CD19^+$ B cells among total $CD19^+$ B cells that had completed the same number of divisions when cultured 4 d in the presence of nil, 10, 20 or 40 μm of CID 1067700 are depicted as line scattered plots (right panels). Cell viability was defined by $7\text{-}AAD^-$ $CD19^+$ staining). Data are representative of three independent experiments.

We analyzed CSR inhibition by stimulating a purified population of B cells under various conditions with IL-4, which directs class-switching to IgG1 or with TGF-β, which directs class-switching to IgA (**Figure 4.5**). We stimulated B cells with primary inducing stimuli, T-cell dependent CD154 to engage CD40 on the surface of B cells, LPS to engage surface TLR4, or R-848 to engage endosomal TLR7/8, all of which play important roles in lupus[20, 21, 22, 23, 24]. In the presence of Rab7 inhibitor, CSR to IgG1 and IgA decreases in a dose dependent fashion, but does so without affecting B cell proliferation, as shown by carboxyfluorescein succinimidyl ester (CFSE) proliferation assay. CFSE couples with intracellular lysine residues and cell division can be analyzed CFSE is distributed to new daughter cells and with each cell division is reflected by the progressive halving of CFSE signal. In addition, with increasing doses of Rab7 inhibitor, there is a dose-dependent increase of IgM-producing $CD138^{+}$ plasma cells.

Having shown that Rab7 inhibitor impairs CSR, we next analyzed levels of germline transcripts and *Aicda* transcripts – which are required for CSR, and analyzed circle transcripts and post-recombination transcripts – which are readouts for ongoing and completed CSR, respectively.

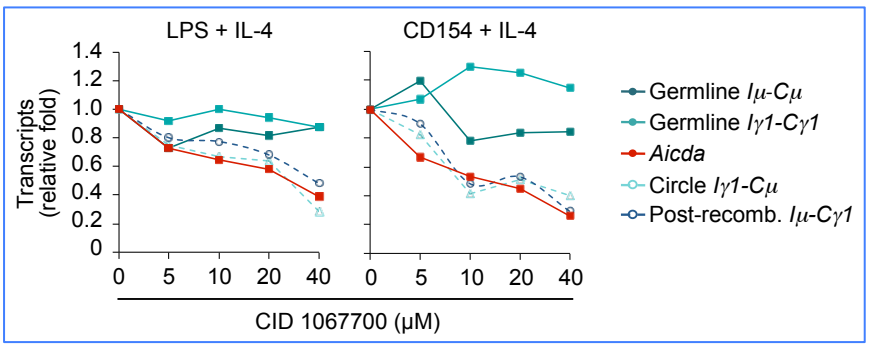

Figure 4.6 CID 1067700 decreases *Aicda* mRNA, circle transcripts and post-recombination transcripts. Germline Iμ-Cμ and germline Iγ-Cγ transcripts and *Aicda* transcripts (are required for CSR, normalized to *CD79b*) from $CD19^{+}$ B cells stimulated with either LPS or CD154 (3 U/ml, to engage CD40) plus Il-4 (4 ng/ml, for CSR to IgG1) were measured by qRT-PCR. Circle Iγ1-Cμ and Iμ-Cγ1 post-recombination transcripts (are accurate readouts for CSR, normalized to *CD79b*) from $CD19^{+}$ B cells stimulated with either LPS or CD154 (3 U/ml, to engage CD40) plus Il-4 (4 ng/ml, for CSR to IgG1) were measured by qRT-PCR.

Similar to the dose-dependent reduction in CSR in B cells that we stimulated with LPS or CD154 with IL-4, there is a dose-dependent decrease in *Aicda* transcripts, circle transcripts and post-recombination transcripts (**Figure 4.6**). However, germline *Iμ-Cμ* transcripts and germline *Iγ1-Cγ1* transcripts were not significantly affected. Thus CID 1067700 impairs B cell CSR by inhibiting *Aicda* expression, without affecting B cell viability or proliferation or Rab7 expression (data not shown).

The CID 1067700-impaired antibody response was associated with reduced CSR, which is initiated by AID, as we showed *in vivo* in MRL/$Fas^{lpr/lpr}$ lupus-mice and *in vitro* B cell cultures. AID expression requires activation of the canonical (phosphorylation of p65 and dimerization with p50) and non-canonical NF-κB (processing of p100 to p52 and dimerization with RelB). The role of NF-κB signaling in disease has been implicated in autoimmune diseases such as Crohn's disease and ulcerative colitis. Treatment studies to decrease NF-κB activation/activity has been shown to clinically reduce symptoms[25].

Mechanistically, canonical NF-κB hyper-activation in lupus B cells would result from higher *Rab7* expression, as Rab7 plays a role in activating the canonical NF-κB pathway, but not non-canonical NF-κB or MAPK (ERK or p38) pathways (data not shown from our manuscript[26]). Nevertheless, despite the statistically significant difference in *Rab7* expression between lupus B cells and normal B cells, B cells from several lupus patients showed normal *Rab7* expression, suggesting that B cells from this subset of lupus patients upregulate Rab7 activities and/or dysregulate genes that functionally interact with Rab7 in controlling canonical NF-κB activation.

4.5 SUMMARY TO CHAPTER 4

We have shown that Rab7 plays a B cell-intrinsic role in the specific activation of the canonical NF-κB pathway for B cell differentiation, particularly CSR, and generation of class-switched specific antibodies in normal mice and pathogenic autoantibodies in lupus mice, in which Rab7 is upregulated in B cells.

In vivo CID 1067700-inhibition of CSR, which "suspend" B cells at an IgM^+ state, as, indicated by the higher proportions of IgM^+ lymphocytes in human or mouse B cell cultures in the presence of CID 1067700. Whether these IgM^+ B cells remained naïve B cells or underwent memory B cell differentiation remains unclear. These would have still been available for the response to microbial pathogens and has been suggested to play a protective role in systemic autoimmunity[27]. In addition, CID 1067700 treatment allowed for some residual AID expression, which resulted in significant reduction but not ablation of secondary antibody isotypes. These can, even at lower titers, mediates a protective anti–microbial immunity, as suggested by the normal risk of infections in *Aicda*$^{+/-}$ mice, which have reduced AID expression[28].

Despite not involving human patients, our study provides a strong rational to target Rab7 in antibody responses, and as therapeutics for systemic autoimmunity and, possibility, IgE-mediate allergic responses. Our studies also provide novel and significant insights into the mechanisms of immunoregulation, as mediated by direct modulation of B cell-intrinsic functions, thereby providing a new target for therapeutic treatments and approaches, which will be discussed in Chapter 5.

4.6 MATERIALS AND METHODS

Quantitative RT-PCR (qRT-PCR)

For quantification of mRNA, RNA from SLE patient PBMCs, lupus-prone MRL/*Fas*$^{lpr/lpr}$ lupus-prone mice or C57BL/6 B cells were extracted from 0.2-5 x 10^6 cells using RNAeasy Plus Mini Kit (Qiagen). cDNA was synthesized from total RNA with the SuperScript™ III First-Strand Synthesis System (Invitrogen) using oligo-dT primer. Transcript expression was measured by qRT-PCR with appropriate primers using the Bio-Rad MyiQ Real-Time PCR Detection System (Bio-Rad Laboratories) to measure the binding of SYBER Green (IQ™ SYBR® Green Supermix, Bio-Rad Laboratories) to cDNA with the following protocol: 95°C for 15 sec, 40 cycles of 94°C for 10 sec, 60°C for 30 sec, 72°C for 30 sec. Data acquisition was performed during 72°C extension step. Melting curve analysis was performed from 72°C-95°C. The ΔΔCt method was used to analyze levels of transcripts and data were normalized to the level of *Cd79b* transcripts, which encodes the BCR Igβ chain that is constitutively expressed in B cells. For qPCR, the following primers were used: *Aicda* transcripts, forward 5'- TGCTACGTGGTGAAGAGGAG-3' and reverse 5'- TCCCAGTCTGAGATGTAGCG-3'; germline Iμ-Cμ transcripts, forward 5'-ACCTGGGAATGTATGGTTGTGGCTT-3' and reverse 5'-TCTGAACCTTCAAGGATGCTCTTG-3'; germline Iγ1-Cγ1 transcripts, forward 5'-TCGAGAAGCCTGAGGAATGTG-3' and reverse 5'-ATGGAGTTAGTTTGGGCAGCA-3'; circle Iγ1-Cμ transcripts, forward 5'- TCGAGAAGCCTGAGGAATGTG-3' and reverse 5'-TCTGAACCTTCAAGGATGCTCTTG-3'; post-recombination Iμ-Cγ1 transcripts, forward 5'-ACCTGGGAATGTATGGTTGTGGCTT-3' and reverse 5'-

ATGGAGTTAGTTTGGGCAGCA-3'; *Cd79b* transcripts 5'- TGTTGGAATCTGCAAATGGA-3' and reverse 5'- TAGGCTTTGGGTGATCCTTG-3'; human *RAB7A* transcripts, forward 5'-ACAGGCTAGTCACGATGCAG-3' and reverse 5'- TTGGGGGCAGTCACATCAAA-3'; human *AICDA* transcripts, forward 5'- ACTGGGCTTTTAGAGCAGCA-3' and reverse 5'-ACAGTGCATTGGCCCTTC-3'; human *CD79b* transcripts, forward 5'-AGGAACACGCTGAAGGATGG-3' and reverse 5'-CCACTTCACTTCCCCTGTCC-3'.

CID 1067700

For *in vivo* and *in vitro* studies, CID 1067700 (Glixx Laboratories) was dissolved in DMSO at 10 mg/ml. For *in vivo* studies, CID 1067700 was administered by intraperitoneal (i.p.) injection at 16 mg/kg. For in vitro experiments, CID was directly diluted in cell culture media at molarities ranging from 5 to 40 μM.

Lupus MRL/Faslpr/lpr mice: clinical pathology, serological autoantibodies and cellular analysis

Female MRL/*Fas*$^{lpr/lpr}$ mice were purchased from Jackson Laboratory (00485) and female C57BL/6 mice were maintained in a pathogen-free vivarium. All protocols were in accordance with the rules and regulations of the Institutional Animal Care and Use Committee (IACUC) of the University of Texas Health Science Center at San Antonio. For double-blind CID 1067700-treatment, 10-week-old (therapeutic treatment) or 15-week-old (late therapeutic treatment) *MRL/Fas*$^{lpr/lpr}$ mice were administered 0 mg/kg or 16 mg/kg of CID 1067700 weekly by intraperitoneal (i.p.) injection until 20 weeks. Skin lesions, lymphadenopathy, urine protein content and serum were collected at 8, 10, 12, 14, 16, 18 and 20 weeks. Spleen, brachial and inguinal lymph nodes and kidneys were harvested from 18-week-old mice. Skin lesions were scored on a scale of 0 to 4, with 0 = none, 1 = mild, snout; 2 = moderate, < 2 cm snout, ears; 3 =

severe, > 2 cm snout, ears; 4 = extremely severe. TL oligos.xlsx Lymphadenopathy were scored on a scale of 0 to 4, with 0 = none, 1 = small (at one site), 2 = moderate (at two sites), 3 = large (at three or more different sites), 4 = extremely severe. Anti–dsDNA IgG and IgG2a antibody titers were measured in sera of MRL/*Fas*$^{lpr/lpr}$ mice by ELISA as previously described [29]. Titers were expressed in RU, defined as the dilution factor needed to reach 50% of binding saturation, calculated using GraphPad Prism® software (GraphPad Software, Inc.).

B cells and CSR

For single B cell suspensions, murine spleens were prepared using a 70 μm cell strainer. Spleen B cells were resuspended in ACK Lysis Buffer (Lonza) to lyse red blood cells and after quenching with RPMI-1640 medium (Gibco) supplemented with FBS (10% v/v, Hyclone), penicillin-streptomycin (1% v/v, Invitrogen) and amphotericin B (1% v/v, Invitrogen) and supplemented with 50 μM β-mercaptoethanol (RPMI-FBS), were resuspended in RPMI-FBS before purification of B cells. Lymph node cells were directly resuspended in RPMI-FBS before purification.

For CSR induction, B cells were purified by depletion of cells expressing CD43, CD4, CD8, CD11b, CD49b, CD90.2, Gr-1 or Ter-119 using the EasySep^{TM} Mouse B cell Isolation kit (Stemcell Technologies) following the manufacturer's protocol, resulting in a preparation of more than 99% Igμ^{+} Igδ^{hi} B cells. After pelleting, B cells were resuspended and cultured at 3 x 10^5 cell/ml in RPMI-FBS. B cells were then stimulated with the following primary stimuli: CD154 (3 U/ml, mouse CD154-containing membrane fragments on baculovirus-infected Sf21 insect cell[30], LPS (3 μg/ml, from *E. coli*, serotype 055:B5, deproteinized by chloroform extraction, Sigma-Aldrich), TLR1/2 ligand Pam_3CSK_4 (100 ng/ml, Invivogen), TLR4 ligand

monophophoryl lipid A (lipid A, 1 μg/ml, Sigma-Aldrich), TLR7 ligand R-848 (30 ng/ml, Invivogen) or TLR9 ligand CpG ODN1826 with a phosphorothioate backbone (CpG, 1 μM, sequence 5'–TCCATGACGTTCCTGACGTT–3'; Operon). Anti–Igδ mAb (clone 11-26c) conjugated to dextran (anti–δ mAb/dex, 3 ng/ml, Fina Biosolutions) was added, as indicated, to crosslink BCRs. Recombinant IL-4 (3 ng/ml, BioLegend) was added for CSR to IgG1 and IgE, IFN-γ (50 ng/ml) for CSR to IgG2a, and TGF-β (2 ng/ml) for CSR to IgG2b (all from R&D Systems). After stimulation, B cells were harvested, stained with fluorochrome-conjugated mAbs in Hank's Buffered Salt Solution (HBSS) with 1% bovine serum albumin for 20 m and analyzed by flow cytometry for Igγ3, Igγ1, Igγ2b and Igγ2a expression (CSR to IgG3, IgG1, IgG2b and IgG2a) and other B cell surface molecules. Dead (7–AAD$^+$) cells were excluded from analysis. FACS data were analyzed by the FlowJo® software (Tree Star).

B cell proliferation and survival

For B cell proliferation analysis *in vivo*, mice were injected i.p. with 2 mg of bromodeoxyuridine (BrdU) in 200 μl PBS twice, at 24 h prior to sacrificing and at 20 h after the initial injection. B cells prepared from spleen were analyzed for BrdU incorporation and DNA contents using a BrdU Flow Kit (BD Biosciences).

For B cell proliferation analysis in vitro, CFSE-labeled naïve B cells were cultured for 96 h in the presence of appropriate stimuli and then analyzed by flow cytometry for CFSE intensity, where after completion of one cell division, CFSE distributes equally into two daughter cells. The number of B cell divisions was determined by the "Proliferation Platform" of the FlowJo® software. Percentages of IgG1$^+$ CD19$^+$ B cells among total CD19$^+$ B cells that had completed the same number of divisions were calculated.

Immunohistochemistry

Kidneys from *MRL/Fas*$^{lpr/lpr}$ lupus mice were fixed overnight in 10% formalin then passed into ethanol (70% in PBS) overnight, paraffin embedded and then sectioned (5 μm) for periodic acid Shiff (PAS) staining.

Immunoblotting

B cells (1 x 10^7) were harvested by centrifugation at 500 *g* for 5 m, resuspended in 0.5 ml of lysis buffer (20 mM Tris-Cl, pH 7.5, 150 mM NaCl, 0.5 mM EDTA, 0.25% (v/v) NP-40) supplemented with phosphatase inhibitors, including sodium pyrophosphate (1 mM), NaF (10 mM) and $NaVO_3$ (1 mM), and a cocktail of protease inhibitors (Sigma-Aldrich). Cell lysates were separated by SDS–PAGE and transferred onto polyvinylidene difluoride (PVDF) membranes. After blocking with milk and overnight incubation with rabbit mAb anti–Rab7 (Abcam) the membrane was incubated with goat anti–rabbit conjugated horseradish peroxidase (HRP) secondary Ab. Membranes were then stripped with 200 mM glycine (pH 2.5) for re-immunoblotting with a mouse HRP–conjugated mouse anti–β-actin (Abcam).

Statistical analysis

All statistic analysis was performed using Excel® software (Microsoft) or GraphPad Prism software. Statistical differences in Ig titers, CSR and RNA transcript expression were analyzed with Student's t-test assuming two-tailed distribution. P values less than 0.05 were considered significant. Statistical differences in lifespan between DMSO control mice or treated CID 1067700-treated mice (by i.p. injection at 16 mg/kg) were compared by Kaplan Meier curves and calculated using the Mantel-Cox log rank test.

4.7 REFERENCES

1. Tsokos GC. Systemic lupus erythematosus. *The New England journal of medicine* 2011, **365**(22)**:** 2110-2121.

2. Harley IT, Kaufman KM, Langefeld CD, Harley JB, Kelly JA. Genetic susceptibility to SLE: new insights from fine mapping and genome-wide association studies. *Nature reviews Genetics* 2009, **10**(5)**:** 285-290.

3. Flesher DL, Sun X, Behrens TW, Graham RR, Criswell LA. Recent advances in the genetics of systemic lupus erythematosus. *Expert Rev Clin Immunol* 2010, **6**(3)**:** 461-479.

4. Taylor KE, Chung SA, Graham RR, Ortmann WA, Lee AT, Langefeld CD*, et al.* Risk alleles for systemic lupus erythematosus in a large case-control collection and associations with clinical subphenotypes. *PLoS genetics* 2011, **7**(2)**:** e1001311.

5. Hughes T, Adler A, Kelly JA, Kaufman KM, Williams AH, Langefeld CD*, et al.* Evidence for gene-gene epistatic interactions among susceptibility loci for systemic lupus erythematosus. *Arthritis and rheumatism* 2012, **64**(2)**:** 485-492.

6. Vaughn SE, Kottyan LC, Munroe ME, Harley JB. Genetic susceptibility to lupus: the biological basis of genetic risk found in B cell signaling pathways. *J Leukoc Biol* 2012, **92**(3)**:** 577-591.

7. Chan OT, Madaio MP, Shlomchik MJ. The central and multiple roles of B cells in lupus pathogenesis. *Immunol Rev* 1999, **169:** 107-121.

8. Anolik J, Sanz I. B cells in human and murine systemic lupus erythematosus. *Curr Opin Rheumatol* 2004, **16**(5)**:** 505-512.

9. Jacob N, Stohl W. Autoantibody-dependent and autoantibody-independent roles for B cells in systemic lupus erythematosus: past, present, and future. *Autoimmunity* 2010, **43**(1)**:** 84-97.

10. Shlomchik MJ, Craft JE, Mamula MJ. From T to B and back again: positive feedback in systemic autoimmune disease. *Nat Rev Immunol* 2001, **1**(2)**:** 147-153.

11. Kiefer K, Oropallo MA, Cancro MP, Marshak-Rothstein A. Role of type I interferons in the activation of autoreactive B cells. *Immunol Cell Biol* 2012, **90**(5)**:** 498-504.

12. Cohen-Solal J, Diamond B. Lessons from an anti-DNA autoantibody. *Mol Immunol* 2011, **48**(11)**:** 1328-1331.

13. Heinlen LD, McClain MT, Ritterhouse LL, Bruner BF, Edgerton CC, Keith MP*, et al.* 60 kD Ro and nRNP A frequently initiate human lupus autoimmunity. *PLoS One* 2010, **5**(3)**:** e9599.

14. Xu Z, Zan H, Pone EJ, Mai T, Casali P. Immunoglobulin class-switch DNA recombination: induction, targeting and beyond. *Nat Rev Immunol* 2012, **12**(7)**:** 517-531.

15. Pone EJ, Zhang J, Mai T, White CA, Li G, Sakakura J*, et al.* BCR-signaling synergizes with TLR-signaling to induce AID and immunoglobulin class-switching through the non-canonical NF-κB pathway. *Nat Commun* 2012, **3:** 767(761-712).

16. Zan H, Zhang J, Ardeshna S, Xu Z, Park SR, Casali P. Lupus-prone MRL/faslpr/lpr mice display increased AID expression and extensive DNA lesions, comprising deletions and insertions, in the immunoglobulin locus: concurrent upregulation of somatic hypermutation and class switch DNA recombination. *Autoimmunity* 2009, **42**(2)**:** 89-103.

17. Lam T, Kulp D, Lou Z, Wang R, LaFleur C, Casali P*, et al.* Inhibition of antibody class switching and blocking of pathogenic autoantibody responses and disease development in lupus-prone mice by a small molecule compound that targets Rab7. *J Immunol* 2014**:** : in preparation.

18. Agola JO, Hong L, Surviladze Z, Ursu O, Waller A, Strouse JJ*, et al.* A competitive nucleotide binding inhibitor: in vitro characterization of Rab7 GTPase inhibition. *ACS chemical biology* 2012, **7**(6)**:** 1095-1108.

19. Gronwall C, Vas J, Silverman GJ. Protective Roles of Natural IgM Antibodies. *Frontiers in immunology* 2012, **3:** 66.

20. Nickerson KM, Christensen SR, Shupe J, Kashgarian M, Kim D, Elkon K*, et al.* TLR9 regulates TLR7- and MyD88-dependent autoantibody production and disease in a murine model of lupus. *J Immunol* 2010, **184**(4)**:** 1840-1848.

21. Wang H, Schlomchik MJ. Regulation of autoreactive anti-IgG (rheumatoid factor) B cells in normal and autoimmune mice. *Immunologic research* 1999, **19**(2-3)**:** 259-270.

22. Fan H, Liu F, Dong G, Ren D, Xu Y, Dou J*, et al.* Activation-induced necroptosis contributes to B-cell lymphopenia in active systemic lupus erythematosus. *Cell death & disease* 2014, **5:** e1416.

23. Lyn-Cook BD, Xie C, Oates J, Treadwell E, Word B, Hammons G*, et al.* Increased expression of Toll-like receptors (TLRs) 7 and 9 and other cytokines in systemic lupus erythematosus (SLE) patients: ethnic differences and potential new targets for therapeutic drugs. *Molecular immunology* 2014, **61**(1)**:** 38-43.

24. Liu B, Yang Y, Dai J, Medzhitov R, Freudenberg MA, Zhang PL*, et al.* TLR4 up-regulation at protein or gene level is pathogenic for lupus-like autoimmune disease. *J Immunol* 2006, **177**(10)**:** 6880-6888.

25. Ardite E, Panes J, Miranda M, Salas A, Elizalde JI, Sans M*, et al.* Effects of steroid treatment on activation of nuclear factor kappaB in patients with inflammatory bowel disease. *British journal of pharmacology* 1998, **124**(3)**:** 431-433.

26. Pone EJ, Lam TS, Edinger AL, Xu Z, Casali P. B cell Rab7 mediates induction of AID expression and class-switching in T-dependent and T-independent antibody responses. *J Immunol* 2014**:** submitted for publication. Not appended in accordance with NIH guidelines.

27. Jiang C, Zhao ML, Scearce RM, Diaz M. Activation-induced deaminase-deficient MRL/lpr mice secrete high levels of protective antibodies against lupus nephritis. *Arthritis and rheumatism* 2011, **63**(4)**:** 1086-1096.

28. Harada Y, Muramatsu M, Shibata T, Honjo T, Kuroda K. Unmutated immunoglobulin M can protect mice from death by influenza virus infection. *The Journal of experimental medicine* 2003, **197**(12)**:** 1779-1785.

29. White CA, Seth Hawkins J, Pone EJ, Yu ES, Al-Qahtani A, Mai T*, et al.* AID dysregulation in lupus-prone MRL/*Fas*$^{lpr/lpr}$ mice increases class switch DNA recombination and promotes interchromosomal *c-Myc/IgH* loci translocations: Modulation by HoxC4. *Autoimmunity* 2011, **44**(8)**:** 585-598.

30. Pone EJ, Zhang J, Mai T, White CA, Li G, Sakakura JK*, et al.* BCR-signalling synergizes with TLR-signalling for induction of AID and immunoglobulin class-switching through the non-canonical NF-kappaB pathway. *Nature communications* 2012, **3:** 767.

CHAPTER 5

FUTURE THERAPEUTIC APPROACHES THAT INHIBIT UNWANTED B CELL CLASS-SWITCHING

5.1. FUTURE DIRECTIONS TO DISRUPT 14-3-3-MEDIATED TARGETING OF CSR

For CSR to unfold, AID and the whole CSR machinery must be targeted to the S regions that are set to undergo recombination to introduce DSBs, the resolution of which leads to S–S DNA recombination – dysregulation of AID targeting has been associated with autoimmunity, chromosomal translocations and lymphomagenesis.

In Chapter 2, we characterized the recruitment and scaffold functions of 14-3-3 adaptors for the stabilization of enzymatic activity of AID and other CSR factors on S regions that require multiple molecular interactions. Here, we have made two important discoveries on 14-3-3-mediated targeting of the AID-centered CSR machinery: (i) we showed that all seven isoforms of 14-3-3 adaptors directly interacted with AID, but failed to interact with AID C-terminal point mutants that have been shown to be defective in mediating CSR[1, 2] and (ii) CSR to IgG1 in primary B cells was significantly reduced in the presence of HIV-1 viral protein R, Vpr; Vpr was also reported to inhibit CSR to IgA in CH12F3 B cells[3].

As we have also shown that AID colocalized with Vpr in HIV-1^+ patients lymph node germinal center B cells. In addition, (HIV-1^-) B cells internalized Vpr when cocultured with HIV-1^+ $CD4^+$ T cells that were infected with an HIV-1 strain (strain HIV-192US657; a clinical isolate of the primary R5 HIV-1 strain). B cell internalization of HIV-1 Vpr is likely facilitated by CD21[4, 5], CD40 and/or binding of DC-SIGN[3] – Vpr can be released from virions or infected T cells in an extracellular form[6], which can be internalized by bystander B cells through protein transduction[7]. Overall, our findings provide evidence that 14-3-3 adaptor proteins nucleate the assembly of the

AID-centered CSR machinery on 5'-AGCT-3' DNA repeats and H3K9acS10ph marks in S regions that are set to undergo S–S recombination. They also suggest that CSR DNA–protein and/or protein–protein complexes can be destabilized by naturally occurring molecules, leading to inhibition of CSR, thereby providing a basis for the identification of synthetic small molecule compounds, such as those that disrupt DNA–protein and/or protein–protein interactions involving 14-3-3[8, 9], or biologics that can effectively inhibit unwanted CSR, such as CSR underlying the generation of IgG and IgA autoantibodies in autoimmunity and atopic IgE antibodies in allergies and asthma.

FUTURE APPROACHES TO IDENTIFY SMALL MOLECULES THAT INHIBIT THE TARGETING OF CSR

Targeting "hot spots" of protein-protein interacting interfaces has proven to be an effective mechanism to screen for small molecules that block cell functions, as the "footprints" of these "hot spots" are not significantly larger than those covered by small molecules[10, 11]. In spite of the "flatness" of many protein-interacting interfaces, we expect to identify "hot spots" of 14-3-3, AID, PKA, Rev1 and/or Ung interactions; we expect proteins with mutations in these "hot spots" to display no scaffolding activity but "normal" structure, enzymatic function or homeostatic interactions with cell molecules. This mutagenesis approach would dissociate the CSR scaffolding functions of 14-3-3, PKA, Rev1 and/or Ung from their other cell functions. It will also provide guidance for target selection of Vpr interference in identifying, by high-throughput screening (HTS), synthetic small molecules that interfere with 14-3-3, AID, PKA, Rev1 and/or Ung interactions, thereby inhibiting CSR.

The rationale for using HTS stems from our published findings that: (i) CSR can be inhibited by

a naturally occurring molecule, Vpr, likely through disruption of scaffolding functions of 14-3-3, AID, PKA, Rev1 and/or Ung; (ii) CSR can be inhibited by difopein, a synthetic high affinity peptide inhibitor of 14-3-3, which we showed to be DNA/protein adaptors; and (iii) a single point-mutation (F193A or L196A) in AID is sufficient to disrupt AID/14-3-3 interaction and inhibit CSR. The interactions critical for CSR, as identified by mutagenesis studies, and disrupted with by Vpr/Vpr peptides, would help in the selection of the first set of HTS targets.

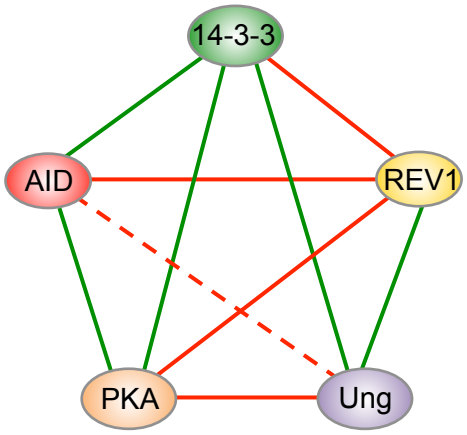

Figure 5.1 HTS of small molecule compounds that interfere with 14-3-3, AID, PKA, Rev1 and/or Ung interactions. The five interactions between 14-3-3, AID, PKA, Rev1 and/or Ung have been confirmed by our published data[12, 13, 14, 15] (total 10 possible interactions; green lines; red lines indicate interactions yet to be analyzed).

Systematically, all ten possible 14-3-3, AID, Rev1, Ung and/or PKA pair-wise interactions can be disrupted (**Figure 5.1**). For instance, screening over 50,000 diversified small molecules to identify those that can disrupt CSR protein-protein interaction. This is supported by our data using Vpr peptides to inhibit B cell class-switching. Vpr peptides with the highest CSR inhibitory effect segregated within three structural clusters (I, II and III) corresponding to the three α-helices of Vpr. Through a "multi-prong" strategy – cluster I peptides encompassed the Ung-binding Vpr region[16] and cluster III peptides straddled the 14-3-3- and PKA-interacting Vpr regions[17, 18].

Enhancing modifications of candidates and select modified compounds that are stable and do not

affect cell cycle, proliferation or survival and analyze their disruption of 14-3-3, AID, PKA, Rev1 and/or Ung scaffolding functions would fully cause the disruption of recruitment/stabilization of these factors to/on S regions. Confirmation would be required, by analyzing inhibition of CSR to different Ig isotypes (IgG, IgA or IgE) by these compounds.

Finally, the effect of these compounds in mice immunized with NP_{16}-CGG, as we described[19], could be confirmed by analyzing for the inhibition of CSR and the generation to NP-specific antibody titers *in vivo*. As an alternative HTS strategy, small compounds that block generation of fluorescence in BiFC involving 14-3-3γ and AID without affecting protein expression can be screened.

Small molecules selected through HTS will interfere with 14-3-3, AID, PKA, Rev1 and/or Ung interactions and inhibit CSR; they, however, need not mimic Vpr to be effective, and they will likely inhibit CSR to all Ig isotypes. A quest for inhibitors of predetermined isotype specificity would require targeting of up-stream signaling pathways, e.g., JAK-STAT for IgE, displaying "druglike" features could be used to delete IgG autoantibodies in systemic autoimmunity (without depleting B cells/IgMs, as anti–CD20 mAb therapy does) or IgE in the respiratory tract when administered topically.

5.2 FUTURE DIRECTIONS TO INHIBIT RAB7-MEDIATED INDUCTION OF CSR

CSR requires AID, – dysregulation of AID expression underpins autoantibody class-switching from the non-harmful, protective IgM class to the potentially pathogenic IgG and IgA classes. Systemic lupus erythematosus (SLE) is a chronic autoimmune disease that is characterized by pathogenic anti–dsDNA IgG autoantibodies and pathogenic IgA in nephropathy produced by autoreactive B cells. As Rab7 modulates AID expression in B cells, we undertook this study to address the role of Rab7 in lupus B cells. *RAB7A* (*Rab7* in mouse) expression and *AICDA* (*Aicda* in mouse) expression were upregulated in SLE patients and in female MRL/$Fas^{lpr/lpr}$ mice.

We proposed that Rab7-dependent mature endosomes in B cells play an important role in mediating signal transduction from CD40 and TLRs, leading to activation of NF-κB to induce AID for CSR and, eventually, generation of class-switched specific antibodies in normal mice and pathogenic autoantibodies in lupus mice, in which Rab7 is upregulated in B cells. Rationale for our hypothesis stems from our data in Chapter 3, in which we show that *Rab7 B-KO* mice/B cells were defective in CSR *in vivo* and *in vitro*. These B cells were also impaired in the canonical NF-κB pathway activation and AID induction. They, however, were normal in IgM production, proliferation, survival and plasma cell differentiation, likely due to their normal activation of the ERK, p38 kinase and non-canonical NF-κB pathways in B cells.

These findings are consistent with our contention that the putative signal functions of Rab7-dependent intracellular membranes are in addition to the basal functions of such membranes, e.g., cargo sorting, recycling and degradation. As these basal functions maintain cell homeostasis,

they are likely carried out by multiple small GTPases in a redundant manner.

Rab7 is a small GTPase that, upon activation and tethering to immature endosomes, promotes formation of mature endosomes[20]. These are part of the larger network of intracellular membrane structures, which, as contended by a new paradigm in signaling[21, 22], would strengthen signals from surface and intracellular (immune) receptors by providing a "platform" for these receptors and their downstream signal molecules to interact. As further contended by us, different intracellular membranes transduce distinct signals, thereby dictating the specificity of cell differentiation, including CSR in B cells. This is prompted by our novel idea that Rab7, likely through mature endosomes, mediates NF-κB activation in B cells. This notion is consistent with and can readily explain our data suggesting that Rab7 plays a B cell-intrinsic role in antibody and autoantibody responses and is a target of lupus therapeutics.

We have made three important discoveries on Rab7-mediated induction of CSR in autoantibody responses: (i) Rab7 plays a B cell-specific role in antibody class-switching; (ii) Rab7 is upregulated in lupus B cells and; (iii) CID 1067700 prevents lupus development in lupus-prone mice and blunts antibody response and autoantibody responses, which are initiated by AID.

Despite not involving human patients, our study provides a strong rational to target Rab7 in antibody responses, and as therapeutics for systemic autoimmunity and, possibly, IgE-mediate allergic responses. Our studies also provide novel and significant insights into the mechanisms of immunoregulation, as mediated by direct modulation of B cell-intrinsic functions, thereby providing a new target for therapeutic treatments and approaches.

FUTURE APPROACHES TO IDENTIFY COMPOUNDS THAT INHIBIT THE INDUCTION OF CSR

Developing new inhibitors with improved specificities to Rab7 would enhance the affect on lupus B cells. New compounds that are screened would be used to verify their inhibitory effects on NF-κB activation and CSR, and to analyze their efficacy in blunting autoantibody responses and in preventing disease development in lupus-prone mouse models. This provides a strong rationale to screen for more specific inhibitors, which has increase affinities to Rab7 (thereby lowering effective doses), or decreased affinities towards other small GTPases (thereby being better tolerated at relatively high doses), or, ideally, both.

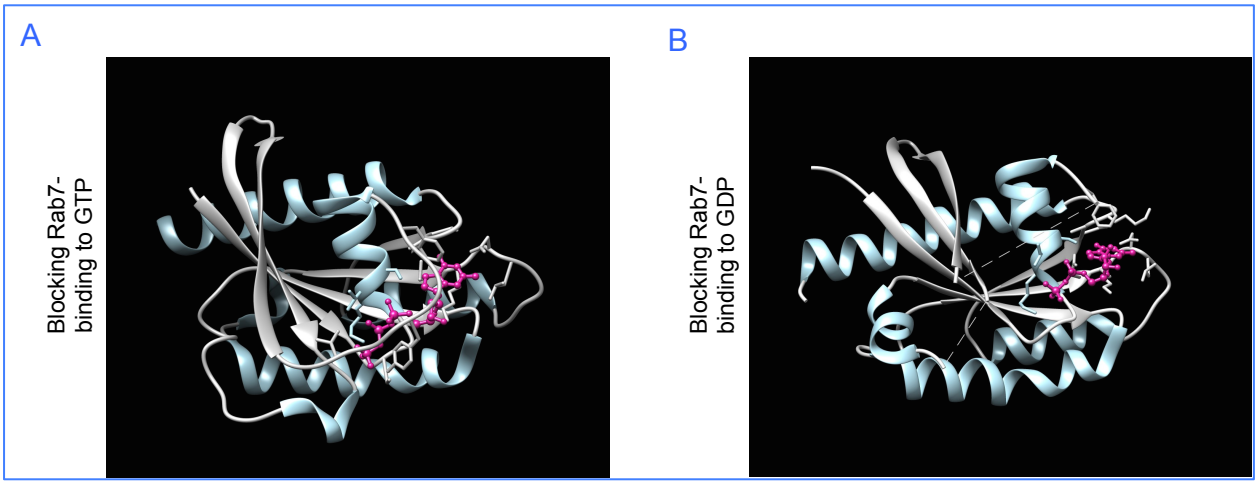

Figure 5.2 CID 1067700 binding to Rab7 can be enhanced. CID 1067700, a recently identified (and the only known) specific inhibitor of Rab7**.** It functions by inhibiting Rab7 GTPase activity by fitting into both the narrow GTP-binding pocket (**A**) and the more open GDP-binding pocket thereby blocking Rab7 function (**B**). For future therapeutic designs, using the high-power Rhodium® Docking software developed by our collaborator Drs. W. E. Bauta and J. Bohmann (SwRI®) can identify CID 1067700 derivatives that maintain affinities and better fit to Rab7 but have diminished binding to non-Rab7 targets (red box indicate where improvements can be made).

Screening approaches would include identifying CID 1067700 analogs with increased specificity towards Rab7 and to screen compound libraries for new Rab7-binding small molecules using an *in silico* approach, and to verify the Rab7 inhibitory activity of these compounds. First, we must identify CID 1067700 derivatives that maintain affinities to Rab7 but have diminished binding to

non-Rab7 targets using the high-power Rhodium® Docking software developed by our collaborator Drs. W. E. Bauta and J. Bohmann (SwRI®, **Figure 5.2**). Next, we will perform the computational screening of 2 x 10^6 small molecules to identify those that could bind Rab7 with high affinities. These new Rab7 inhibitors will be tested *in vitro* for their inhibitory activities in NF-κB activation, AID expression and CSR in B cells. We will also test them *in vivo* by treating MRL/*Fas*$^{lpr/lpr}$ mice starting at 10-week of age, when they begin to exhibit significant autoantibody levels but no disease signs. We will analyze clinical, histological, serological, cellular and molecular parameters, and generate a survival curve, as we described[23, 24]. We will follow basic principles of preclinical animal studies[25].

These compounds may ameliorate lupus symptoms by also affecting immune elements other than B cells. A "global" analysis of homeostasis and functions of other immune cells and cytokine signatures is beyond the scope of this proposal, and, in the absence of genetic studies, such analysis may not necessarily yield definitive information on the contribution of these elements in mediating the effect of Rab7 inhibitors. These would not affect IgM, including natural antibodies important in the defense against microbial pathogens, making them attractive candidates for further clinical evaluations.

Our study is highly relevant to the healthcare needs of human health. Therapeutic interventions (e.g., using Rab7-specific inhibitors, as we contend here) would inhibit further generation of pathogenic autoantibodies, thereby preventing nephritis, myocardial infarction, neuropsychiatries and other diseases that are life debilitating and expensive to manage. Our work will also re-emphasize the use of highly specific and inexpensive small molecules as new therapeutics.

5.3 REFERENCES

1. Geisberger R, Rada C, Neuberger MS. The stability of AID and its function in class-switching are critically sensitive to the identity of its nuclear-export sequence. *Proc Natl Acad Sci USA* 2009, **106**(16)**:** 6736-6741.

2. Doi T, Kato L, Ito S, Shinkura R, Wei M, Nagaoka H*, et al.* The C-terminal region of activation-induced cytidine deaminase is responsible for a recombination function other than DNA cleavage in class switch recombination. *Proc Natl Acad Sci USA* 2009, **106**(8)**:** 2758-2763.

3. Begum NA, Izumi N, Nishikori M, Nagaoka H, Shinkura R, Honjo T. Requirement of non-canonical activity of uracil DNA glycosylase for class switch recombination. *J Biol Chem* 2007, **282**(1)**:** 731-742.

4. Moir S, Malaspina A, Li Y, Chun TW, Lowe T, Adelsberger J*, et al.* B cells of HIV-1-infected patients bind virions through CD21-complement interactions and transmit infectious virus to activated T cells. *J Exp Med* 2000, **192**(5)**:** 637-646.

5. Stoiber H, Speth C, Dierich MP. Role of complement in the control of HIV dynamics and pathogenesis. *Vaccine* 2003, **21 Suppl 2:** S77-82.

6. Tungaturthi PK, Sawaya BE, Singh SP, Tomkowicz B, Ayyavoo V, Khalili K*, et al.* Role of HIV-1 Vpr in AIDS pathogenesis: relevance and implications of intravirion, intracellular and free Vpr. *Biomed Pharmacother* 2003, **57**(1)**:** 20-24.

7. Sherman MP, Schubert U, Williams SA, de Noronha CM, Kreisberg JF, Henklein P*, et al.* HIV-1 Vpr displays natural protein-transducing properties: implications for viral pathogenesis. *Virology* 2002, **302**(1)**:** 95-105.

8. Zhao J, Du Y, Horton JR, Upadhyay AK, Lou B, Bai Y*, et al.* Discovery and structural characterization of a small molecule 14-3-3 protein-protein interaction inhibitor. *Proc Natl Acad Sci USA* 2011, **108**(39)**:** 16212-16216.

9. Zhao J, Meyerkord CL, Du Y, Khuri FR, Fu H. 14-3-3 proteins as potential therapeutic targets. *Semin Cell Dev Biol* 2011, **22**(7)**:** 705-712.

10. Stockwell BR. Chemical genetics: ligand-based discovery of gene function. *Nat Rev Genet* 2000, **1:** 116-125.

11. Wells JA, McClendon CL. Reaching for high-hanging fruit in drug discovery at protein-protein interfaces. *Nature* 2007, **450**(7172)**:** 1001-1009.

12. Lam T, Thomas LM, White CA, Li G, Pone EJ, Xu Z*, et al.* Scaffold functions of 14-3-3

adaptors in B cell immunoglobulin class switch DNA recombination. *PloS one* 2013, **8**(11)**:** e80414.

13. Zan H, White CA, Thomas LM, Mai T, Li G, Xu Z*, et al.* Rev1 recruits ung to switch regions and enhances du glycosylation for immunoglobulin class switch DNA recombination. *Cell reports* 2012, **2**(5)**:** 1220-1232.

14. Xu Z, Fulop Z, Wu G, Pone EJ, Zhang J, Mai T*, et al.* 14-3-3 adaptor proteins recruit AID to 5'-AGCT-3'-rich switch regions for class switch recombination. *Nature structural & molecular biology* 2010, **17**(9)**:** 1124-1135.

15. Mai T, Pone EJ, Li G, Lam TS, Moehlman J, Xu Z*, et al.* Induction of activation-induced cytidine deaminase-targeting adaptor 14-3-3gamma is mediated by NF-kappaB-dependent recruitment of CFP1 to the 5'-CpG-3'-rich 14-3-3gamma promoter and is sustained by E2A. *Journal of immunology* 2013, **191**(4)**:** 1895-1906.

16. Selig L, Benichou S, Rogel ME, Wu LI, Vodicka MA, Sire J*, et al.* Uracil DNA glycosylase specifically interacts with Vpr of both human immunodeficiency virus type 1 and simian immunodeficiency virus of sooty mangabeys, but binding does not correlate with cell cycle arrest. *J Virol* 1997, **71**(6)**:** 4842-4826.

17. Kino T, Gragerov A, Valentin A, Tsopanomihalou M, Ilyina-Gragerova G, Erwin-Cohen R*, et al.* Vpr protein of human immunodeficiency virus type 1 binds to 14-3-3 proteins and facilitates complex formation with Cdc25C: implications for cell cycle arrest. *J Virol* 2005, **79**(5)**:** 2780-2787.

18. Barnitz RA, Wan F, Tripuraneni V, Bolton DL, Lenardo MJ. Protein Kinase A phosphorylation activates Vpr-induced cell cycle arrest during Human Immunodeficiency Virus Type-1 infection. *J Virol* 2010, **In press**.

19. Pone EJ, Lam TS, Edinger AL, Xu Z, Casali P. B cell Rab7 mediates induction of AID expression and class-switching in T-dependent and T-independent antibody responses. *J Immunol* 2014**:** submitted for publication. Not appended in accordance with NIH guidelines.

20. Wang T, Ming Z, Xiaochun W, Hong W. Rab7: role of its protein interaction cascades in endo-lysosomal traffic. *Cell Signal* 2011, **23**(3)**:** 516-521.

21. O'Neill SK, Veselits ML, Zhang M, Labno C, Cao Y, Finnegan A*, et al.* Endocytic sequestration of the B cell antigen receptor and toll-like receptor 9 in anergic cells. *Proceedings of the National Academy of Sciences of the United States of America* 2009, **106**(15)**:** 6262-6267.

22. Chaturvedi A, Martz R, Dorward D, Waisberg M, Pierce SK. Endocytosed BCRs sequentially regulate MAPK and Akt signaling pathways from intracellular compartments. *Nature immunology* 2011, **12**(11)**:** 1119-1126.

23. Zan H, Zhang J, Ardeshna S, Xu Z, Park SR, Casali P. Lupus-prone MRL/*Fas*$^{lpr/lpr}$ mice display increased AID expression and extensive DNA lesions, comprising deletions and insertions, in the immunoglobulin locus: concurrent upregulation of somatic hypermutation and class switch DNA recombination. *Autoimmunity* 2009, **42**(2)**:** 89-103.

24. White CA, Pone EJ, Lam T, Tat C, Hayama KL, Li G*, et al.* HDAC inhibitors upregulate B cell microRNAs that silence AID and Blimp-1 expression for epigenetic modulation of antibody and autoantibody responses. *J Immunol* 2014**:** in revision.

25. Landis SC, Amara SG, Asadullah K, Austin CP, Blumenstein R, Bradley EW*, et al.* A call for transparent reporting to optimize the predictive value of preclinical research. *Nature* 2012, **490**(7419)**:** 187-191.